An investigation of the influence of co-morbid anxiety on functional connectivity changes in the MIA model of OA pain

Thesis submitted to the University of Nottingham

for the

Degree of Doctor of Philosophy

Amanda Lillywhite

November 29th 2019

School of Life Sciences

University of Nottingham Medical School

Queen's Medical Centre

Nottingham

NG7 2UH

Chapter 1 Table of Contents

List of Figures

List of Tables

Abstract

Background

Pain, although universally experienced and adaptive, can negatively impact daily functioning and quality of life when it becomes chronic. Osteoarthritis is one of the most commonly experienced chronic pain conditions, with a huge personal and societal impact. The treatment of OA can be challenging and is complicated by a number of frequently experienced co-morbid conditions.

Anxiety is often co-morbid in chronic pain conditions, including OA. Co-morbid anxiety is associated with an increase in levels of pain, an increased need for medication and worse outcomes after treatment than patients without these co-morbidities, particularly with opioids. The investigation of how anxiety mediates pain and responses to treatment, and the brain changes that occur in response to co-morbid anxiety and pain is still unclear. This thesis hypothesised that animal models of OA pain are associated with changes in functional connectivity in the brain, and anxiety exacerbates OA pain via alterations in these pathways and changes in endogenous opioid receptor tone.

Objectives

1) To validate methods for measuring alterations in spontaneous fluctuations in the BOLD signal using resting-state fMRI in the rat.

2) To compare resting-state fMRI differences in the monosodium iodoacetate (MIA) model of OA in Wistar rats and Wistar-Kyoto rats, an inbred genetic strain which has a high anxiety behavioural phenotype.

3) To investigate to the potential contributions of alterations in opioid receptors and endogenous opioid tone in WKY rats and if this impacts upon the manifestation of pain behaviour in the model of OA.

Methods

In this thesis, the Wistar-Kyoto inbred rat strain, which displays anxiety-related behaviour, was used with outbred Wistar rats as normal anxiety controls. Intra-articular administration of MIA (1mg) was used to model osteoarthritis pain in the knee.

fMRI was used to investigate resting-state functional connectivity changes in the two rat strains after intra-articular MIA, and ECoG was used to explore the temporal nature of neuronal activity. Medetomidine and isoflurane were used together to provide anaesthesia during these experiments.

Behavioural pharmacological studies were conducted to investigate responsiveness to morphine after intra-articular MIA in the WKY rats, and subsequently the endogenous opioidergic system was investigated through administration of naloxone.

Results

The medetomidine and isoflurane anaesthetic regime was tested for the functional connectivity work and decided to be suitable for the study of resting-state fMRI in these rat models.

Functional connectivity differences were observed following induction of the MIA model of OA pain and correlation analysis revealed that the relationship between pain behaviour and functional connectivity from

the vmPFC to S2/caudate putamen was altered in the high anxiety WKY strain of rats.

Using ECoG, increases in power of somatosensory evoked potentials, over the somatosensory cortex, were observed in response to noxious electrical stimulation after intra-articular MIA

Behaviourally, in the WKY rats, responses to morphine were attenuated, with increased endogenous opioidergic tone, suggesting that some of the differences in the sensitivity to morphine may reflect differences in the endogenous opioid system.

Conclusions

The work in this thesis provided new evidence of the influence of anxiety on functional brain changes in the MIA model of OA pain, and possible involvement of the opioidergic system but further work is required to replicate the new functional connectivity data and focus on molecular mechanisms underpinning these alterations.

Acknowledgements

This thesis would not have been possible without the help and support of my supervisors, colleagues, friends and family

I would firstly like to thank my supervisors, Victoria Chapman, Gareth Hathway and Dorothee Auer. I am exceptionally grateful for the opportunity to have studied for this PhD, and for everything I've learned over the past four years. Vicky was ever present throughout the course of my PhD for practical and theoretical guidance, no matter how busy, providing a vast amount of support, time and knowledge. I would like to thank Gareth for both the scientific and practical contributions to my thesis but his enthusiasm for science was particularly important to me and kept me motivated during every study and challenge. I would like to thank Dorothee for all of her practical support and scientific input for the imaging experiments, she was a steady source of advice, knowledge and inspiration.

I want to thank all of my colleagues and PhD students in the research group, and in Dorothee's research group for all of the vast amounts of practical help needed during these experiments but also for the emotional support and friendship, without which this PhD would have been a very different experience.

I would like to thank the technical staff, in particular Dave Watson and Clare Spicer, for being present for almost every experiment, and solving every practical problem and mishap. These studies would not have been possible without them.

Lastly, I would like to thank my husband Danny and my family, mostly for their continued love and support over the past four years but also for not asking about the thesis too often.

Abbreviations

ACC: Anterior cingulate cortex

BLA: Basolateral amygdala

BOLD: Blood oxygen level dependent

CeA: Central nucleus of the amygdala

CNS: Central nervous system

CPS: Central pain syndrome

CT: computerised tomography

CBF: cerebral blood flow

DMN: Default mode network

DRG: Dorsal root ganglion

DRt: Dorsal reticular nucleus

ECoG: Electrocorticography

EEG: Electroencephalography

EPI: Echo planar imaging

ERP: Event related potential

FC: functional connectivity

fMRI: Functional magnetic resonance imaging

FWHM: Full width half maximum

GRF: Gaussian random field

HPA: Hypothalamic-pituitary-adrenal

HRQoL: Health related quality of life

ICA: Independent component analysis

IL: Infra-limbic cortex

MEG: Magnetoencephalography

MIA: Monosodium iodoacetate

MRI: Magnetic resonance imaging

NKI: neurokinin 1

OA: Osteoarthritis

PAG: Periaqueductal grey

PET: Positron emission tomography

PFC: Prefrontal cortex

PWT: Paw withdrawal threshold

RS: Resting state

RS-FC: Resting state functional connectivity

RVM: rostral ventromedial medulla

Sl: primary somatosensory cortex

S2: secondary somatosensory cortex

SEP: somatosensory evoked potential

vmPFC: ventromedial prefrontal cortex

WB: Weight bearing

WKY: Wistar Kyoto

YDL: Years lived with disability

Chapter 1: General Introduction

1.1 Pain

Pain is a phenomenon that is experienced nearly universally by mankind. It is largely a necessary and adaptive experience and plays a significant role in allowing us to recognise when we are being harmed, and to subsequently avoid harm. Although pain is primarily a sensory experience, it is now well recognised that it also encompasses a significant affective component. These affective and sensory components combine to produce a typically highly unpleasant experience. While pain *is* primarily an adaptive response, it can also negatively impact daily functioning and quality of life when it extends beyond the necessary physiological healing of injuries and illnesses.

Given the unpleasantness of the pain experience, individuals seek to avoid or alleviate pain on a daily basis, through a number of physical, pharmacological or psychological means. Pharmacological analgesics: drugs that are used to alleviate pain, comprise the largest share of the over the counter (OTC) drugs market in the United States (• *OTC medicines: breakdown of sales value 2017-2018 | UK Statistic*).

Chronic pain conditions comprise a large portion of the world's disease burden, as represented by years lived with disability (YDL). 4 of the most common chronic pain conditions are featured in the top 10 most impactful conditions and osteoarthritis is the 13th biggest contributor to YDL (Rice, Smith and Blyth, 2016). This demonstrates the impact of chronic pain on disease and disability, and the importance of its treatment at both a societal and individual level.

This chapter will introduce how pain signals are transmitted from the peripheral to the central nervous system, how pain is modulated by the

nervous system and altered during chronic pain, with a focus on knee osteoarthritis, and how neuroimaging has been used to investigate these changes.

1.1.1 Peripheral mechanisms of pain

1.1.1.1 Nociceptors

The sensory perception of pain begins in the peripheral nervous system, most often arising from the skin, in order to warn of actual or potential tissue damage. Noxious stimuli are detected by nociceptors which are located on the terminals of small diameter unmyelinated and myelinated sensory afferent fibres. Sensory afferent neurons are pseudo-unipolar neurons, with an axon that bifurcates towards both the sensory organ and the dorsal horn of the spinal cord. They do not have dendrites (Fig 1.1).

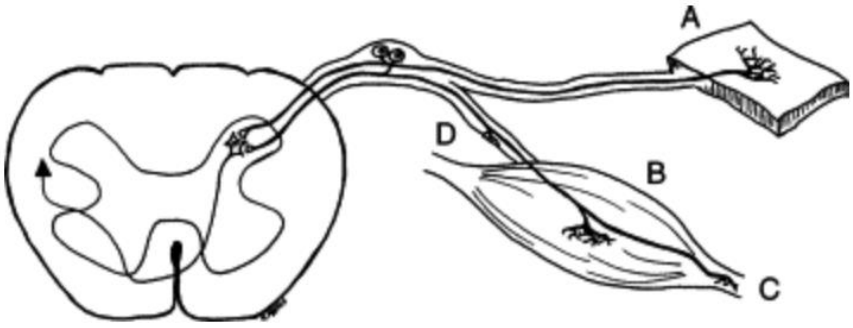

Figure 1.1: The process of nociception, originating from primary afferents innervating the skin (A) or the muscle (B) and tendon (C). The primary afferent fibre extends to the dorsal horn of the spinal cord (Bove and Swenson, 2006)

These sensory receptors were first defined by Charles Sherrington, who discovered that nociception in the skin begins in a set of nerve endings whose specific role it is to detect stimuli that "do the skin injury, stimuli that in continuing to act would injure it still further" (Sherrington, 1903). However, nociceptors are not only present in the skin and are also present in the muscles, joints, bladder, gut and digestive tract.

Two main sensory afferent fibres are activated by noxious stimuli: A-δ and C fibres.

- A-δ fibres are myelinated nerve fibres with a small diameter (1-5 micrometres), and a conduction velocity of 5-40 m/s. They can respond to both mechanical and thermal stimuli, although approximately half of A-δ fibres are classified as mechanically insensitive afferents (McMahon, 2013). A-δ fibres produce a quick sharp pain sensation (See refs in Stucky, 2016).

- C fibres make up 70% of all nociceptors; they are not typically myelinated but are encased in a schwann cell sheath (Stucky, 2016). They have a smaller diameter (0.3 – 1.3µm), and a conduction velocity of 0.1-2m/s. They are polymodal and the majority of C fibres respond to mechanical, thermal and chemical stimuli such as low pH, although approximately 30% of C fibres are mechanically insensitive (McMahon, 2013).

Noxious stimuli trigger the depolarisation of the sensory endings of nociceptors and the opening of voltage gated Na^+ channels, leading to action potential generation and their conduction to the dorsal horn of the spinal cord. All primary sensory neurons have cell bodies in dorsal root or trigeminal ganglia. The peripheral branch of this axon innervates the tissue and the central branch of this axon enters the central nervous system (CNS) via the dorsal horn of the spinal cord (Fig 1.1) (Woolf and

Ma, 2007). Normally, nociceptors are electrically silent and only transmit action potentials when stimulated.

1.1.2 Central mechanisms of pain

1.1.2.1 Ascending pain pathways

The dorsal horn of the spinal cord is segregated into several different laminae. Most A-δ and C fibres terminate in the superficial layers of the dorsal horn with a small number reaching into the deeper layers, while A-β fibres tend to innervate laminae IV – V (Todd, 2010). In practice, laminar organisation of the dorsal horn is far more complex than this, and differences in termination within the dorsal horn are influenced not only by fibre type but also by functional class and neurochemical properties (Todd, 2010), although discussion of this is beyond the scope of this thesis.

Spinal projection neurons from the dorsal horn, located primarily in lamina I and V, relay nociceptive information from primary afferents supraspinally to the brainstem and thalamic nuclei (Todd, 2010). The primary regions in which these projection neurons terminate include the caudal ventrolateral medulla, the nucleus of the solitary tract, the lateral parabrachial area, the periaqueductal grey (PAG) and the thalamus (Todd, 2010). Most of the lamina I projection neurons express the neurokinin 1 (NK1) receptor, the primary target for substance P which is the neuropeptide released during nociceptive input *(Todd et al*, 2002).

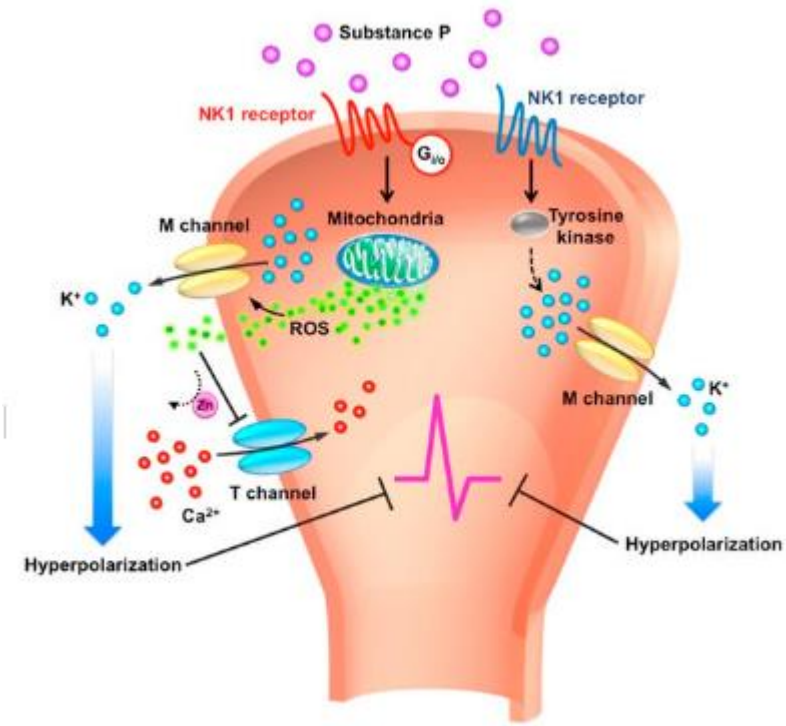

Figure 1.2: A schematic illustrating substance P mediated signalling and ion channels in the peripheral nervous system. Substance P acts on NK1 receptors via two pathways modulating the M K+ and T Ca^{2+} channels, resulting in neuronal hyperpolarisation (Chang, Jiang and Chen, 2019).

The spinothalamic tract, which transmits signals towards supraspinal regions, is divided into two separate pathways each of which are involved in the transmission of pain. The ventral spinothalamic tract is located in the ventral lateral funiculus and is involved in the transmission of pain and temperature (Paxinos, 2014). The dorsal spinothalamic tract is located in the dorsolateral funiculus and is nociception specific. Although the two pathways of the spinothalamic tract ascend separately, they merge at the level of the medulla (Rea and Rea, 2015).

The ascending projections in the spinothalamic tract terminate in the thalamus and contralateral projections target mesencephalic nuclei including the dorsal reticular nucleus (DRt), the rostral ventromedial medulla (RVM) and the periaqueductal gray (PAG) (Todd, 2010). Supraspinally, a number of cortical and subcortical regions are then

involved in the perception of pain (Tracey and Mantyh, 2007). A distinction is often made between regions that encode the sensory perception of pain, such as the somatosensory cortices and the regions involved in the emotional processing of pain, including regions such as the amygdala, ACC and insula (Tölle *et al.*, 1999; Dunckley *et al.*, 2005).

1.1.4 Descending modulation of pain

The CNS is not solely involved in the transmission of pain signals for the perception of pain but is also central to the modulation of pain (Tracey and Mantyh, 2007; Ossipov, Dussor and Porreca, 2010). The central processing of pain is bidirectional and just as the transmission of information extends to brain, the brain also transmits information back to the spinal cord. The endogenous mechanisms that modulate pain are involved in both the facilitation and the inhibition of pain (Ossipov, Dussor and Porreca, 2010). Descending inhibition of pain involves a network of supraspinal regions, including the prefrontal cortex, hypothalamus, amygdala and the anterior cingulate cortex (ACC), which feed into the PAG, and the RVM which projects down to the dorsal horn of the spinal cord (Millan, 2002).

The discovery of descending pain mechanisms began with the observation that electrical stimulation of PAG or RVM lead to suppression of behavioural responses to nociceptive stimuli (Reynolds, 1969; Mayer and Price, 1976). The PAG not only receives input from ascending projections from the spinal cord, but also a number of cortical and subcortical regions including the prefrontal cortex, the amygdala, the hypothalamus and the ACC (Veening *et al.*, 1991; An *et al.*, 1998).

The PAG relays to the dorsal horn through the RVM, which contains the raphe magnus and the reticular formation. The RVM contains serotonergic (5-HT) and GABAergic neurons which project to the dorsal

horn (Bowker, Westlund and Coulter, 1981; Antal *et al.*, 1996). Neurons within the RVM are classified as 'on cells' 'off cells' and 'neutral cells'(Bajic *et al.*, 2017). These physiological definitions are based on the firing properties of cells following noxious stimulation of the periphery (Fields *et al.*, 1983). ON cells are anatomically inactive, with low frequency basal firing rates. OFF cells conversely have higher basal firing rates. Upon noxious stimulation ON cells increase firing rate whilst OFF cells significantly reduce their firing frequency (Fields, 1991). Both ON and OFF cell firing is intimately linked with the initiation of reflex nocifensive behaviours (Fields *et al.*, 1983; Devonshire *et al.*, 2015). NEUTRAL cells have no consistent change in firing properties in response to noxious stimulation, but are the majority of spinally projecting 5-HT containing neurons (Fields *et al.*, 1983).

The prefrontal cortex (PFC) is implicated in pain but also more broadly in executive and cognitive functioning (Robbins, 1996; Koechlin, Ody and Kouneiher, 2003). The PFC is connected extensively to other cortical and subcortical areas, including a number of regions relevant to the processing of pain (See refs in Ong, Stohler and Herr, 2019). Evidence for the influence of a prefrontal influence on descending modulation of pain come from early studies demonstrating that anaesthetisation of the prefrontal cortex leads to anti-nociception in the rat (Cooper, 1975).

Output from the hypothalamus has been shown to be involved in the descending modulation of pain, and stimulation of the hypothalamus has also been shown to produce anti-nociception in rats (Wardach *et al.*, 2016). Mechanistically, although this effect has not been fully determined, it is thought to be mediated by spinally descending orexin neurons (Wardach *et al.*, 2016). Descending dopaminergic projections from hypothalamic A11 neurons have also been implicated in pain signalling, and in chronic pain in studies of hyperalgesic priming, the

ablation of D5 receptors reduces pain responses and prevents hyperalgesic priming (Megat *et al.*, 2018).

The amygdala has been heavily implicated not only in pain but also in the processing of fear and emotions (Davis *et al.*, 2010; Pare and Duvarci, 2012). Outputs from the thalamus, the secondary somatosensory cortex (S2) and the insula cortex (Veinante, Yalcin and Barrot, 2013), project to the basolateral amygdala (BLA) or the central nucleus of the amygdala (CeA) and subsequently to the PAG (Veinante, Yalcin and Barrot, 2013). Innervation of the PAG by the CeA is extensive and highly organised, with terminations primarily centred in the ventral half of the PAG (Rizvi *et al.*, 1991).

1.2 Peripheral and central mechanisms of pain plasticity

1.2.1 Sensitization of the peripheral nervous system

The process by which the nervous system functions in response to pain is not fixed and plasticity in the peripheral sites and central nervous system can give rise to a number of features commonly experienced during pain (Latremoliere and Woolf, 2009a). These functional changes are referred to as either peripheral or central sensitization.

The changes that occur in the peripheral nervous system are dependent both on the type of noxious input, the type of tissue receiving the noxious input, and result in an increased responsiveness to nociceptive inputs. Sensitisation of the peripheral nervous system is thought to give rise to primary hyperalgesia, a phenomenon commonly experienced

during pain. Primary hyperalgesia refers to the process by which sensitivity to stimuli that are normally already painful is increased, within the area of injury. When the peripheral nervous system is sensitised, thresholds for nociceptive stimulation decrease and responses to supra-threshold stimuli are increased, with additional ongoing spontaneous neuronal activity (McMahon, 2013). Although the mechanisms behind primary hyperalgesia are likely to vary based on the type of injury and the nociceptors that are sensitised, they are thought to involve the release of inflammatory mediators during injury (McMahon, 2013). The inflammatory mediators released during mechanical stimulation include bradykinin, histamine, serotonin and prostaglandin E1 and are thought to contribute to the lowered thresholds for mechanical stimulation in afferents that are primarily mechanically insensitive (Meyer *et al.*, 1991). For mechanically sensitive Aδ and C afferents, responses to suprathreshold stimuli are enhanced, with spontaneous activity and an increase in the size of peripheral receptive fields of the dorsal horn neurones (McMahon, 2013).

5-HT, as an inflammatory mediator, acts directly on the membrane ion channel protein altering permeability and cell excitability. However, the majority of inflammatory mediators act indirectly. These mediators activate membrane receptors, coupled to G proteins or secondary messengers, leading to the activation of kinases and subsequent phosphorylation of cellular proteins and leading to changes in membrane ion channel proteins (Dray, 1995).

1.2.2 Central sensitisation mechanisms

A number of features of pain, such as secondary hyperalgesia, dynamic tactile allodynia and temporal summation of pain are not explained by

sensitisation of the peripheral nervous system and are thought to be explained by augmentation of processing within the central nervous system (CNS) (Mendell and Wall, 1965; Urban, Zahn and Gebhart, 1999).

Sensitisation of the CNS, and its role in pain processing has been widely accepted for decades. Evidence for central sensitisation was first demonstrated in motor neurons when it was observed that neurons that initially required a nociceptive stimulus in order to become activated, only required a light touch for activation after repeated nociceptive stimulation (Woolf, 1983). After initiation of central sensitisation, neurons in the dorsal horn of the spinal cord exhibit increased spontaneous activity, enlargement of their peripheral receptive fields, a reduction in activation thresholds and increased responses to suprathreshold stimuli (see refs in Latremoliere and Woolf, 2009a).

Sensitisation of the central nervous system results in facilitation of nociceptive transmission, which is thought to lead to an adaptive response of hyperawareness to nociceptive input, in order to protect the body from additional injury (Latremoliere and Woolf, 2009b).

The changes in nociceptive processing underpinning central sensitization give rise to a number of a phenomena experienced during pain. Temporal summation is commonly experienced during chronic pain conditions and refers to the heightened sensitivity to pain that occurs when noxious stimuli are applied repeatedly in a certain time period. Dynamic allodynia is the sensation of pain in response to brushing stimuli that are not normally painful, in contrast to static allodynia, which occurs in response to pressure. Secondary hyperalgesia is another common feature of chronic pain, referring to an increase in sensitivity to nociceptive stimuli in the area surrounding, but not including, the region of injury.

1.3 Opioids

For patients experiencing debilitating levels of pain, opioids are a common method of analgesic treatment, despite rising controversy over the use of these medications (Guy *et al.*, 2017). Endogenous opioids and endocannabinoids in particular, are involved in the descending inhibition of pain (Ossipov, Dussor and Porreca, 2010). This thesis will focus primarily on the influence of opioid receptor system.

Work confirming the existence and location of opioid receptors in nervous tissue began in the 1970s (Pert and Snyder, 1973), with varying distribution and expression within different areas of the body. For pain modulation, the opioid receptors within the nervous system are of primary interest, particularly in the spinal cord and the brain.

1.3.1 Opioid receptors

Four receptors are involved in the binding of opioid compounds throughout the body: the μ, δ, κ, and nociception opioid receptors, belonging to the rhodopsin family of the G_i/G_o protein coupled receptor (GPCR) group. GPCRs have 7 transmembrane domains, connected by 3 intra-cellular and 3 extracellular domains, an extra-cellular N terminal and an intra-cellular C terminal tail (Fig 1.2) (Strader *et al.*, 1994). Signalling of GPCRs is mediated by interaction with G proteins, and opioid receptors interact preferentially with pertussis toxin (PTX) sensitive G proteins.

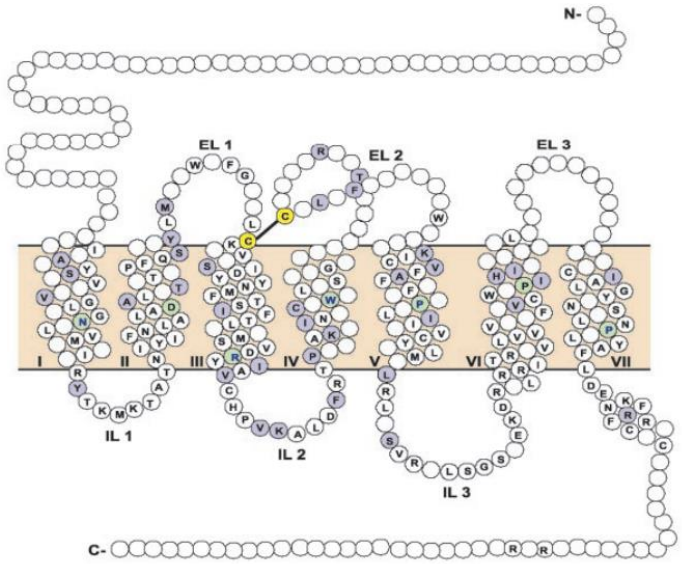

Figure 1.3: GPCR opioid receptor structure showing the intra-cellular and extra-cellular loops and the N and C terminals (Waldhoer, Bartlett and Whistler, 2004a).

On activation of the receptor, subunits α and βγ are released which leads to the inhibition of adenyl cyclase and a decrease voltage gated Ca^{2+} entry resulting in a decrease of presynaptic neurotransmitter release, including neuropeptides from sensory afferent fibres. In parallel an activation of K^{+} channels leads to hyper-polarisation of post synaptic neurons and a decrease in synaptic transmission. Activation of opioid receptors additionally leads to the inhibition of the secondary messenger cyclic adenosine monophosphate (cAMP).

In the CNS opioid receptors modulate both ascending pain transmission and descending modulation of pain and the analgesic effects of opioids are mediated by multiple sites of action. At the level of the spinal cord, opioid receptors are located on the sensory afferent fibres terminating in the superficial laminae (I and II) of the dorsal horn, where the majority of C and A- δ fibres terminate (Faull and Villiger, 1987). μ opioid receptors, the primary receptor involved in opioid analgesia, is located pre-

synaptically on the terminals of primary afferent neurons and post-synaptically on neurons within the dorsal horn (Moriwaki *et al.*, 1996). μ and δ receptor agonists have been shown to have an anti-nociceptive effects in lamina I of the dorsal horn, whereas κ opioids have been shown to exert a greater effect in laminae III-V (Hope, Fleetwood-Walker and Mitchell, 1990).

The PAG and RVM have been shown to be particularly involved in descending inhibition of pain. Early studies demonstrated that microinjection of morphine directly into these regions produced powerful anti-nociception (Yaksh, Yeung and Rudy, 1976; Akaike *et al.*, 1978).

This effect is thought to be mediated by disinhibition of excitatory outputs from the PAG (Lueptow, Fakira and Bobeck, 2018). Activation of the descending pathway normally results in increased inhibitory signalling in the dorsal horn of the spinal cord.

1.3.2 Opioid ligands

Most opioid ligands bind preferentially, but not exclusively, to one opioid receptor. Discrimination of opioid receptors, by ligands, is thought to occur through differences in the extracellular loops, situated above the binding cavity which is located in an inner helical region comprised of the transmembrane domains 3-7. The heterogeneity of these extracellular loops is thought, in part, to lead to opioid peptide binding selectivity (Waldhoer et al, 2004).

The endogenous opioid ligands are cleaved from four precursors: Pro-encephalin, pro-opiomelancortin, pro-dynorphin and pre-pro-N/OFQ (Nakanishi *et al.*, 1979; Comb *et al.*, 1982). Six main endogenous opioid peptides exist: beta-endorphin, endomorphin, Leu-enkephalin, Met-

encephalin, Dynorphin and N/OFQ, each with a different affinity for the opioid receptors (Waldhoer et al, 2004).

The endogenous ligands with highest affinity for μ opioid receptors are β -endorphin and endomorphin, although β-endorphin also displays high affinity for κ and δ opioid receptors. β-endorphin is particularly relevant for pain, as it is cleaved from pro-opiomelancortin and is released into plasma following exposure to painful stimuli (Rasmussen and Farr, 2009). In the peripheral nervous system β-endorphins bind to both pre and post synaptic opioid receptors, although they exert their effects primarily through binding at pre synaptic receptors, through the inhibition of tachykinins, including substance P (Yaksh 1988). Encephalin, an endogenous opioid ligand with some affinity for μ opioid receptors, has also been implicated in pain processing, with evidence of involvement during descending modulatory systems, in on-going pain (Haywood et al, 2018).

1.4 Chronic pain

Chronic pain is defined in the international classification of diseases, version 11 (ICD-11) as pain lasting longer than 3 months (Treede *et al.*, 2015). Chronic pain can originate from several causes; some of these are due to injury or illness but not all sources of pain are easily identified. The prevalence of chronic pain is high, with estimates ranging from 35-51% of the UK population, and severe chronic pain ranging from 10-14% of the population (Fayaz *et al.*, 2016).

The effects of experiencing chronic pain on health-related quality of life (HRQoL) are numerous. Movement in individuals with chronic pain is impaired, levels of physical exercise are decreased and carrying out daily tasks can become difficult. The ability to work is often affected, with approximately 1 in 4 individuals experiencing an impact of chronic pain

on their employment. Additional effects have been seen on relationships, with difficulties in attending social activities (Breivik *et al.*, 2006).

When acute pain transitions to chronic pain, sensitisation is evident in the peripheral and central nervous system, although the mechanisms of this transition are not well understood. The study of chronic pain is complicated by heterogeneous patient populations, co-morbid conditions and the range of chronic pain conditions. The influence of co-morbid conditions on chronic pain is complex and it is difficult to unravel the directionality of any relationships between affect, behaviours and pain. It is likely that pain influences affect and physical activity but also that negative affect impacts on pain, and that a lack of physical activity could impact on pain (Fig 1.3).

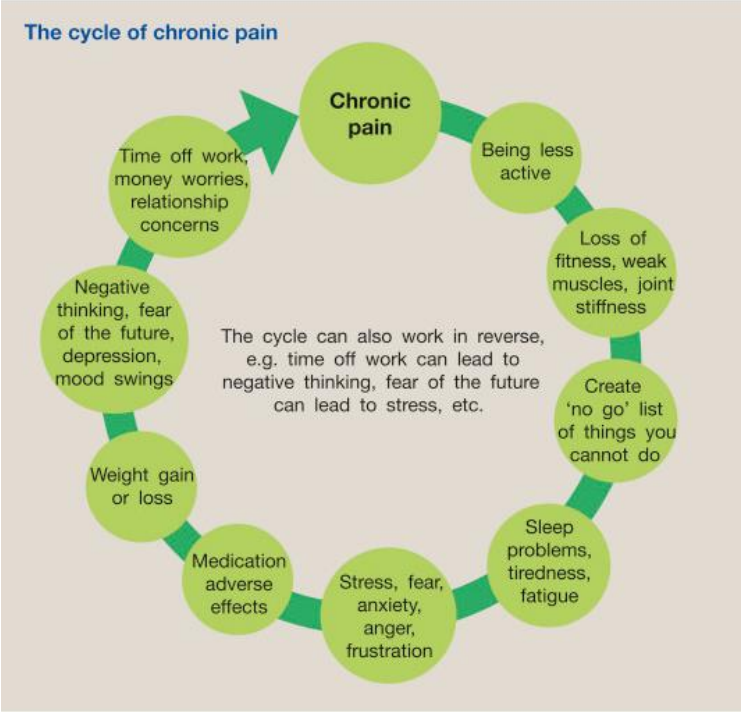

Figure 1.4: The effects of chronic pain on daily functioning. A number of biological and psychosocial factors are involved in the cycle of chronic pain and the direction of causality can be difficult to infer (Blackburn 2018).

1.4.1 Osteoarthritis

Arthritis describes the group of conditions that result in pain and inflammation and stiffness of joints. Osteoarthritis is a chronic condition of the synovial joints and is a leading cause of disability in adults. In comparison, rheumatoid arthritis is an inflammatory auto-immune condition. Osteoarthritis and rheumatoid arthritis are the most common cause for an individual to experience chronic pain, making up 42% of the chronic pain population in Europe (Breivik *et al.*, 2006). This thesis will focus exclusively on osteoarthritis. Up to 80% of individuals suffering with OA experience limitations in movement and around 25% of those will experience serious limitations in carrying out basic tasks on a daily basis (Ma, Chan and Carruthers, 2014).

Osteoarthritis most commonly occurs in the knee joint, and ACR (American College of Rheumatology) guidelines classify an individual as having knee OA if they have pain in the knee and meet a number of criteria from physical examination, radiography or from lab findings: e.g. over 50 years of age, less than 30 minutes of morning stiffness, bony tenderness, radiographic findings such as osteophytes or laboratory findings such as ESR levels or alterations in the synovial fluid (*ACR Diagnostic Guidelines*, 2002).

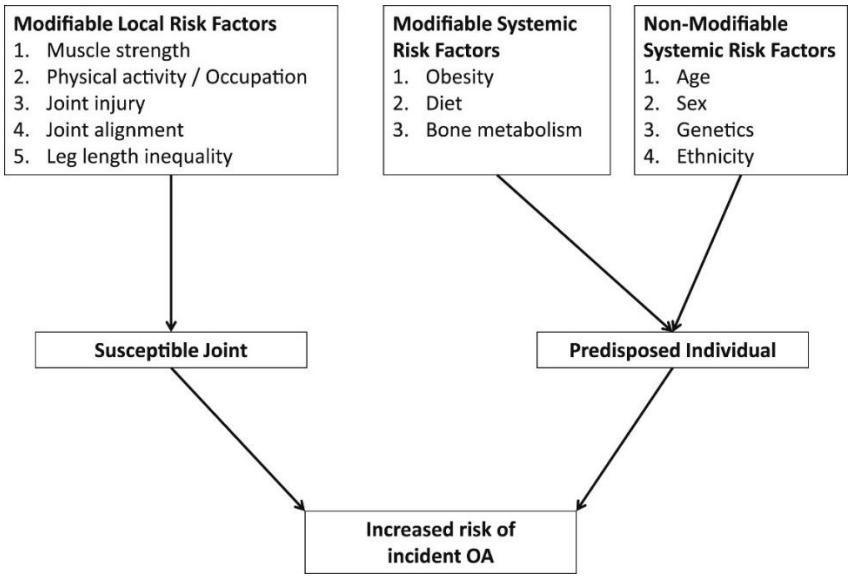

Figure 1.5: Risk factors for the development of OA (Johnson and Hunter, 2014)

Many risk factors predispose an individual to develop OA (Fig 1.5). One of the biggest risk factors for the development of OA is age. Although the exact mechanism behind this relationship is not thoroughly understood, it is thought to be related to cellular senescence, loss of muscle mass during the ageing process and increases in bone turnover (Johnson and Hunter, 2014). Another major risk factor for OA in the hips and knees is obesity, with a strong positive relationship between weight and the risk of developing knee OA. For every 5 unit increase in body mass index, there is a 35% increase in the incidence of knee OA (Jiang *et al.*, 2012). This is not thought to be entirely biomechanical, as this also influences hand OA. Women are more likely to experience OA than men, with epidemiological studies demonstrating that women experience an increase in radiological severity of OA (Srikanth *et al.*, 2005). There are a number of additional risk factors for OA that stem from stresses that the joint undergoes. Repetitive joint use, elite level sport and prolonged standing have been demonstrated to increase the likelihood of OA (Johnson and Hunter, 2014). A number of injuries to the joints predispose an individual to OA, although the pathogenesis of post-

traumatic OA is thought to be different to OA without previous identifiable trauma (Riordan and Little, 2014).

1.4.2 Pathogenesis of OA

1.4.2.1 Cartilage

OA has a complex pathophysiology and affects the whole joint (Fig 1.6). Several pathological changes occur within the joint, although investigation into the changes in articular cartilage, in particular, form the bulk of the research into the pathophysiology of OA.

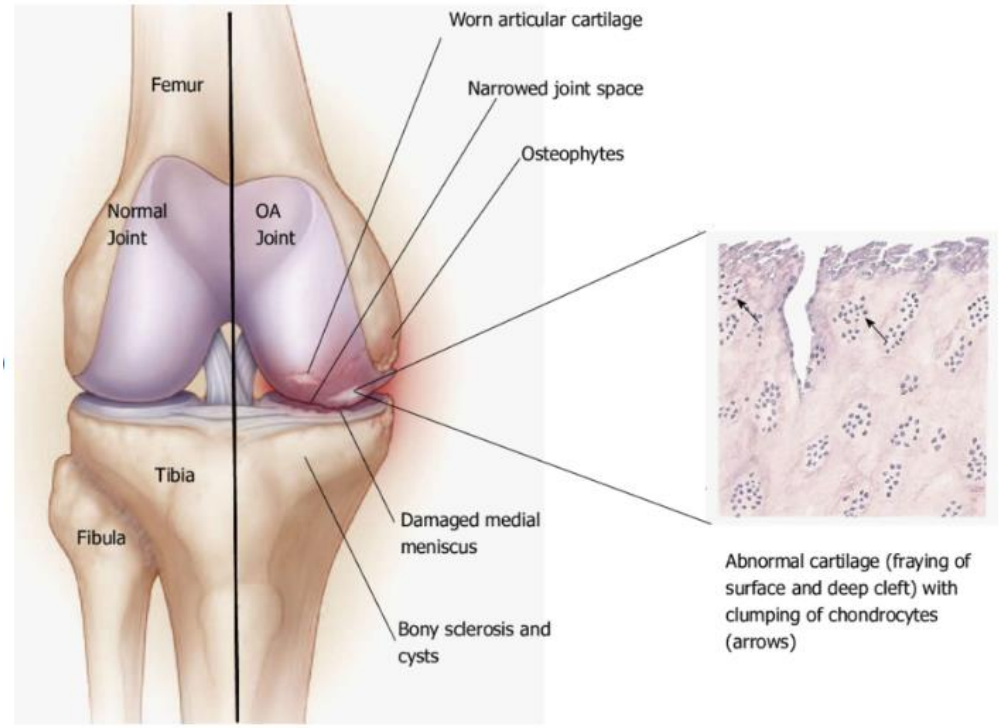

Figure 1.6: Pathophysiology of knee 0A, showing both a healthy joint (left) and a diseased joint (right) with worn cartilage, a narrowed joint space, osteophytes, damaged meniscus and bone changes (Uth, 2014).

Articular cartilage is a flexible connective tissue at the end of the bones. It is aneural and avascular and is formed of chondrocytes which receive nutrients from the synovial fluid (Karuppal, 2017). Articular cartilage allows the joint to move without friction and counteracts compressional forces onto the joint. In the cartilage, chondrocyte-extracellular matrix interactions are altered, resulting in a decrease in the tensile strength of the extra-cellular matrix, as well as a phenotypic shift of the chondrocytes (van der Kraan and van den Berg, 2012). Chondrocytes become activated, and begin to show low levels of proliferative activity, which are not seen in non-OA chondrocytes, resulting in the formation of chondrocyte clusters (Hoshiyama *et al.*, 2015). Eventually, this leads to chondrocyte death, although it is not well understood what effect this has on cartilage degradation (Sandell and Aigner, 2001).

1.4.2.2 Synovium

The majority of OA patients experience inflammation of the synovium (Mathiessen and Conaghan, 2017), which is a connective tissue that lines the joint sealing the synovial cavity within the joint, containing the synovial fluid. The synovium is made up of two layers: the sub intima and the intima. In OA, the synovium undergoes a number of changes, with hyperplasia of the inner lining of the synovium, sub lining fibrosis and stromal vascularization with an influx of macrophages and lymphocytes (See refs in Scanzello and Goldring, 2012). Development of synovitis in OA is associated with worse pain and an increase in joint dysfunction (Hill *et al.*, 2007).

1.4.2.3 The meniscus

The menisci play an important role in the biomechanics of the knee joint, aiding load distribution within the joint as well as shock absorption from impact (Englund, Guermazi and Lohmander, 2009). Meniscal tears are

commonly seen in OA patients, although the directionality and causality of this relationship is unclear (Lange *et al.*, 2007).

1.4.2.4 Subchondral bone

During OA, the subchondral bone undergoes a number of changes, including osteophyte formation, sclerosis and cyst formation (Man and Mologhianu, 2014). Osteophytes refer to bony outgrowths, capped by fibrocartilage and are thought to contribute to pain and loss of function in OA (Man and Mologhianu, 2014). Changes to the subchondral bone can be measured using radiography, although high or low radiographic scores of joint damage do not always correlate well with joint pain experienced (Cubukcu, Sarsan and Alkan, 2012).

1.4.3 OA Pain and treatment

The predominant symptom of knee OA is chronic pain (Hadler, 1992). It has been shown that the relationship between changes in the knee structure and levels of pain experienced are generally weak and some OA patients experience high levels of pain despite relatively low levels of damage to the knee whereas some experience comparatively little pain despite extensive changes to the knee joint (Finan *et al.*, 2013). Treatments for knee OA pain are limited and total knee replacement surgery is often the only effective treatment (Steinhaus, Christ and Cross, 2017). Pharmacological treatments, such NSAIDS and opioids, focus on managing inflammation and pain levels until a joint replacement is required. Improved treatment of OA pain requires better understanding of how changes both within and outside of the damaged knee joint affect the experience of chronic pain and to what extent this pain may be mediated by activity in and changes to the central nervous system.

1.5 Neuroimaging of pain

Neuroimaging encompasses a number of different techniques and methodologies to produce images of either the structure, function or metabolism in the central nervous system. Structural neuroimaging shows contrasts between different tissues in the brain, for example grey and white matter. Functional neuroimaging is concerned with transient biological fluctuations that are linked to how the brain functions; measurement of blood flow, or electrical activity that relate to underlying neuronal activity, for example.

A major benefit of neuroimaging is that it allows for the non-invasive study of the *whole* brain in humans or animals, either anatomically or functionally. It also allows for focus on cortical or subcortical regions within the brain at a higher resolution. Although many different neuroimaging techniques have been used to advance understanding of central nervous system mechanisms underpinning the perception of pain, magnetic resonance imaging (MRI) is the primary method of *anatomical* neuroimaging used in the study of pain. Computerised tomography (CT) is commonly used within medicine, but is less common for pain research. This is largely because MRI does not rely on ionizing radiation to achieve anatomical images and the images acquired with MRI typically have a higher resolution than those obtained with CT and are superior for the imaging of soft tissue (Apkarian, 2015).

MRI studies of structural changes associated with pain have demonstrated volumetric differences in the brain in a number of pain conditions: In painful osteoarthritis (OA), a reduction in grey matter volume was shown in the anterior cingulate cortex, albeit with no reversal by analgesic intervention (Russell *et al.*, 2018). In trigeminal neuralgia, a reduced volume has been observed in a number of affective

regions, including the hippocampus, posterior cingulate, nucleus accumbens and ventral diencephalon (Hayes *et al.*, 2017). Overall however, structural imaging forms a very small part of the pain imaging literature.

1.5.1 Functional MRI

Functional neuroimaging investigates fluctuations in haemodynamic activity over time and these techniques are used to provide information about brain function, usually on a global scale, underpinning nociception and the experience of pain. There are four main functional neuroimaging techniques that are used for the investigation of functional changes in response to pain (See refs in Morton, Sandhu and Jones, 2016). Functional magnetic resonance imaging (MRI) gives an indirect measure of neuronal activity by measuring the blood oxygen level dependent signal (BOLD), electroencephalography (EEG) measures electrical activity from the brain and gives a more direct measure of neuronal activity albeit at the expense of spatial resolution. Magnetoencephalography (MEG) measures the magnetic fields produced by electrical activity in the brain and positron emission tomography (PET) requires the use of radioligands in order to observe metabolic processes. The focus of this thesis is on the use of fMRI in studies of acute and chronic pain.

Functional neuroimaging studies within the pain field have implicated a number of cortical and subcortical regions in pain processing, and have primarily been conducted in humans (See refs in Morton, Sandhu and Jones, 2016). The majority of studies aimed to identify brain regions are involved in pain perception in response to acute nociceptive stimuli (Jones *et al.*, 1991; Apkarian *et al.*, 1992; Bingel *et al.*, 2004; Brooks *et al.*, 2005; La Cesa *et al.*, 2014). Commonly identified brain regions are sensory, limbic and motor areas including: primary sensory cortex (S1);

secondary sensory cortex (S2); anterior cingulate cortex; insular cortex; prefrontal cortex; thalamus and the cerebellum (Tracey and Mantyh, 2007). Beyond the investigation of *which* regions are involved in the processing of pain, there has been a shift to identify *how* these regions contribute to the experience of pain, and which aspect of pain they likely underpin. Given that pain encompasses a number of features, such as the location of pain, the intensity of pain and the unpleasantness of pain, a greater understanding of the role(s) of different brain regions to the pain experience is important.

The primary somatosensory cortex (S1) is a key region of interest in studies of pain, however functional neuroimaging studies of the involvement of S1 in pain have been particularly discordant (Bushnell *et al.*, 1999). Early studies of the primary somatosensory cortex reported significant activation in response to noxious thermal stimuli of the arm (Jones *et al.*, 1991), but also deactivation in response to noxious thermal stimulation of the fingers (Apkarian *et al.*, 1992). S1 is also thought to be the most somatotopically organised region implicated in pain, with organisation resembling that of the tactile input homunculus (Apkarian *et al.*, 2005; Ploner *et al.*, 2017). However, studies of nociception are often complicated by the fact that pain rarely occurs in the absence of other sensations, such as heat or touch, and BOLD activity in S1 and S2 has been shown to be better correlated with perceptions of heat intensity than with pain intensity (Moulton *et al.*, 2012). The discordance of findings between these studies reflects either the complexity of S1 involvement in pain, or the challenging nature of studying S1 involvement in pain.

The anterior cingulate cortex, a region that is regularly implicated in affective aspects of pain, has been associated with the perceived unpleasantness of pain and has shown increases in activity in response to the watching of painful experiences, without receipt of any noxious input

(Rainville *et al.*, 1997; Morrison *et al.*, 2004). These imaging results support findings from electrophysiological studies in rodents that have proposed a role for mirror neurons in the ACC, for emotional processing of pain (Carrillo *et al.*, 2019).

The insular cortex has been heavily implicated in the affective processing of pain and forms a key part of the salience network (SN) alongside the cingulate cortex (Critchley *et al.*, 2007). The insula, like the somatosensory cortex, has been shown to have a relatively fine somatotopic organisation of nociceptive inputs, and it has been suggested that the insula may play a role in the localisation of pain (Brooks *et al.*, 2005).

Increases in BOLD responses have been shown in the PAG during noxious electrical stimulation, when compared to non-painful stimulation (Hahn *et al.*, 2013), as well as during visceral pain (Dunckley *et al.*, 2005). Interestingly, PAG activation has been shown to correlate with pain thresholds and inversely with perceived pain intensity in humans (La Cesa *et al.*, 2014). Although brainstem nuclei can be challenging to image due to size and vulnerability to physiological noise, the brainstem has also been implicated in the processing of pain using fMRI (Napadow, Sclocco and Henderson, 2019).

The regions discussed above, among many others, have been shown to be activated consistently across a wide range of studies and have been accepted as key regions of the brain that are responsible for the conscious perception of pain (Tracey and Mantyh, 2007). The role that these regions play in pain is complex, further highlighting the complex and distributed contribution of the brain in pain processing.

1.5.2 Neuroimaging functional connectivity

The study of regional activation in response to pain has been largely successful, with imaging studies providing functional confirmation of previous pharmacological results. However, in recent years there has been a shift to study the brain on a more global scale, given that the brain contains in the order of 10^{10} million neurons that are organised into complex networks (Hagmann *et al.*, 2008). Understanding of how these networks function in a healthy brain, how they are altered in certain conditions or disease states, and what this means for both the understanding and treatment of disorders, is not well understood.

The connectome is a structural framework that describes connections, both structural and functional across the entire brain, as a network (Griffa *et al.*, 2013). Connectomics refers to the study of this network activity, aiming to ultimately provide complete coverage of the connections in the central nervous system. The study of connectomics aims to uncover how the principles of connectivity support network function. In pain, connectomics focuses on how regions implicated in pain processing interact in networks and how brain network interactions underlie the complexity of the perception of pain, including sensory, emotional and cognitive fluctuations and the dynamics of these fluctuations (Kucyi and Davis, 2017). Studies of the connectome are recent, with the first full human brain connectome created in 2008 by Hagmaan using diffusion MRI in order to map structural fibre trajectories in the brain, through the diffusion of water molecules (fig 1.7).

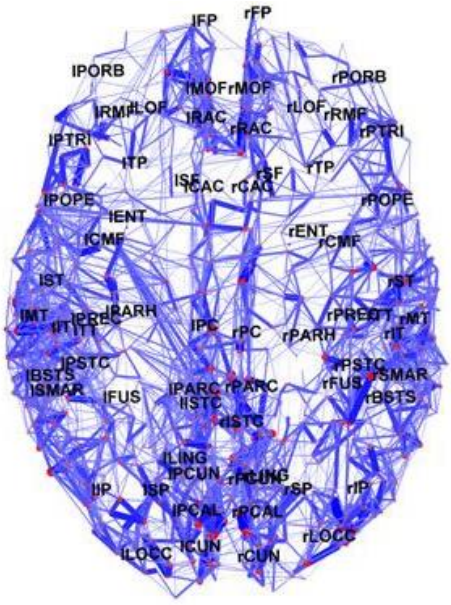

Figure 1.7: The first human connectome map, visually displaying structural connections between regions of interest in the brain, identified using diffusion imaging (Hagmann *et al.*, 2008).

1.2.3 Preclinical neuroimaging

Although the number of studies employing fMRI to investigate functional changes in the brain has increased over the last few decades, fMRI has mainly been used to study human participants.

The majority of animal fMRI pain studies have been conducted in rodents, primarily in rats. In rodents, much as in humans, the bulk of fMRI studies have focused on supraspinal responses to a range of acute nociceptive stimuli, for example injections of noxious substances such as formalin, or following electrical or mechanical stimuli (Zhao *et al.*, 2012). The use of acute stimuli allows for good temporal control of nociceptive inputs and mapping to BOLD responses. As in humans, the most common aim of these studies is to map the brain regions involved in nociceptive processing in order to better understand the mechanisms

behind processing of nociception in the brain. Activation is typically spread over the previously mentioned set of regions, such as the cingulate, somatosensory regions, insula, the PAG and the thalamus. However, as these regions are not considered to be pain specific, the relative importance of each of these regions to the pain experience is debated in the literature (Iannetti and Mouraux, 2010). In addition, rodent neuroimaging faces additional confounds from the anaesthesia that is commonly used to preserve welfare and reduce motion (Da Silva and Seminowicz, 2019). Anaesthesia is discussed in more detail in chapter 3, and functional connectivity in pain is discussed in chapter 4.

1.6 Hypothesis

In this thesis, I hypothesise that anxiety is associated with exacerbated joint pain, and that this is accompanied by changes in the brain. Animal models of OA pain are associated with changes in functional connectivity in the brain and I hypothesis that anxiety is associated with higher OA pain levels, accompanying changes in functional connectivity via changes in endogenous opioid receptor tone.

1.6.1 Aim:

To use fMRI and behavioural methods in the monosodium iodoacetate (MIA) model of OA pain in rats to investigate the contribution of anxiety and opioid receptor tone to OA pain.

1.6.2 Objectives

1) To validate methods for measuring alterations in spontaneous fluctuations in the BOLD signal using resting-state fMRI in the rat.

2) To compare resting-state differences in the MIA model of OA in Wistar rats and Wistar-Kyoto rats, an inbred genetic strain which has a high anxiety behavioural phenotype.

3) To investigate the potential contributions of alterations in opioid receptors and endogenous opioid tone in WKY rats and if this impacts upon the manifestation of pain behaviour in the model of OA.

Chapter 2 General Methods

All experiments using animals conformed to the regulations set out by the UK Home Office in accordance with the Animal (Scientific Procedures) Act 1986. Experiments were conducted under project licenses 40/3647 and PB3DA999F. All experiments were conducted in adult male rats. Male rats were chosen to provide consistency with data previously collected in the field, in order to minimise additional experimental confounds. Rats were housed in open top cages in groups of 4 with access to food and water ad libitum. A tunnel, nesting and a wooden chew were provided to each cage for environmental enrichment. The rats were weight matched at the start of study. Wistar and Sprague Dawley rats were provided by Charles River, UK and WKY rats were provided by Envigo, UK. Number of animals used are reported separately in each results chapter.

2.1 Models:

The studies in this thesis used two preclinical models: a model of osteoarthritis pain and a model of endogenous anxiety, in order to model the influence of anxiety on osteoarthritis pain. Full details of the background of these models are provided in chapter 4.

2.1.1 Induction of the MIA model

In these studies, a single injection of 1mg of MIA was used to induce the model of OA. MIA (1mg/50µl; Sigma, UK; vehicle: saline) or saline; for control rats (50µl) was administered into the left knee through the infra-patellar ligament, using a 0.5ml insulin syringe. All intra-articular

injections were given under general anaesthesia (isoflurane 2.5% in 1L/min oxygen).

To induce anaesthesia, the rat was placed into a Perspex chamber into which 3% isoflurane in 1l/min oxygen was delivered. When the rat was fully anaesthetised, as assessed by loss of its righting reflex, the animal was placed in a supine position onto a heated mat, with the nose placed into a cone attached to the anaesthetic delivery system, which provided continued anaesthesia during the injection process. The rat's hind legs were shaven and both knee diameters were recorded with electronic callipers. The level of anaesthesia was assessed again to ensure that the rat was areflexic, by giving a toe pinch on the hind paw, and the ipsilateral leg was disinfected with a mixture of chlorhexidine and water. The experimenter's hands were disinfected, and the leg was gently extended with the knee joint bent to 90° or until the intra-articular space, below in the infrapatellar ligament was clearly located. The needle of the insulin syringe was placed through the infra-patellar ligament into the intra-articular space and the syringe was depressed, releasing 50µl of MIA or saline into the knee joint. The rat was then weighed, to provide a baseline for future health checks and was placed into a recovery cage, which was placed on a heated mat, until conscious. Rats were identified using numbers written onto the tail with permanent marker.

Post injection, rats were health checked and returned to their home cages after recovery. Health was monitored daily for 5 days and then weekly. The experimenter was blinded to the treatment given to each rat.

2.1.2 Behavioural assessment of pain

All animals were handled prior to habituation and then habituated twice prior to baseline behavioural measurements. Habituation consisted of allowing the rats to explore the weight bearing box and the von Frey

cages, as well as acquainting them with the positioning of the paws in the weight bearing box and the application of the von Frey hairs in the von Frey cages.

2.1.2.1 Weight bearing

Weight bearing is a commonly used measure of disease progression in the MIA model of OA, as well as of the efficacy of treatments (Bove *et al.*, 2003). These studies use a static weight bearing approach in order to test the distribution of weight across the hind paws, using an incapacitance tester (Linton Instrumentation, UK). The incapacitance tester (Fig 2.1 A) was calibrated prior to use using a 50g brass weight.

The incapacitance tester was then set to collect the average weight placed on each hind paw, giving a measure of joint pain, over a 3 second period. Typically, rats bear less weight on an injured limb, generating a degree of weight bearing asymmetry.

During testing, the rat was placed into a Perspex chamber with a slanted front placed onto the incapacitance tester (Fig 2.1 A), with hind paws placed onto two weighing scales and the tail resting through a cut out in the centre of the back of the Perspex box. This ensured even positioning and excluded the tail from weight measurements. Weight measurements were taken when the rat's forepaws were placed onto the slanted front of the Perspex box, with one hind paw placed on each of the scales. Measurements were only recorded during trials in which the rat remained still, central and upright.

Testing of weight bearing asymmetry occurred in the same room as testing of paw withdrawal thresholds. All rats received two habituation sessions prior to testing in order to minimise both stress, and thereby

stress induced analgesia, as well as exploratory movement. Full details on testing schedules in provided in the relevant results chapter.

2.1.2.2 Evoked pain behaviour: von Frey

Von Frey hairs are calibrated nylon filaments used to determine thresholds for mechano-sensitivity (Fig 2.1B) (Deuis, Dvorakova and Vetter, 2017). The hairs have different thicknesses which alter the discrete force applied when pressed against the glaborous surface of the hind paw. As the MIA model is induced in the knee and von Frey hairs are applied to the paw, withdrawal responses to von Frey stimulation reflect referred pain. In these experiments the up-down approach described by Dixon and refined by Chaplin was used (Dixon, 1980; Chaplan *et al.*, 1994). A hair was applied to the surface of the hind paw and if fewer than 2 applications elicited a withdrawal response, the hair with the next highest force was applied to the paw. If 2/3 applications induced a withdrawal response, the next lowest hair was applied to the paw until no withdrawal response was elicited. The von Frey hairs used in these experiments ranged from 2g to a maximum of 26g in force.

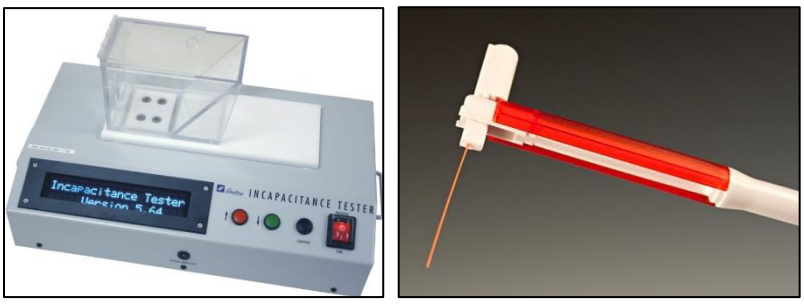

Figure 2.1 A) Incapacitance tester with Perspex box for assessing weight bearing asymmetry; B) von Frey hair with handle and filament for assessing mechanical sensitivity

2.1.3 Quantifying changes to the joint after MIA injection

On the final day of the MIA model (21 or 28 days), after the rats were humanely killed in accordance with schedule 1 of the Animal (Scientific Procedures) Act 1986, knee joints were dissected from the rats, by cutting through the mid femur and mid tibia, and stored in 4% paraformaldehyde (PFA). Prior to quantifying joint changes, the knee joints were manually disarticulated. Excess muscle tissue was removed from around the joint, using scissors, and a scalpel was used to cut the ligaments surrounding the joint. The knee joint was gently twisted, a cut was made through the meniscus and the joint was gently pulled apart exposing the articular surfaces.

Cartilage lesions were subsequently scored using the macroscopic methods of Guingamp (Guingamp *et al.*, 1997). Scores were separated into different regions on the articular surface: the medial and lateral femoral condyles, the medial and lateral tibial plateaus, the patella and the femoral groove. The cumulative total was then taken as the indicator of total joint damage (Table 1).

Score	Appearance
0	Normal appearance
1	Slight yellowish discoloration
2	Little cartilage erosions in load-bearing areas

3	Large erosions extending down to the subchondral bone
4	Large erosions with large areas of subchondral bone exposure

Table 1: Joint damage scores from Guingamp et al (1997) used in macroscopic assessments of joint damage.

2.1.4 Model of Anxiety: Wistar-Kyoto Rat Strain

The Wistar-Kyoto rat strain was chosen to model anxiety vulnerability in these studies (McAuley *et al.*, 2009). The use of a genetic model of anxiety was selected to provide a model of endogenous anxiety (Detailed explanation provided in chapter 3).

2.1.5 Behavioural testing of anxiety

2.1.5.1 Elevated Plus Maze

The elevated plus maze is used to test anxiety-related behaviour in rodents. The maze is raised from the ground and has four arms: two of these arms have high sides and are enclosed at the end; two of the arms have no sides and are open at the end (Fig 2.2). In these experiments the rats were placed in the centre of the maze, nose facing into an open arm and the rat was allowed to explore for a period of 10 minutes.

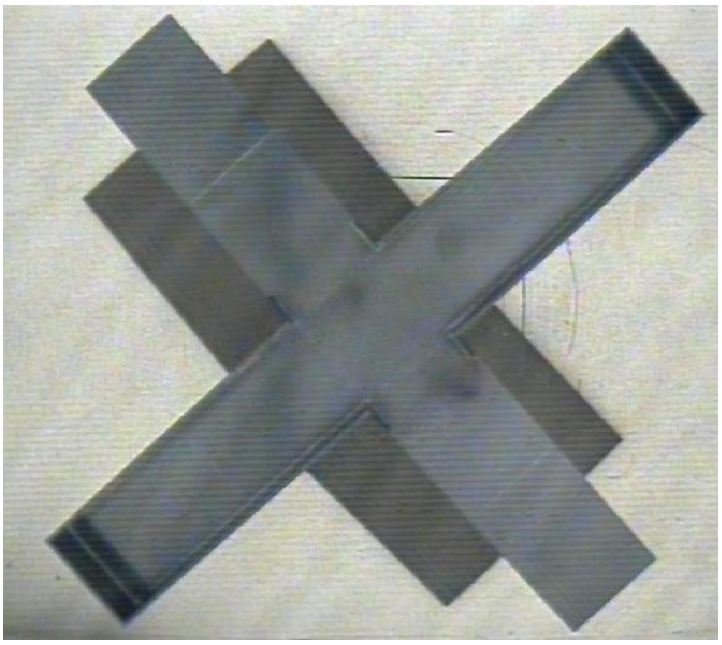

Figure 2.2: Screenshot of the elevated plus maze with open arms (top left and bottom right) and closed arms (top right and bottom left) and foam padding underneath for safety.

Monitoring of the rat was conducted through the use of a ceiling mounted camera and the rat was tracked using the Ethovision XT software (Noldus, Wageningen). For analysis purposes the maze was further divided into segments: the arms are subdivided into the inner open/closed and the outer open/closed arms. The inner open/closed arm is the portion of the arm that is located adjacent to the centre of the maze. Exploration in the closed arms of the maze was taken as an indicator of anxious behaviour whereas exploration in the open arms of the maze was taken as an indicator of lower levels of anxiety. A number of parameters are recorded by the software whilst the rat is in the maze.

- Distance: The distance that the rat travels in the maze as a whole, as well as each segment of the maze is measured in cm.
- Latency: The latency to enter each segment of the maze is measured in s.

- Speed: The speed of travel in the maze and in each segment of the maze is measured
- Time: The time spent in the maze and in each segment of the maze is measured.

The rat is tracked from both the nose point and from the centre point. In these experiments the centre point of the rat has been used for analyses to avoid any inaccuracy in tracking in situations in which the nose point of the rat meets the tail.

2.1.6 Locomotor testing

2.1.6.1 Open field

A custom made opaque cylindrical arena (90cm diameter) was used to test locomotion in the rats. The rats were placed into the centre of the arena and activity was monitored for a period of 10 minutes. As described for the elevated plus maze, all activity was monitored using Ethovision software and the aforementioned parameters were measured. The open field was subdivided into the centre of the arena and the periphery, allowing for an additional investigation of anxiety, with time spent at the periphery taken as a measure of anxious behaviour.

2.1.7 Statistical analyses of behavioural data

All behavioural data were analysed with GraphPad Prism 7 (GraphPad Software, California) using parametric statistics when appropriate, as determined by the presence of a normal distribution, using the D'Agonstino and Pearson test.

Analyses between strains (Wistar and WKY) and treatments (saline and MIA) at different time points/doses were wherever possible, analysed with a two-way ANOVA with Tukey's multiple comparisons, as recommended by GraphPad. Although many measurements were repeated, RM ANOVAs were not able to be used due to missing behavioural data points. For welfare reasons, on days where rats experienced problems with weight bearing on the ipsilateral limb, weight bearing measurements and PWTs were not taken.

Comparisons between two groups were conducted using t-tests (Wistar vs WKY) or non-parametric equivalents.

2.2 MRI

Full details of MR sequences are provided in the relevant results chapter.

2.2.1 Physiological monitoring

Physiological monitoring was, excluding blood pressure, conducted using an MRI compatible monitoring and gating system (Small Animal Instruments Inc.; New York). Physical parameters measured include: Blood pressure (MmHg), heart rate (beats per minute (bpm)), oxygen saturation (% O_2), respiratory rate (breaths per minute) and temperature (° Celsius).

2.2.2 Surgery

All surgeries were conducted under isoflurane anaesthesia. The rats were induced at 4% isoflurane in 1l/min oxygen until loss of the righting reflex was observed. The rats were then removed from the induction chamber and placed in a supine position onto a warming mat with a nose cone providing continued anaesthesia.

2.2.2.1 Tail artery/vein cannulation

The tail was chosen as a cannulation site in order to allow for a smaller incision site, reducing the risk of bleeding and body temperature reduction during scanning, as observed during previous experiments. After confirming that the rat was areflexic, using a toe pinch, an incision was made, through the tail skin using a pair of small surgical scissors. A pair of blunt forceps scored down the side of the vessel, through the connective tissue and the vessel was dissected away and isolated. A pair of forceps were placed under the vessel to lift it from the connective tissue and to provide tension. A small amount of 0.5% lidocaine was applied to the vessel to ensure that the vessel did not lose moisture or elasticity while providing some local analgesia at the surgical site. Two pieces of cotton thread were passed under the vessel, with a loose knot tied at the portion of the vessel closest to the animal and a tight knot at the portion of the vessel closest to the end of the tail. Using a microscope, a hole was made into the top of the vessel using a 25 gauge needle.

A custom tool, created in the department, entered the previously made hole lifting the top of the vessel in order for easier insertion of the cannula. This tool consisted of a piece of wire bent at 90°, fixed into an insulin syringe holder. The cannula was then inserted into the hole and, where possible, was inserted several centimetres into the vessel. When the cannula was satisfactorily placed, the upper knot was tied around both the vessel and the cannula and the lower knot was again tied around the cannula to ensure that it was securely placed. The arterial cannula was attached to a syringe containing heparinised saline (50%) and the venous cannula was attached to a syringe containing 0.1mg/ml medetomidine in 0.9% saline.

2.2.3 Anaesthetic regime

The anaesthetic regime used in these experiments is described fully in chapter 3.

2.2.4 MRI: Data collection

All data were collected on a 30cm bore Bruker Biospec 7T scanner using a Bruker Avance III console (Bruker BioSpin, Ettlingen) and a 2x2 rat brain, surface, receive only, array coil with Paravision V (Bruker BioSpin, Ettlingen).

2.2.5 MRI: analysis

2.2.5.1 File conversion

Raw Bruker ParaVision data files are not ready for use within standard analysis software. The Bru2Nii converter (neurolab, USC) was used in order to convert all Bruker ParaVision files into the NIFTI file format. In addition to converting the file type, the Bru2Nii converter additionally multiplied the size of the image by 10, in order to increase the size of the rat brain to a size that is more comparable to that of a human brain. This allows conventional fMRI software to be used for analysis for the much smaller rat brain (Fig 2.3).

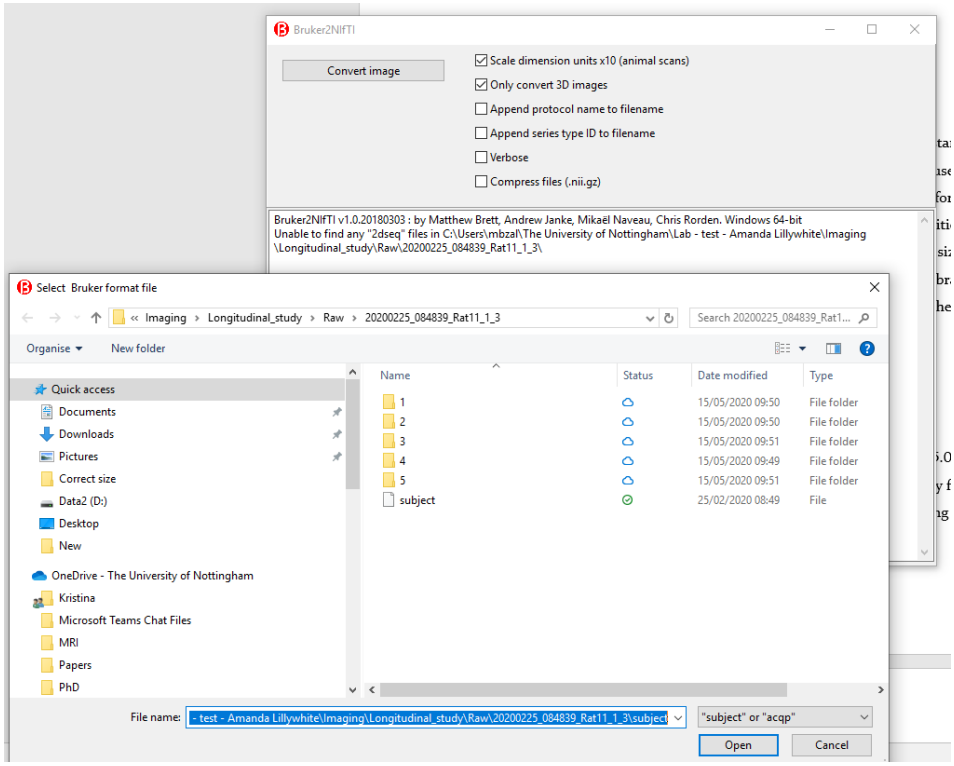

Figure 2.3: File conversion from Bruker ParaVision 5 to Nifti file format using the bru2nii converter. Subject files were used to convert relevant images, and image dimensions were scaled x 10.

2.2.5.2 Pre-processing

The majority of pre-processing was conducted in FSL version 5.0.1 (fMRIB, Oxford). Where standard processes designed primarily for human brains were not suitable for the rat brain, pre-processing was conducted manually in ITK-SNAP (Figure 2.4, www.itksnap.org, Yushkevich et al., 2006).

2.2.5.2.1 Motion correction

Motion can occur during scanning and causes problems for analysis of fMRI data, inducing artefacts or false positive results. It is therefore important to correct for this motion, where possible. In these studies,

motion correction was conducted in FSL with MCFLIRT (Jenkinson *et al.*, 2002) which is an automated tool for affine intra and inter-modal brain image registration. It uses the middle volume of an image as an initial template and a coarse 8mm search is conducted to look for motion parameters, followed by two searches at 4mm each using trilinear interpolation.

2.2.5.2.2 Spatial smoothing

Spatial smoothing increases the signal to noise ratio and gives the data a more Gaussian distribution, at the expense of some spatial resolution. Spatial smoothing was conducted in FSL with the application of a kernel, which averages a portion of the signal from neighbouring voxels together. Data was spatial smoothed using FSL at the individual ICA stage 1 mm full width half maximum (FWHM) based on the literature.

2.2.5.2.3 Slice timing correction

The data was collected in an interleaved formation, therefore interleaved slice timing correction was conducted at the individual ICA stage using MELODIC.

2.2.5.2.4 Masking of non-brain tissue

Removal of non-brain tissue from both functional EPI and anatomical t2 weighted images was conducted using a manually created masks in ITK-SNAP that were applied using FSLmaths (Fig 2.4).

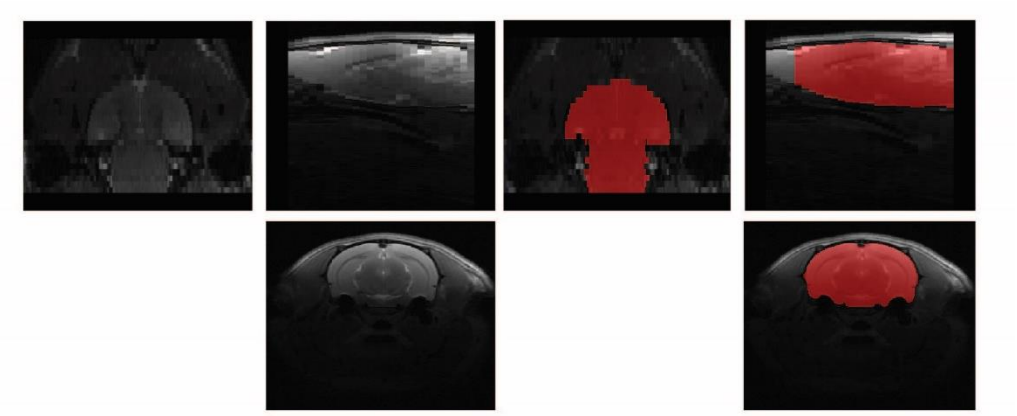

Figure 2.4: A single subject T2 weighted anatomical image (left) with a mask created manually in ITKSNAP (right), covering the brain but excluding the olfactory bulb.

2.2.5.2.5 Registration

Registration was conducted in FSL using FLIRT linear registration. The functional EPI images were registered to their respective anatomical images using a rigid body 6 parameter model. Brain extracted T_2-weighted anatomical images were first registered to a brain extracted template using a full search, affine, 12 parameter model. The registrations were manually inspected for quality at each stage using FSLeyes.

2.2.6 Resting state functional connectivity analysis

Resting state fMRI is concerned with low frequency fluctuations of less than 0.1Hz in the BOLD signal, which occur spontaneously when the brain is at rest (Biswal *et al.*, 1995).

The term 'at rest' can refer to a number of different states, with subtle differences, that primarily involve a task/stimulation/attention free environment. In humans, typically the distinction is between eyes open and eyes closed, with or without visual fixation (Snyder and Raichle, 2013). In preclinical research the distinction occurs between anaesthetised and non-anaesthetised animals (Paasonen *et al.*, 2018).

These experiments all occur under general anaesthesia of 0.1 mg/kg/hr medetomidine combined with 0.5% isoflurane delivered in oxygen at 1l/min.

The purpose of RS-fMRI is to look at networks that occur in this resting state. A number of these reproducible networks have been identified; the most commonly studied of which is the default mode network (DMN), first identified by Raichle et al (Raichle *et al.*, 2001; Snyder and Raichle, 2013). This network consists of a number of regions that are more active during a restful state, and less active during an attentional state. The DMN is particularly relevant to studies of a number of clinical conditions as it is commonly found to show differences in these clinical populations. The discovery of these networks and the differences that occur within them functionally is highly relevant and aids the understanding of how conditions can alter how the brain functions as well as whether treatments may reverse this functional differences.

It is also important to consider not just what happens within these functional networks but also how they might be functionally linked to other regions associated with pain.

There are a number of ways to investigate resting state networks, including seed based connectivity, independent component analysis and graph network analysis. In these studies, independent component analysis using MELODIC (multivariate exploratory linear optimized decomposition into independent components) in the FSL package has been used for initial exploratory analyses, followed by seed based functional connectivity based on a priori regions of interest from the affective/pain literature.

2.2.7 Independent component analysis (ICA)

Independent component analyses (ICA) were conducted for resting state datasets. ICA decomposes 4D fMRI data sets into a number of time courses and associated spatial maps (Beckmann *et al.*, 1995). A 4D fMRI data set refers to a volume (typically the whole brain) made up of a number of cross sectional images collected over a short period of time. These volumes are collected repeatedly for a period of time, in order to show temporal fluctuations in the BOLD signal. It is an exploratory and model free approach.

2.2.7.1 Individual ICA

In these studies, individual ICA maps were generated using MELODIC in FSL. ICA maps were created with an unspecified number of components, with the number of components given individually for each data set by MELODIC.

Pre-processing was conducted as part of the individual ICA analysis in MELODIC, FSL, as previously discussed, with motion correction, spatial smoothing, slice timing correction and registration happening automatically as part of MELODIC.

The resting state datasets were then individually, manually denoised by assessing each of the independent components identified by MELODIC using the methods used by Griffanti et al (Griffanti *et al.*, 2017). These components were assessed based on their spatial map, the time course of the data and the power spectrum. In these studies, a liberal approach was taken and any components that were not clearly identified as noise were kept in, to minimise any loss of valid signal as recommended by Griffanti (Griffanti *et al.*, 2017).

Spatial features: Spatial maps should contain fewer and larger clusters (as shown in Fig 2.5). In contrast, ringing around the outside of the brain is related to motion artefact and signal in the CSF is related to physiological noise (Griffanti *et al.*, 2017).

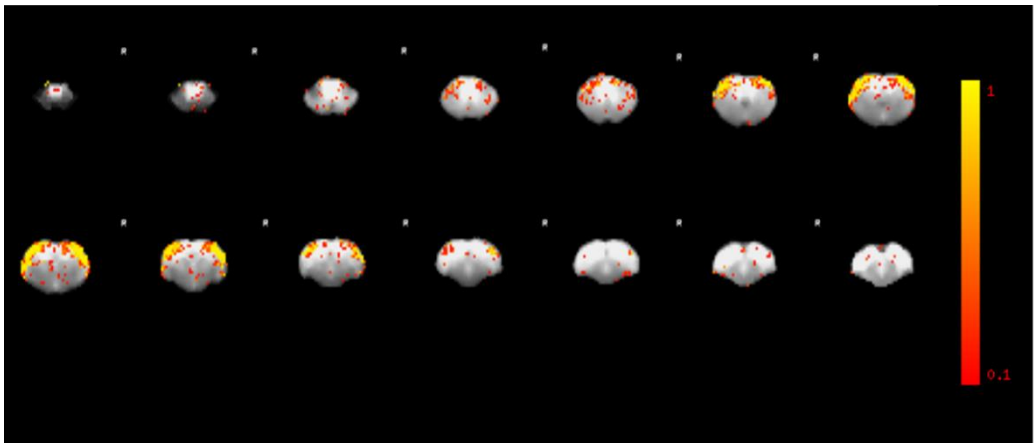

Figure 2.5: Individual ICA component (from one rat), assessed during the denoising process. This component was retained due to the large bilateral clusters that were present, consistently, in several slices of the volume, averaged over the total acquisition period (300 volumes, 6 minutes).

Temporally, there should be no significant trends, very high frequency patterns, or jumps in the time series. A smooth, fluctuating time course was taken as an indicator of a BOLD timecourse (as shown in Fig 2.6) (Griffanti *et al.*, 2017).

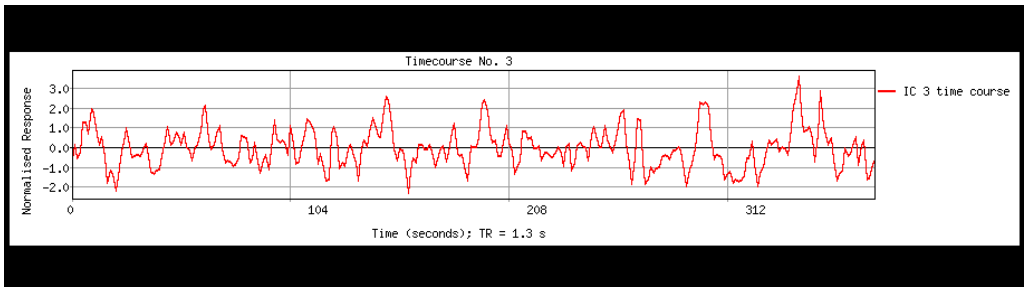

Figure 2.6: Example of an optimal time course from the above component. No jumps in the time course were seen and the time course did not have any high frequency fluctuations.

An optimal component should have power concentrated at the lower end of the power spectrum with the majority of the power centered in the lower half of the power spectrum, preferably with an early spike below 5Hz and vastly reduced power thereafter (as shown in Fig 2.7) (Griffanti *et al.*, 2017).

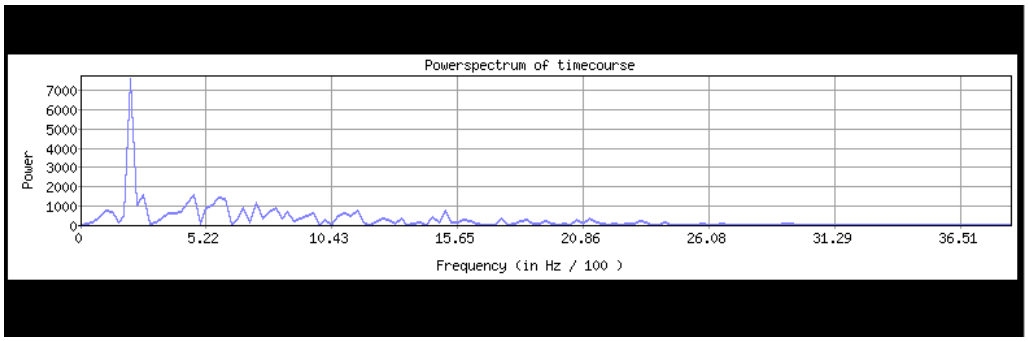

Figure 2.7: Example power spectrum from a good component. The power is predominantly at the lower frequency end of the spectrum.

2.2.7.2 Group ICA

After manual denoising of the individual ICA maps, the denoised images were used for the group ICA analysis.

2.2.8 Seed based functional connectivity analysis

Seed based functional connectivity is a hypothesis driven approach, which looks for a correlation in the fMRI time series between seed regions and the time series of other regions in the brain (Fig 2.8). Seed regions can either be specified a priori, using knowledge from the literature to inform choices about which regions are likely useful to test or they can be selected from a task dependent fMRI experiment. The time course from the seed region is compared to the time series of all other voxels, resulting in a map of which regions are temporally correlated with the seed region.

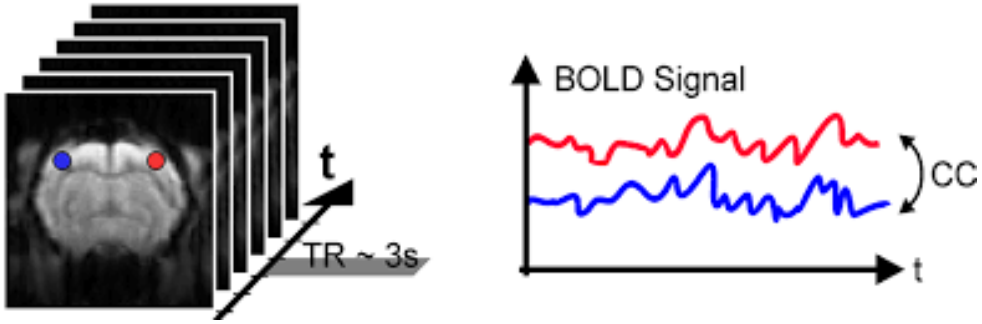

Figure 2.8 Schematic detailing the seed based functional connectivity. The timecourse of the seed region (blue) correlated with the time series of the region in red and therefore these two regions are said to functionally connected (Daniel Kalthoff and Matthias Hoen, no date).

2.2.8.1 Construction of a seed region mask

All masks for seed regions were created using FSL, with the fslmaths command. Masks were created in standard space and the registered to each individual rat's RS fMRI space to ensure consistency. The time courses for each region of interest were then extracted using the fslmaths command and used as a regressor in FEAT. Placement of each seed mask was confirmed in each animal's functional image. Seed regions are shown in Chapter 4.

2.2.9 Post analysis Statistics

Statistical thresholding in images was conducted using FEAT, with a Z value set at 2.3 and a corrected cluster significance of $p< 0.05$. This Z value is standard in the field, albeit at the less conservative end of the spectrum. A lower threshold was chosen due to the small sample sizes used in the imaging study and the novelty of the data collected. Sample sizes were calculated based on studies with markedly different methodologies and it was felt important to minimise risk of false positives in these early stages. This cluster thresholding is based on Gaussian Random Field (GRF) theory.

2.3 ECoG

2.3.1 Background

Electrocorticography (ECoG) is a neurophysiological technique that records electrical signals directly from surface of the cerebral cortex. By recording intra-cranially, signal distortions from the skull and from intermediate tissues such as the scalp are avoided (Buzsáki, Anastassiou and Koch, 2012).

ECoG measures the local field potential (LFP), which is made up of electrical activity from a number of different sources. Contributions to the LFP can arise from any excitable membrane, for examples spines, dendrites or axons and from transmembrane current (Buzsáki, Anastassiou and Koch, 2012). ECoG measures the LFP signal primarily from the superficial layers of the cortical surface (Buzsáki et al., 2012).

In these experiments, electrodes were placed onto the surface of the dura, through holes placed in the skull. In order to measure signal from the surface of the brain, a craniotomy must be performed, making this an invasive procedure.

2.3.2 Single electrode ECoG over the somatosensory cortex

2.3.2.1 Surgery

The surgeries were conducted under isoflurane anaesthesia. The rats were induced at 3% isoflurane delivered in 1l/min oxygen, which was reduced to 2 ½ - 2% isoflurane for the duration of the surgery.

2.3.2.2 Tail artery/vein cannulation

Tail artery and vein cannulations were conducted as previously described (page 52).

2.3.2.3 Craniotomy

A craniotomy was performed and one small hole was drilled above the hind-limb somatosensory cortex (AP = -1.5mm, ML = 2.0mm) and a reference electrode was placed frontally (AP = 5mm, ML = 2mm. Loop tipped twisted silver wire electrodes were placed under the surface of the skull for EEG recording (Fig 2.9).

Figure 2.9: Loop tipped silver wire electrode

2.3.2.4 Data recording

The electrodes were mounted onto a NeuroLog head-stage (NL100AK; Digitimer, Welwyn Garden City, UK) and signals were acquired using a microCED1401 data acquisition unit (Cambridge Electronic Design, Cambridge). Signals were amplified x2000, band-pass filtered between 0.5-100Hz and recorder at 2 kHz using Spike2 software (Fig 2.10, Cambridge Electronic Design, Cambridge UK).

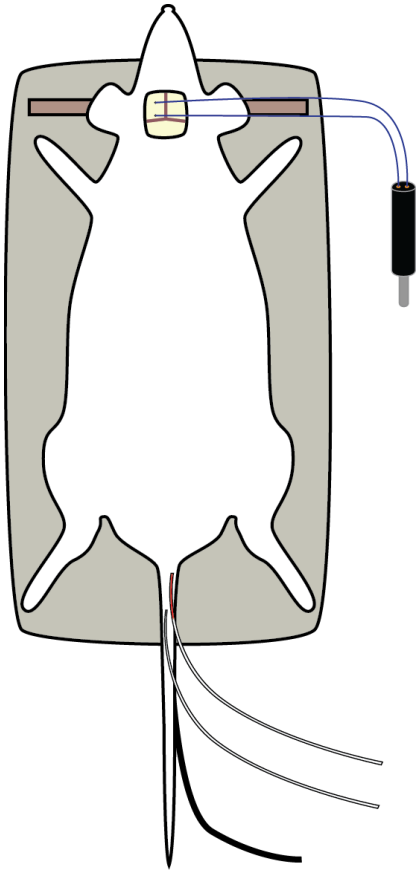

Figure 2.10: Diagram of the ECoG set up, showing both the s1 and reference electrode as well as the tail cannulae.

2.3.3 12 Channel ECoG

A 12 channel electrode was built in house and was used to conduct these experiments (Fig 2.11). A Connect HST/8o50 adaptor was used to

connect the 16 channel head stage (HSt/16o25-18p-xR; 1x gain; Plexon, USA) via a custom flexible connector (Omnetics, USA). The electrodes were formed by exposing the ends of 12 28 AWG, flexible multiple strand tinned copper wires, coated with silicone (BNTECHGO, Los Angeles) and soldering them to the adaptor. A gold pin was inserted into the adaptor for the purpose of attaching a reference and grounding cable, which was attached to the scalp of the animal via a bulldog clip.

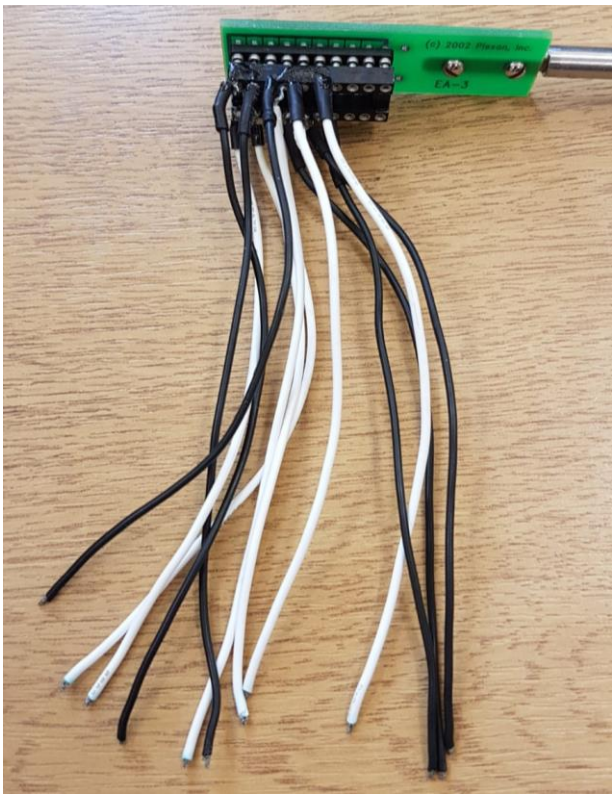

Figure 2.11: 12 Channel electrode set up with 12 individual wires with ends exposed for recording.

2.3.3.1 Data recording

The electrodes were attached to a head stage (HST, 16O25-18P-xR 1x gain; Plexon, Dallas), using a flexible connector, connected to the PBX preamplifier (Plexon, Dallas) and transferred to the multichannel

acquisition processor (Plexon, Dallas), which analysed the signals. LFP data were then exported to MATLAB using Neuroexplorer 4 (Plexon, Dallas), where data were analysed using a custom made script from the lab, primarily written by Charles Greenspon.

2.3.3.2 Surgery

All surgeries were conducted under isoflurane anaesthesia. The rats were induced at 4% isoflurane in 1l/min oxygen until loss of the righting reflex was observed. The rats were then removed from the induction chamber and placed in a supine position onto a warming mat with a nose cone providing continued anaesthesia.

2.3.3.4 Tail artery/vein cannulation

Tail artery and vein cannulations were conducted as previously described (page 52).

2.3.3.5 Craniotomy

12 holes were made in the skull, in a pre-defined set of co-ordinates adapted from Xia et al, 2012 (Xia *et al.*, 2016). Marks were first made onto the skull using a permanent marker secured into a stereotaxic arm (Fig 2.12).

The co-ordinates in respect to bregma were (in mm; positive X and Y axis values indicate right and anterior locations, respectively). FL1: X = – 1.5, Y = 4.5; FR1: X = 1.5, Y = 4.5; FL2: X = – 1.5, Y = 1.5; FR2: X = 1.5, Y = 1.5; LFL: X = – 4.5, Y = 0; RFR: X = 4.5, Y = 0; PL1: X = – 1.5, Y = – 1.5; PR1:

X = 1.5, Y = – 1.5; LPL: X = – 4.5, Y = – 3; RPR: X = 4.5, Y = – 3; PL2: X = – 1.5, Y = – 4.5; PR2: X = 1.5, Y = – 4.5 (Xia *et al.*, 2016).

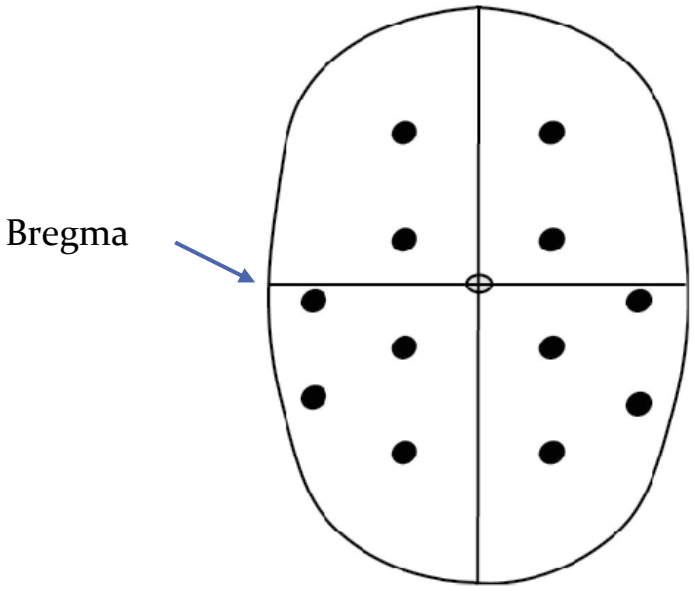

Figure 2.12 Electrode placement map, showing the locations of the 12 holes drilled during the craniotomy in respect to bregma.

2.3.3.6 Physiological monitoring

Physiological monitoring was, excluding blood pressure, conducted using the same MRI compatible monitoring and gating system for consistency between experiments (Small Animal Instruments, Inc.; New York).

2.3.3.7 Anaesthetic switchover

The anaesthesia was switched from isoflurane to the isoflurane and medetomidine combination as previously described in chapter 3.

2.3.3.8 Electrical stimulation

Electrodes made from 30 gauge needles were inserted into the pads of the hind-paw on each side of the paw and attached to a stimulus generator (DS3, Digitimer Ltd, Welwyn Garden City). Electrical stimulation was conducted at 3 different amplitude, 0.1mA, 2.5mA and 7.5mA.

2.3.3.9 Mechanical stimulation

Mechanical stimulation was conducted using Von-Frey hairs set into a pneumatic pump (World Precision Instruments) in order to provide accurate timings of stimulus onset/offset on the data recording. The pump drove a spring loaded pneumatic pin cylinder (CJ1B4-10su4, SMC) in which the von Frey hair was set, positioned perpendicular to the glaborous surface of the hind paw. Once triggered, the pneumatic pump drove the von Frey hair onto the paw and released pressure after 3 seconds.

2.3.3.10 Thermal stimulation

Thermal stimulation was conducted using an aluminium heating block (created in house UoN, Medical Engineering) set into a pneumatic pump (World Precision Instruments) in order to provide accurate timings of stimulus onset/offset on the data recording. The pump drove a spring loaded pneumatic pin cylinder (CJ1B4-10su4, SMC) with the heating block positioned perpendicular to the glaborous surface of the hind paw. Once triggered, the pneumatic pump drove the heating block onto the paw and released pressure after 3 seconds

2.4 ELISA

Rats were humanely killed via overdose of sodium pentobarbital (Euthatal, 2mL, i.p.) and exsanguinated to generate blood samples. Whole blood was collected in ice cold tubes containing 200µl heparin and processed within one hour. Samples were centrifuged at 13,000 rpm, 4°C for 20 mins, and the supernatant plasma collected and stored at -80°C prior to assay. Plasma samples were assayed in duplicate using a commercially available EIA kit (Phoenix Pharmaceuticals, Burlingame, CA, USA) according to the manufacturer's instructions. The optical density of each well was determined at 450nm.

Chapter 3 Feasibility testing of methods for functional connectivity studies in rat models of OA pain

3.1 General background

Magnetic resonance imaging (MRI) is a powerful and versatile technique for the investigation of brain changes, allowing for studies of both structure and function through the manipulation of a number of carefully selected parameters. Functional MRI (fMRI) measures neuronal activity indirectly through the blood oxygen level dependent (BOLD) signal, either in response to external stimuli or the spontaneous fluctuations that occur when the brain is at rest. The latter; resting state fMRI (rs-fMRI) is an important and relevant tool for the investigation of spontaneous fluctuations of the BOLD signal in a number of disorders that affect the central nervous system (see Chapter 2 for detailed background). Significant alterations in resting functional connectivity (rs-fc) have been shown in disorders that result in chronic pain, as well as affective disorders such as anxiety and depression (Baliki, Chang, Baria, Centeno, & Apkarian, 2014; Cottam, Iwabuchi, Drabek, Reckziegel, & Auer, 2018; Liao et al., 2010).

While the biological source of rs-fc is not precisely understood, it is thought to reflect both underlying neuronal activation patterns which are indirectly measured through the BOLD signal, as well as physiological signals from cardiac and respiratory oscillations (Birn *et al.*, 2006). Support for the neuronal basis of rs-fc comes from evidence that networks are formed between regions that are functionally, rather than spatially related: signals can be split into functional networks such as the auditory network, the motor network and the sensory network amongst others (Damoiseaux *et al.*, 2006). Combined rs-fMRI and EEG datasets

provide some evidence for the association of low frequency EEG signals with rs-fc (Deligianni *et al.*, 2014).

3.1.1 Rodent neuroimaging

Neuroimaging in rodents, although technically conducted quite similarly to neuroimaging in humans, is routinely conducted under general anaesthesia. Bespoke coils, suitable for the smaller size of the rat brain and preclinical MRI scanners with increased field strengths are generally used in conjunction with stronger gradients, yet the principles of neuroimaging remain unchanged (Hoyer *et al.*, 2014). Nonetheless, adapting these techniques to the rat brain creates a number of additional challenges which require careful consideration before any questions of interest can be reliably addressed (Jonckers *et al.*, 2015).

Neuroimaging data collection using MRI in particular, requires subject motion to be minimised. The length of time required for MRI data collection, often 2 seconds for EPI images and longer for anatomical imaging, predisposes images to distortions or artefacts from subject motion that can be challenging to correct, if correction is possible at all (Zaitsev, Maclaren and Herbst, 2015). Thus, these types of studies use anaesthetic agents to restrict motion while preserving welfare (Jonckers *et al.*, 2015). Nevertheless, several experiments have recently been conducted in awake rats trained to restraint environments within the scanner (Pei-Ching Chang *et al.*, 2016). An awake neuroimaging set up for some types of studies can be justified, but is not ideal for studies in which stress may confound the primary measures, which is the case for studies of pain mechanisms and anxiety. While training has been shown to keep stress levels theoretically relatively low during scanning time (Chang *et al.*, 2016), the repeated handling and exposure to restraint

might be inappropriate for strains of rats that have increased vulnerability to anxiety or in models of chronic pain.

The use of anaesthesia to reduce motion introduces additional challenges. The physiology of the rat, including heart rate, breathing rate and pulse oximetry must be comprehensively monitored to ensure that the animal is both appropriately and stably anaesthetised and that these parameters are within a physiological range. The anaesthetic agent must also be carefully chosen to ensure that any effects on the haemodynamics, cerebrovascular coupling, temperature and neural responsiveness, while inevitable, are well understood and minimised. Several studies exist within the rodent neuroimaging literature which either propose new anaesthetic regimes or test commonly used anaesthetic regimes for studies of functional connectivity (Williams *et al.*, 2010; Grandjean *et al.*, 2014; Bukhari *et al.*, 2017; Paasonen *et al.*, 2018).

Isoflurane is a commonly used as an anaesthetic agent in MRI and fMRI experiments. It is an inhalational anaesthetic agent that is generally well tolerated but has been shown to affect neurovascular coupling in a dose dependent manner (Masamoto *et al.*, 2007). Although studies have been carried out using isoflurane, including those investigating pain (Abaei *et al.*, 2016; Wells *et al.*, 2017a), the dampening effects that isoflurane has on the BOLD signal call into question whether isoflurane is the optimal choice for fMRI experiments. Under isoflurane, burst-suppression firing is observed under deeper anaesthesia. Periods of high-voltage waves are interspersed with periods of isoelectric epoch, and this firing pattern has been shown to occur at isoflurane doses recommended for fMRI studies (Vincent *et al.*, 2007). This type of activity contrasts with the slow wave activity commonly seen in the resting state (Steriade, Amzica and Contreras, 1994; Vincent *et al.*, 2007). Isoflurane has been shown to have an inverted U shape effect on the BOLD signal, with BOLD signal increases at moderate doses (2% and 2.5%) and BOLD signal decreases at

lower (1.5%) and higher (3%) doses (Tsurugizawa, Takahashi and Kato, 2016). Due to the complexities of isoflurane anaesthesia, alternative anaesthetic agents such as alpha-chlorolose, propofol, medetomidine, or combinations of low levels of isoflurane with neuromuscular blockers are employed (Paasonen et al. 2018; Weber et al. 2006; Grandjean et al. 2014; Wells et al. 2017).

A goal of this thesis was to identify a suitable anaesthetic for measures of rs-fMRI in the rat. Initial experiments tested alfaxalone, a neuroactive steroid which acts as a positive modulator on $GABA_A$ receptors. However, it quickly became apparent that a stable level of anaesthesia was difficult to reach with alfaxalone. Given that rats cannot be visually monitored in the scanner environment, alfaxalone was decided to be unsuitable for welfare reasons.

Medetomidine is racemic mixture of 50% dexmedotomidine and 50% levomedetomidine which is a full agonist at α2 adrenoreceptors. Medetomidine acts centrally to produce sedation, predominantly via an action at α2 adrenoreceptors in the locus coeruleus (Correa-Sales, Rabin and Maze, 1992). Medetomidine has additional physiological effects, including increases in mean arterial blood pressure, pulmonary arterial blood pressure and heart rate. It is also provides a degree of antinociception (Flecknell *et al.*, 2015).

For functional imaging research, medetomidine has been evaluated in several comparison studies against alternative anaesthetic agents including isoflurane, alpha-chloralose and propofol (Grandjean *et al.*, 2014). It has been reliably used in somatosensory experiments (Zhao *et al.*, 2012, 2014) and has been shown to be superior for rs-fMRI studies, specifically in terms of preservation of functional connectivity in both cortical and subcortical structures (Grandjean *et al.*, 2014). The utility of this anaesthetic for rs-fMRI studies was shown to be improved by combining medetomidine with a low dose (approximate 0.5%) of

isoflurane (Grandjean *et al.*, 2014; Paasonen *et al.*, 2018). With this combination, the functional connectivity pattern better resembled the functional connectivity pattern of an awake rat than either agent alone (Paasonen *et al.*, 2018). Although some suppression of intra-subcortical and thalamo-cortical connections was demonstrated, interhemispheric and intracortical connectivity remained largely intact with this combination of anaesthetics. Biologically, these beneficial effects are thought to occur due to the offset of the vasoconstrictive effects of medetomidine by the vasodilatory effects of isoflurane (Table 3.2).

Physiological effect	Medetomidine	Isoflurane
Heart rate	Decreases	Decreases
Blood pressure	Typically increases but can decrease	Decreases
Cerebrovascular	Vasoconstrictive	Vasodilatory

Table 3.2: comparison of physiological effects of medetomidine and isoflurane (Sinclair, 2003; Yang *et al.*, 2014)

3.1.2 Aims:

Before embarking on neuroimaging studies of models of OA pain, it was important to test the feasibility and suitability of the combined medetomidine/isoflurane anaesthetic regime for this experimental set up, specifically taking into account the use of noxious stimulation (Fig 3.1). The anaesthetic regime needed to be practical for fMRI experiments, both in terms of producing a stable level of anaesthesia whilst preserving neuronal activity. Both of these requirements were tested using ECoG, with direct visual monitoring of physiology and welfare, as well as

qualitative examination of raw EEG traces under each anaesthetic regime. The anaesthetic regime was also required to be suitable for the study of nociceptive processing, allowing for the maintenance of nociceptive responses in the presence of the anaesthesia. This was tested using nociceptive electrical stimulation delivered to the hind paw under combined medetomidine and isoflurane anaesthesia, both with ECoG and fMRI. Finally, the suitability of the nociceptive stimulation equipment in the MR scanning environment was tested to confirm that it did not distort the acquired images, it did not cause heating in the paw and it produced observable BOLD signal increases in fMRI.

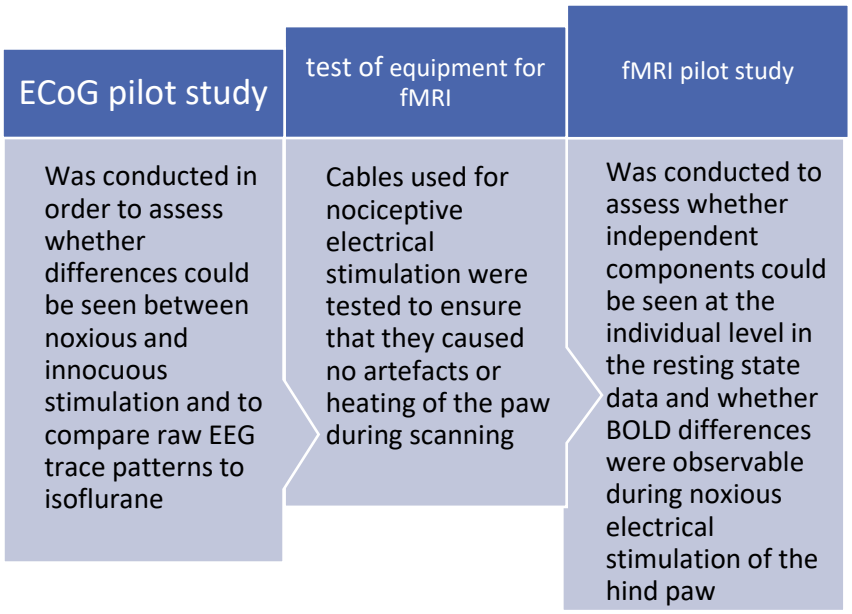

Figure 3.1: Process of implementation and testing of the anaesthetic regime, beginning with the ECoG to look at neuronal activation, followed by testing of equipment for fMRI and the assessment of BOLD activity under the medetomidine and isoflurane anaesthetic regime.

3.2 ECoG: Nociceptive stimulation under medetomidine with isoflurane

The experiments described were conducted in accordance with the Animals (Scientific Procedures) Act 1986, which incorporates Council Directive 2010/63 EU of the European Parliament. These experiments were conducted under project license 40/3647.

3.2.1 Animals

Adult male Wistar rats were used for these experiments weight 250-300g (Charles River, Margate, UK). A total of 4 rats were used for the ECoG experiments and 4 rats were used for the resting state fMRI.

1 male Sprague Dawley rat was used ex vivo to test heating in the hind paw and levels of interference from the electrical stimulation equipment.

3.2.2 Anaesthesia

All rats were transferred from isoflurane (for induction and surgery) to medetomidine anaesthesia (0.05 – 0.1mg/kg + 0.5% isoflurane). The transfer from isoflurane to medetomidine occurred gradually. After surgery, the isoflurane was reduced to 1.5% and the animal was left to acclimatise until physiology and temperature levels reached optimum levels (respiratory rate approximately 60 breaths per minute, temperature 37.5°c). The isoflurane was then reduced further to 1% and a bolus of 0.05mg/kg medetomidine in 0.9% saline, was then given subcutaneously. After a further 5 minutes, the isoflurane concentration was then reduced to 0.5% and physiology was watched carefully in order to ensure that the rat was still fully anaesthetised. After an additional 5

minutes, the continuous rate infusion began with 0.1mg/ml/hr in 0.9% saline. Respiratory rate was monitored visually and paw withdrawal reflexes were measured by using forceps to apply gently pressure to one hind paw to ensure the animal was at an appropriate (areflexic) anaesthetic depth.

3.2.3 Cannulation and electrode placement

For the ECoG and fMRI experiment, surgeries were conducted under isoflurane anaesthesia. The rats were induced at 3% isoflurane delivered in 1l/min oxygen, which was reduced to 2 ½ - 2% isoflurane for the duration of the surgery. The tail artery was cannulated for measurement of blood pressure (mmHg) using an MR compatible blood pressure transducer (Samba sensors, Gothenburg, Sweden) and fine flexible tubing. The tail vein was chosen for cannulation for intravenous (IV) administration of medetomidine (Sedastart, Produlab Pharma, The Netherlands) as it is less invasive than the femoral artery and allows for better control of core body temperature. A continuous infusion of medetomidine was delivered using a continuous infusion pump. Core body temperature was monitored using a rectal probe and controlled using a thermostatic heating mat (Harvard Apparatus, Edenbridge, UK).

In those rats undergoing ECoG, a craniotomy was performed and one small hole was drilled above the hind-limb somatosensory cortex (AP = -1.5mm, ML = 2.0mm), and frontally (AP = 5mm, ML = 2mm) for placement of a reference electrode. Loop tipped twisted silver wire electrodes were placed under the surface of the skull for EEG recording. The electrodes were mounted onto a NeuroLog head-stage (NL100AK; Digitimer, Welwyn Garden City, UK) and were recorded using Spike2 software (CED, Cambridge, UK).

For the fMRI pilot study, data were collected on a 30cm bore Bruker Biospec 7T scanner using a Bruker Avance III console and a rat brain 2 x 2 array coil (Bruker BioSpin, Ettlingen). Functional data were collected with a gradient-echo echo-planar imaging (GE EPI) sequence (TE = 23ms, TR = 2000ms, In-plane spatial resolution 0.46x 046mm^2, slice thickness = 1mm, matrix size = 64 x 64 x 17, flip angle 62.2°). Both resting state images (300 volumes (6 minutes)) and images during intradermal electrical stimulation of the hind paw were collected.

3.2.4 Stimulation paradigm

Pins were placed intradermally into the hind paw for electrical stimulation. The first train of stimulation given was innocuous: 1 train of 20 stimulations at 0.1mA, with 2ms duration. Each noxious train of stimuli was given 3 times, with 20 stimulations per train at 2.5mA and 7.5mA, with 2ms duration and 15 minutes between stimulation trains. This protocol was used as standard for spinal electrophysiology and was chosen to minimise variability between spinal cord and brain electrophysiology. This protocol is commonly used in order to observe wind up of neurons in the spinal cord (Latremoliere and Woolf, 2009a).

3.2.5 Analysis

ECoG data were processed using MATLAB 2016b (MathWorks, Massachusetts) and analyzed using GraphPad Prism (GraphPad, California) with a repeated measures (RM) one way ANOVA and Tukey's multiple comparisons. Fast Fourier Transform (FFT) functions were applied to the 30s post stimulation period to analyze EEG frequency composition.

fMRI analyses were conducted using FSL (fMRIB, Oxford). One animal was excluded due to noise by visual inspection. Files were first converted from the Bruker Paravision to NIFTI file format using the Bru2Nii converter (neurolabusc). Manual masks were created in ITK-SNAP (Piampring, 2016) and applied with FSLmaths. Preprocessing was conducted in FSL with FLIRT Linear registration and MCFLIRT for motion correction with 1mm FWHM spatial smoothing and interleaved slice timing correction (Jenkinson *et al.*, 2002). Data were analysed with MELODIC and FEAT in FSL.

3.3 Somatosensory evoked potential under medetomidine + isoflurane

The EEG activity of the hind limb somatosensory area was visually inspected, in order to compare traces between rats under isoflurane anaesthesia (1.5%) and medetomidine with isoflurane anaesthesia (0.1mg/kg + 0.5%) (Fig 3.2).

A: Medetomidine plus isoflurane

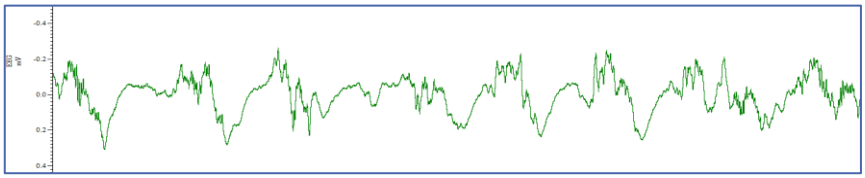

B: Isoflurane

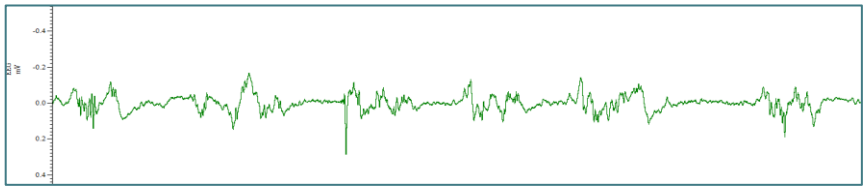

Figure 3.2 A) EEG activity from the S1HL region in a rat anaesthetised with medetomidine and isoflurane (0.1mg/kg & 0.5%). B) EEG activity from the S1HL region in a rat anaesthetised with isoflurane (1.5%), showing burst-suppression firing.

3.3.2 ECoG: Somatosensory evoked potentials

Somatosensory evoked potentials (SEPs) are signal averaged field potentials, acquired over a period of time and then averaged at the point of stimulation.

SEPs were recorded during nociceptive electrical stimulation of the hind paw, in order to confirm that they were visible under the medetomidine and isoflurane anaesthetic regime (fig 3.3).

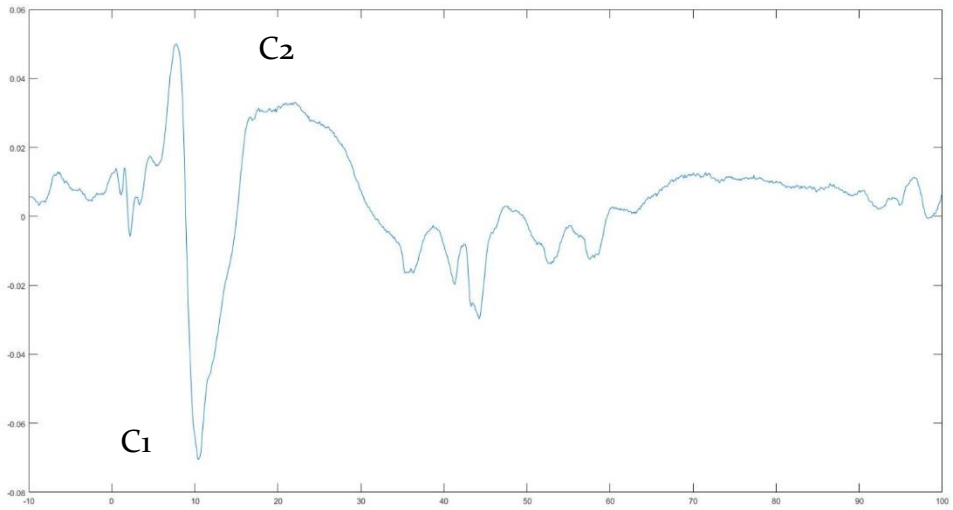

Figure 3.3: Somatosensory evoked potentials averaged over 10 stimulations (5mA) in a single rat, displaying 2 components used for analysis. C1: depolarisation after stimulation, c2: maximum amplitude after the depolarisation

To ensure that the combination of medetomidine and isoflurane did not modulate nociceptive responses overtly and mask electrical activity evoked by nociceptive stimulation, SEPs following electrical stimulation of the hind paw at 2.5mA and 7.5mA were compared to those evoked by a non-nociceptive train of electrical stimulation (0.1mA). Results were analysed in GraphPad Prism with a two-way ANOVA and Tukey's multiple comparisons (Fig 3.4).

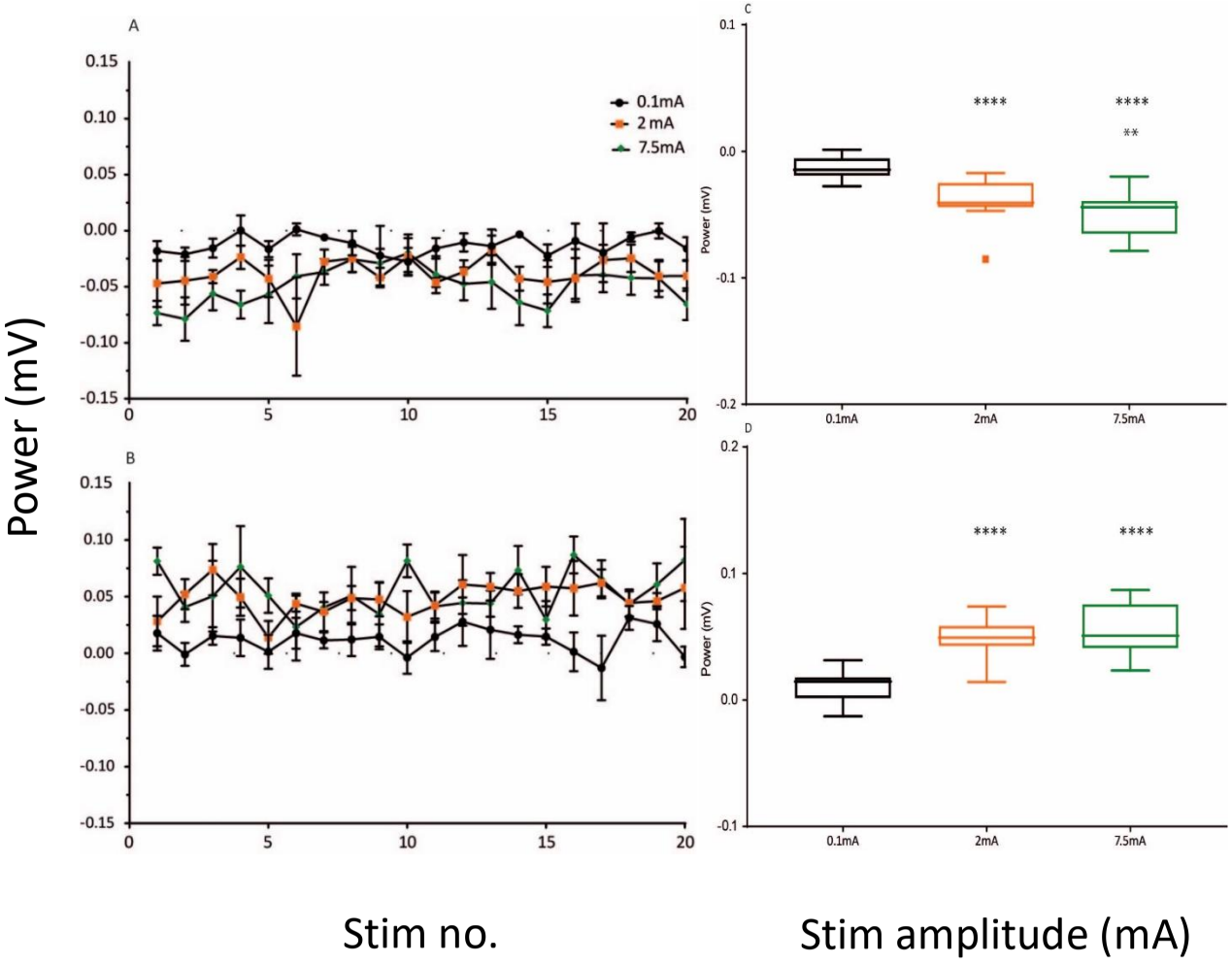

Figure 3.4 A, C: minimum depolarisation values (mV) at C1 for each stimulation amplitude. Significant differences were evident in power (mV) of neuronal activity over the S1HL area (n=4). Differences were evident between 0.1mA and both 2mA and 7.5mA (2mA: p= 0.0001; 7.5mA: p=<0.0001). There was also significant difference between 2mA and 7.5mA.

Figure 3.4 B, D: Significant differences were evident between 0.1mA and both 2mA and 7.5mA (2mA: P= 0.0001; 7.5mA: p = <0.0001). No significant difference was seen between 2mA and 7.5mA (p =0.455).

Data analysed with one-way ANOVA and Tukey's multiple comparisons **** P<0.0001, ** P<0.01

3.3.3 ECoG: Frequency differences after nociceptive electrical stimulation

Given that differences in SEPs were observable after noxious stimulation under the medetomidine and isoflurane anaesthetic regime (Fig 3.3), further analysis was conducted to explore in which frequency bands differences in power were evident following noxious electrical stimulation of the hind paw. Fast Fourier transform (FFT) functions were applied to the 30s period post stimulation to analyse frequency composition. Significant differences in power were observed only in the delta frequency band, for both the depolarisation and the polarisation phase of the SEP at both 2.5mA and 7.5mA ($p<0.0001$, fig 3.5). During depolarisation, a difference in power was also evident between the low and high amplitude stimulation ($p<0.05$, fig 3.5).

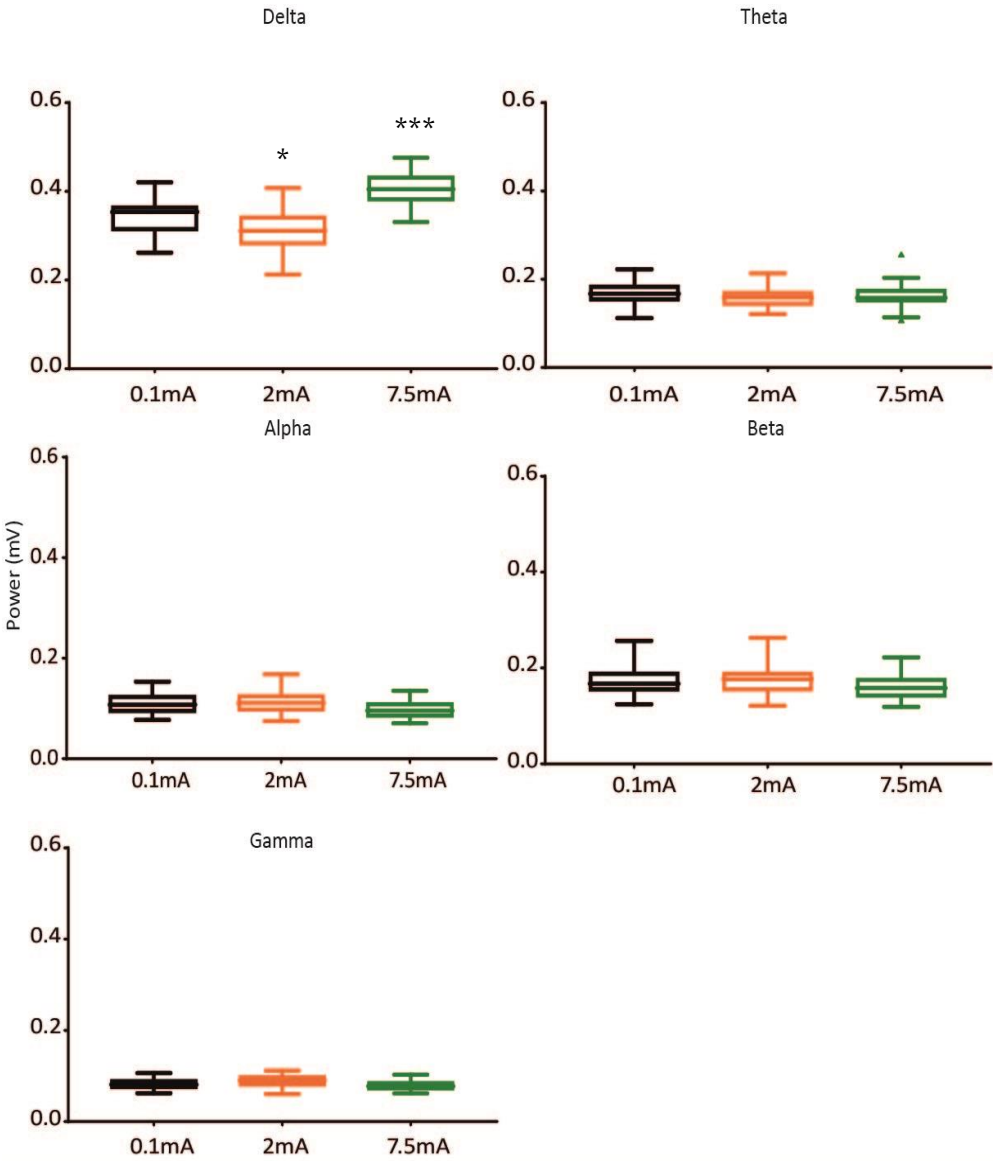

Figure 3.5: Significant differences in power were observed in the delta frequency band only, after noxious electrical stimulation (20 stimulations x 3 trains, 0.5hz) to the hindpaw (N=4). Differences were seen between 0.1 and 2mA (p= 0.0024), 0.1 and 7.5mA (p = <0.0001) and between 2 and 7.5mA (p = <0.0001). Data were analysed with a one way ANOVA and Tukey's multiple comparisons. **** P < 0.0001.

3.3.4 Summary

Qualitatively, there were marked differences between the ECoG traces recorded under isoflurane anaesthesia and medetomidine with isoflurane anaesthesia. Specifically, there was evidence of burst-suppression firing

in the isoflurane anaesthesia protocol, which was not present under the medetomidine and isoflurane anaesthesia combination (Fig 3.2A).

Noxious electrical stimulation of the hind paw of rats anaesthetised with medetomidine and isoflurane evoked SEPs over the hind limb somatosensory cortex, and these differences in power were significant in the delta frequency band.

3.4 Testing of cables for electrical stimulation during fMRI

3.4.1 Methods

3.4.1.1 Animal

One male Sprague Dawley rat was used in this experiment (weight = 297g). The rat was humanely killed in accordance with Schedule 1 of the Animals (Scientific Procedures) Act 1986.

3.4.1.2 Stimulation equipment

Stimulation cables were approximately 2m in length to account for separation between the stimulation equipment and the bore of the magnet. The cables were tested using a multimeter to ensure that the length of the cable did not affect the amplitude of stimulations.

To ensure that the stimulation cables were not causing heating of the paw during the EPI scans, the temperature of the stimulated paw was measured before and after stimulation and compared to the temperature of the non-stimulated paw (fig 3.6). A thin flexible thermometer, approximately (SAII Instruments, New York, USA) was taped to left paw

containing the stimulation cables and a Digitron 2046T digital thermometer (Digitron, Torquay, UK) was taped to the right paw, with the paw temperature of the cadaver averaging about 20°C. To ensure consistency between the thermometers, temperatures were measured at several time points prior to echo planar imaging (EPI).

3.4.1.3 Acquisition

Imaging was performed on a 30cm bore, Bruker Biospec 7T scanner using a Bruker Avance III console and a rat brain 2 x 2 array coil (Bruker BioSpin, Ettlingen, Germany). Images were acquired with Paravision 5 (Bruker Biospin). Images were collected with a gradient-echo EPI sequence with a TE = 23ms, TR = 2000ms, In-plane spatial resolution 0.46x 046mm^2, slice thickness = 1mm, Matrix size = 64 x 64 x 17, flip angle 62.2 and 330 volumes.

This was based on a T1 grey matter estimation of 1800ms, based on measurements of similar regions such as the caudate putamen, in the rat brain at 7T (Behroozi *et al.*, 2017)

The flip angle was calculated using the Ernst Angle equation (Ernst and Anderson, 1966):

$$\alpha E = \arccos(e^{-TR/T1})$$

3.4.1.4 Stimulation paradigm

The cables were tested under two different stimulation paradigms, at different frequencies of stimulation. The first protocol consisted of 20 x 2ms electrical pulses at 7.5mA intensity and a frequency of 0.5 Hz. The second consisted of 20 x 2ms pulses at 7.5mA and a frequency of 10 Hz. The higher stimulation frequency was included in case low frequency

stimulation was not able to induce observable BOLD changes in the upcoming fMRI work, due to the lower temporal resolution of fMRI when compared to electrophysiology.

3.4.2 Hind paw temperature after electrical stimulation

No differences in temperature were detected after electrical stimulation of the hindpaw, at either the lower (0.5Hz) or higher (10Hz) frequency.

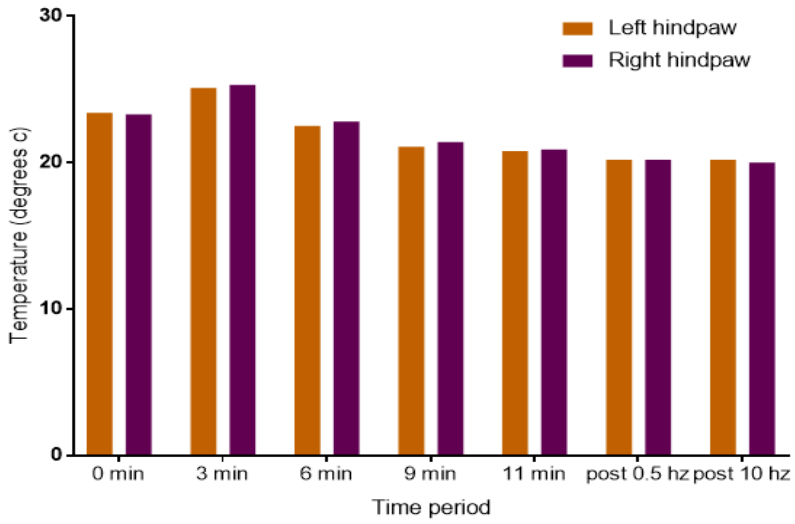

Figure 3.6: Comparison of temperature (degrees C) between the stimulated paw (left) and the non -stimulated paw (right) after electrical stimulation of the hindpaw during EPI imaging (N=1).

3.4.3 Qualitative inspection of raw images during electrical stimulation

In order to assess the effect of electrical stimulation of the hind paw on the data quality of raw fMRI images, an image from before electrical stimulation was qualitatively, visually, compared to an imaging acquired

during electrical stimulation at both the lower (0.5hz) and higher (10hz) frequencies, post mortem in a single rat (Figs 3.7, 3.8).

A slice from volume 25 (pre stimulation) and volume 375 (during stimulation) were taken from both the 0.5 Hz and 10 Hz stimulation protocols. An image showing the difference between the two images was created for each run and visually inspected. Qualitatively, no differences were seen between the images and no radiofrequency artefacts were observed.

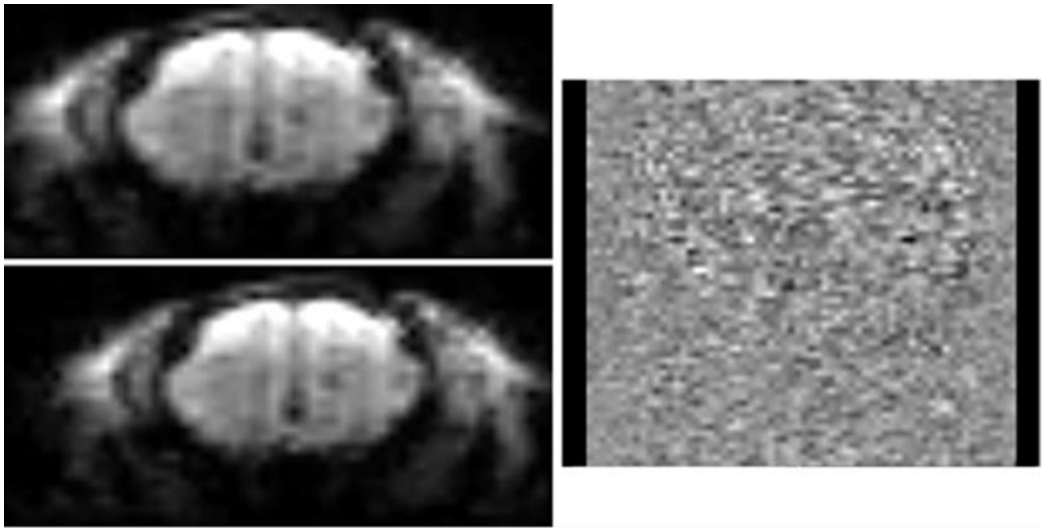

Figure (3.7): Raw ex-vivo fMRI images from the 0.5Hz, 7.5mA stimulation: top - Slice 25 (pre stimulation), and bottom: slice 375 (during stimulation). Right: Image showing the subtraction of the slice 375 image from the image of slice 25 showing no significant distortions during electrical stimulation.

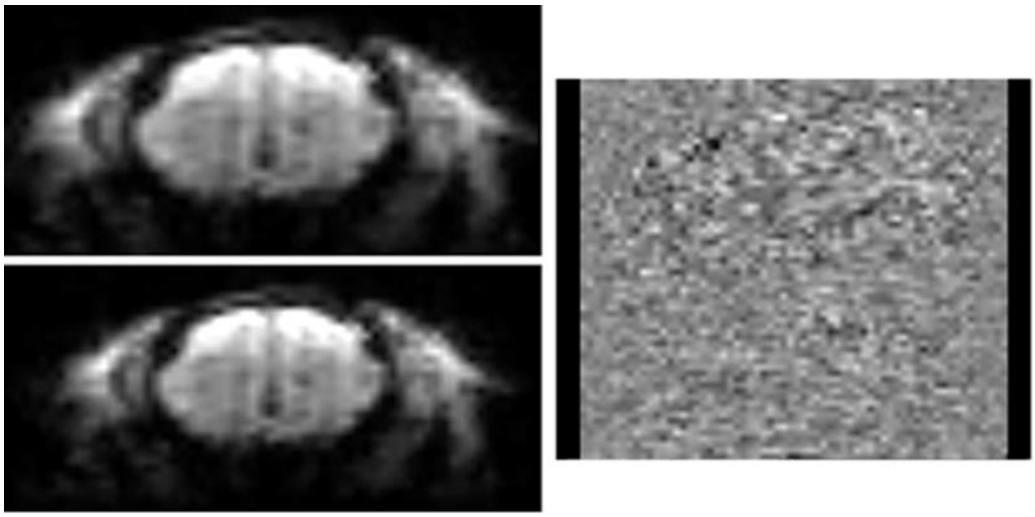

Figure 3.8: Raw ex vivo fMRI images from the 10Hz, 7.5mA stimulation: top - Slice 25 (pre stimulation), and bottom: slice 375 (during stimulation). Right: Image showing the subtraction of the slice 375 image from the image of slice 25 showing no significant distortions during electrical stimulation.

3.5 A pilot resting-state fMRI study to confirm the suitability of medetomidine and isoflurane in the rat

3.5.1 Resting state networks under medetomidine and isoflurane

Single subject ICA, an exploratory statistical analysis which decomposes resting state fMRI data into a number of spatio-temporal components (see Chapter 2) was used to examine single-subject data under the medetomidine and isoflurane anaesthetic regime.

A number of these components were observed at the single subject level (Fig 3.9). Both noise and resting state maps showing preliminary interhemispheric functional connectivity.

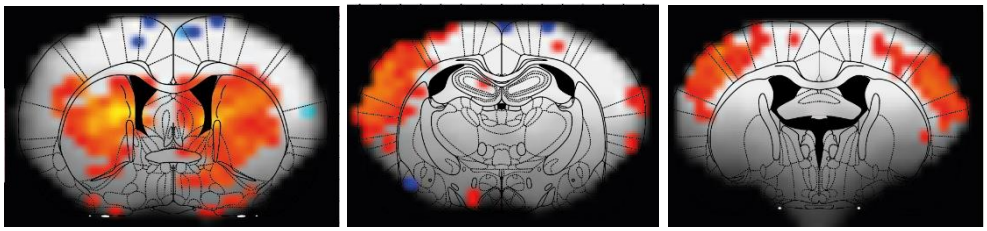

Figure 3.9: Example single subject resting-state ICA maps located over the thalamus and somatosensory areas. Images were thresholded at $p<0.05$, uncorrected, with red/yellow areas indicating correlated increase in BOLD activity over time and blue indicated a correlated decrease in the BOLD signal over time.

3.6 Effects of nociceptive electrical stimulation on BOLD activation

The effects of electrical stimulation of the hind paw on resting state networks was studied using BOLD. There were no significant differences in BOLD activity during nociceptive stimulation at 2.5mA or 7.5mA at a stimulation frequency of 0.5 Hz level (n=3). By contrast at the higher frequency of stimulation (10Hz), there was a significant increase in BOLD activity in the cingulate cortex following nociceptive stimulation of the hind paw (Fig 3.10).

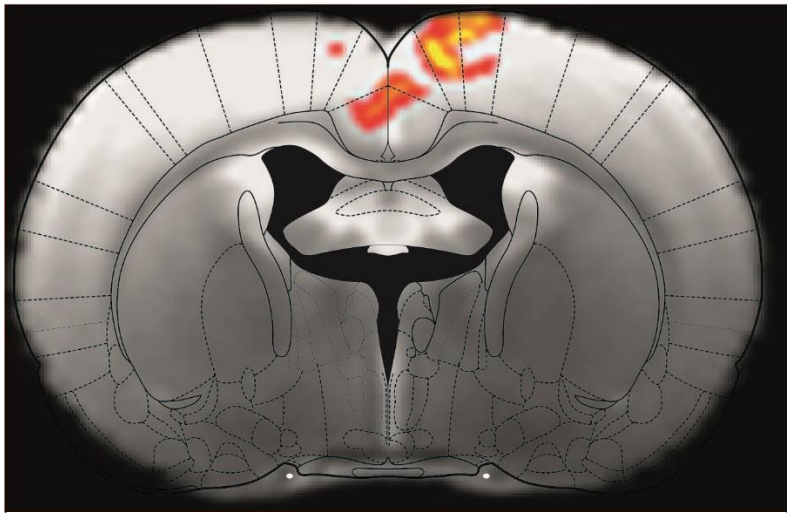

Figure 3.10: Significant clusters of increased BOLD activity were observed in the cingulate and motor cortices after noxious electrical stimulation of the left hindpaw at 10 Hz (2s stimulation block, 30s rest x 3) (n=3) at p=0.05 (uncorrected).

3.7 Discussion

3.7.1 Choice of anaesthetic agent

Medetomidine with isoflurane combination provided us with a number of ICA components with preserved inter-hemispheric connectivity, which were not evident under the isoflurane only protocol from within the research group (Abaei *et al.*, 2016). It is however, still important to understand the impact that this anaesthetic regime might have on the data collected, in order to aid interpretation of results and comparisons with human neuroimaging results.

The suitability of the medetomidine and isoflurane anaesthetic regime for these studies is consistent with the literature, which has reported that this combination is superior for the preservation of networks seen in the non-anaesthetised rat, albeit at the cost of sensitivity in subcortical

networks (Paasonen *et al.*, 2018). Given that this is largely an exploratory study built on a small rodent neuroimaging chronic pain literature, this trade-off was optimal. However, it is important to bear in mind that any changes not seen in subcortical networks may be due to the dampening effects of anaesthesia, rather than a lack of changes created by the OA pain.

Although BOLD increases were observed in the cingulate during nociceptive electrical stimulation of the hind paw, this BOLD signal increase was not observed during the low frequency stimulation under which changes were seen during the ECoG pilot study. It is possible that while this type of stimulation does cause sufficient change to neuronal activity, changes in the BOLD signal occur on a different timescale and current methods may not have been sensitive to very fast, small fluctuations in neuronal activity. However, given the small group size (n=3), this may simply be related to lack of statistical power.

3.7.2 Stimulation equipment

The lack of artefact from the stimulation cables allows for the use of these cables and electrical stimulation in future fMRI experiments. This adds consistency to experimental designs as these cables, stimulation equipment and paradigm are used for both electrophysiology and MRI experiments and allows for the closest comparison of data between the neuronal activity and the BOLD signal. Electrical stimulation is particularly useful as it can be controlled from outside the scanner environment and allows for good temporal control of nociception.

The preliminary EEG experiments allow us to characterise neuronal responses with this stimulation protocol and anaesthetic combination while providing a positive control for the stimulation protocol between the neuroimaging methods. This ensures that in the event of negative

results, it is possible to confirm that they are not due to a lack of neuronal activity from inappropriate stimulation or suppression of neuronal activity from inappropriate anaesthetic depth.

3.7.3 ECoG

The unique burst suppression pattern qualitatively observed under isoflurane was lost under the medetomidine isoflurane combination, which gave a pattern of neuronal activity more closely resembling that of the awake rat.

SEPs were preserved under the new anaesthetic regime and differences were not only seen between innocuous and noxious stimulation but also between 2.5mA and 7.5mA electrical stimulation. This suggests that our anaesthetic regime is sensitive to changes in nociceptive electrical stimulation and is likely suitable for studies of nociception.

In this study, significant changes in ECoG power were solely observed in the delta frequency band (1-4Hz). Although electrical brain changes after nociception have been shown for all frequency bands, increases are most often seen for the theta (4-8Hz) and alpha frequency bands (8-12Hz) Dos Santos Pinheiro *et al.*, 2016).

The lack of significant changes in the theta band in these rats is not surprising, giving that the majority of the ECoG power is observed in the delta band in anaesthetised subjects. These changes have been shown in humans, under a range of anaesthetic agents and so are likely not specific to ECoG studies in the rat or under this anaesthetic regime. Studies of combined intra-cellular recording with EEG suggest that increases in delta power occur when membrane potentials of thalamocortical relay neurones decrease, with increasing levels of anaesthesia (Steriade *et al.*, 1993).

The primary findings from these feasibility studies were that the medetomidine and isoflurane mixture preserved neuronal activity during nociceptive stimulation and MRI detectable large range functional connectivity. Large range functional connectivity is likely to be the primary interest in the study of chronic pain and anxiety, given the number of regions that have been implicated in the processing of both. This will provide additional considerations for results obtained under anaesthesia but will complement human findings from studies conducted on anaesthetised subjects.

Chapter 4 An investigation of the influence of endogenous anxiety on resting state functional connectivity in the MIA model of OA pain

4.1 Introduction

Although the influence of anxiety on chronic pain is not yet well understood, it is gaining increasing recognition. Investigation of the effects of co-morbid conditions on the chronification of pain have highlighted worse outcomes, differences in analgesic drug usage and prescribing as well as some evidence of brain changes, when individuals suffer from co-morbid anxiety, depression or other negative affect (Wasan, Davar and Jamison, 2005a; Valdes *et al.*, 2015; Cottam *et al.*, 2018).

This chapter will focus on the influence of anxiety on OA pain and its related brain changes. Anxiety is described as "a psychological, physiological and behavioural state induced in animals and humans by a threat to wellbeing or survival, either actual or potential" (Steimer 2002). Anxiety is a complex phenomenon and anxiety levels can be elevated, causing physiological changes, even when anxiety levels are not high enough to represent a clinical anxiety disorder (Laeger *et al*, 2012).

Clinically, diagnostic criteria for anxiety disorders outline excessive anxiety and worry, occurring for at least 6 months, difficulties in controlling the worry, feelings of restlessness, easily fatigued, difficulty concentration, irritability, muscle tension and sleep disturbance. These symptoms cause clinically significant distress or impairment in social, occupational or other important areas of functioning (DSM V).

A subtype of anxiety, a stable and enduring form of anxiety referred to as 'trait' anxiety. Trait anxiety has been shown to correlate with high levels of state anxiety, particularly in situations of interpersonal threat (Leal *et al*, 2017).

Although anxiety is primarily a psychological phenomenon, it is also linked with a group of physiological changes including autonomic activation (i.e. tachycardia, blood pressure and respiratory rate increases), as well as muscle tension and sweat production (Hoehn-Saric & McLeod 2000), although these physiological differences are not evident in the same way in those who experience prolonged clinical anxiety (Hoehn-Saric et al, 1989).

Individuals with higher levels of anxiety often display a number of characteristics that have been shown to influence pain processing. Pain catastrophizing, defined as a "tendency to magnify or exaggerate the threat value of seriousness of pain sensations" as well as "pain related worry and fear, coupled with an inability to divert attention away from pain, has been shown to be associated with an increase in anxiety during pain induction (Spanos *et al*, 1979; Chaves and Brown, 1987; Quartana, Campbell and Edwards, 2009).

Distress intolerance, referring to the inability to tolerate negative somatic and emotional states (McHugh and Otto, 2012), has been shown to be associated with negative affect and reduced tolerance of a psychosocial stressor (McHugh *et al*, 2019). In response to pain, distress intolerance has additionally been shown to be associated with the likelihood of opioid misuse and is associated with increased levels of anxiety after pain experiences (McHugh *et al.*, 2019).

Physiologically, a number of changes occur in the hypothalamic-pituitary adrenal axis (HPA), which plays a role in mediating stress (Micale and Drago, 2018). Although the influence of the HPA axis on pain is less

clear, altered cortisol levels (a marker of HPA axis function) have been demonstrated in subacute versus chronic back pain patients, which were mediated by anxiety (Nees *et al*, 2019).

4.1.2 Chronic pain and anxiety

As previously discussed (chapter 1), the brain is involved in the processing and modulation of pain, and there is evidence to suggest that brain changes can occur in response to chronic pain, although reproducibility across the field is low (Baliki *et al.*, 2008; Marwan N Baliki *et al.*, 2014; Tanasescu *et al.*, 2016; Cottam *et al.*, 2018).

A number of chronic pain conditions, including osteoarthritis, back pain fibromyalgia, are associated with co-morbid psychological disorders such as clinical anxiety disorders, major depressive disorder and bipolar disorder (Buskila and Cohen, 2007). Beyond clinical comorbid conditions, features of negative affect such as catastrophizing: an exaggerated negative orientation to actual or anticipated pain have been shown to impact pain, as well as outcomes after treatment for chronic pain (Valdes *et al.*, 2015). Related factors such as strain in family relationship have also been shown to be significantly associated with development of chronic pain over a 10 year timescale (Woods *et al.*, 2019), highlighting that negative affect and psychosocial factors can influence the development of chronic pain.

At a brain level, catastrophizing has been shown to be associated with increases and decreases in grey matter morphology, as well as with functional connectivity and brain changes during task-related fMRI (Gracely *et al*, 2004; Hubbard *et al*, 2014; Chehadi *et al*, 2017). The evidence for associations between anxiety symptoms and brain changes in chronic pain is not conclusive however, and no consistent associations have been demonstrated between self-reported depressive symptoms and

brain changes in chronic pain, as shown by meta-analysis (Malfliet *et al.*, 2017). These studies span a heterogeneous chronic pain population, with conditions ranging from lower back pain to fibromyalgia and migraines. It is not clear whether these types of chronic pain share the same brain changes, given the likely different contributions of nociceptive, neuropathic and central components of pain to these conditions, and whether these, if demonstrated, reflect the same underlying neuronal mechanisms.

These data are largely correlational in nature and as such, although the relationship between psychosocial factors and pain is clear, the directionality and mechanisms underlying this relationship is not. Although human patients obviously provide the most accurate account of how chronic pain and anxiety is experienced in humans, animal resting-state functional connectivity (rs-fc) studies, while logistically challenging to implement, allow for direct manipulations of variables by modelling chronic pain and anxiety in a controlled environment. This can provide useful back-translation of relationships and phenomena observed in humans, to allow for carefully controlled studies in which physiology can be more directly investigated or pharmacological interventions can be easily implemented, providing additional information regarding underlying mechanisms.

The regions of the brain underpinning anxiety and depression are co-located with those involved in the processing of painful inputs and the processing of pain. The anterior cingulate cortex, prefrontal cortex, thalamus, nucleus accumbens, amygdala, PAG and ventral tegmental area implicated in both disorders (Graeff *et al*, 1993; Shin and Liberzon, 2010; Barthas *et al*, 2015; Li *et al*, 2016). Not only is there an anatomical rationale for this interaction between anxiety, depression and chronic pain, but the neurochemistry of these conditions coalesces around the

noradrenergic and serotonergic systems (Borsook *et al.*, 2016; Li *et al.*, 2017).

4.1.3 rs-fMRI in pain

The investigation of rs-fc changes in response to chronic pain still comprises a relatively small proportion of the neuroimaging literature within the pain field, with only approximately 80 papers published in 2018, in comparison to 3000 general fMRI papers (Fig 4.1). Studies of functional connectivity can provide important insights into how pain conditions can alter spontaneous fluctuations in brain activity and whether treatments alter these changes.

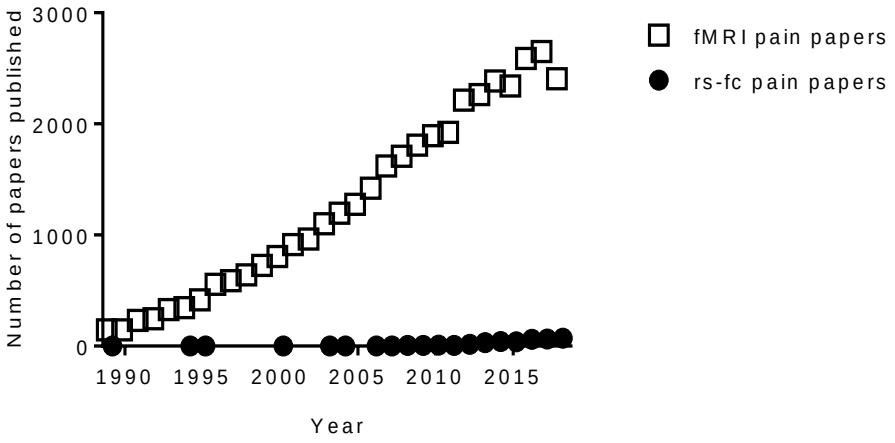

Figure 4.1: Number of papers using fMRI to investigate pain published every year compared to number of papers using rs-fc to investigate pain (PubMed).

4.1.4 Rationale

Alterations in rs-fc have been demonstrated in few preclinical chronic pain models, including the MIA model (Abaei *et al*, 2016; Spisák *et al*, 2017) but results are discordant, and as yet, there is no evidence to suggest how and whether alterations in rs-fc, in animal models, are influenced by the presence of anxiety.

To investigate the involvement of endogenous opioids, rs-fc will be measured after administration of the μ opioid receptor antagonist naloxone. In humans, increases in BOLD signal amplitude have previously been shown after administration of naloxone in the cingulate, prefrontal cortex, insula, as well as subcortical regions including hippocampus and the entorhinal cortex (Borras *et al*, 2004). However, it is not clear whether these effects are a) observable under anaesthesia and b) altered in the presence of anxiety.

4.1.5 Models:

MIA: The monosodium iodoacetate (MIA) model of OA pain was first described by Kalbhen in the 1980s (Kalbhen, 1987). MIA exerts its effects on the joint through the inhibition of glyceraldehydes-3-phosphate dehydrogenase. The inhibition of glycolysis disrupts chondrocyte metabolism, which in turn leads to thinning of the articular cartilage and the appearance of osteophytes (Marker and Pomonis, 2012). At the later stages of the MIA model, damage also occurs to the synovium with exposure of the subchondral bone.

The joint changes developed during the MIA model create a number of pain related behavioural changes that are relevant to the pain experienced in humans with OA. Changes caused by the MIA model

include progressive hypersensitivity in sites distal to the affected joint, which is observed and measured primarily in the hindpaws in rodents. Weight bearing deficits are seen on the injured limb with limping and alterations in gait and a number of other changes are observed including diminished hind-limb grip force, cooling hypersensitivity, vocalisation in response to knee bend, conditioned place preference, locomotive changes including rearing, depressed wheel-running and alterations in sleep (Malfait, Little and McDougall, 2013).

WKY: The WKY rats were initially developed as a control strain for spontaneous hypertensive rat (SHR), but are now commonly used as a model of anxiety or depression (McAuley *et al.*, 2009; Nam *et al.*, 2014). In previous studies WKY rats have exhibited behaviours indicative of increased anxiety in a number of behavioural tests such as the open field and elevated plus maze, and have displayed other signs of anxiety such as ulcer formation, peripheral and central stress responses as well as learning and memory alterations (Ferguson and Cada, 2004). They also show signs of avoidant behaviour, a common feature of all anxiety disorders (Servatius *et al.*, 2008). Physiologically WKY rats have been shown to have different HPA axis function with altered acetylcholinesterase activity, suggesting abnormal cholinergic functioning (McAuley *et al.*, 2009).

Experiments in this thesis used rats supplied by Envigo (UK), the supplier/location most commonly used as a provider for this model of anxiety.

4.1.6 Aims:

1. To compare differences in rs-fc (ICA and seed based) between normal anxiety Wistar rats and high anxiety behavioural

phenotype WKY rats after intra-articular injection of MIA or saline.

2. To look at the relationship between pain behaviour and rs-fc in these groups of rats.

3. To assess differences in BOLD activity after nociceptive electrical stimulation of the hind paw.

4. To investigate whether any brain changes are evident after administration of naloxone.

4.2 Methods

The experiments described were conducted in accordance with the Animals (Scientific Procedures) Act 1986 which incorporates Council Directive 2010/63 EU of the European Parliament.

4.2.1 Animals:

All rats were kept in conventional open top cages and on a reversed 12 hour dark/artificial light cycle. Holding rooms were maintained at a temperature of 22°C and at a humidity of 55%. Food and water were available ad libitum.

42 Adult male Wistar (Charles River, UK) and Wistar Kyoto rats (Envigo, UK) were used in this study. Rats from each strain (N=21) received intra-articular injection of MIA (n=11) or saline (n=10) into their left knee. MIA and saline animals were housed together in groups of 4, within their strains.

4.2.2 Intra-articular injections

All rats received a singular 50µl intra-articular injection into the left knee, through the infra-patellar ligament under isoflurane anaesthesia (3% 1L/min 02). 22 rats received 1mg/50µl in 0.9% saline of monosodium iodoacetate (MIA) and 20 rats received 50µl 0.9% saline using a 50 gauge hypodermic needle.

Sample sizes were determined using a power calculation based on results from the imaging literature. Sample sizes aligned with sample sizes typically used in MIA experiments, based on the power required for behavioural results.

The MIA model of osteoarthritis pain was induced under isoflurane anaesthesia (3% 1L/min $0_{2)}$. A singular intra-articular injection of monosodium iodoacetate (1mg/50µl; Sigma, UK) or saline (50µl) was given into the left knee, through the infra-patellar ligament, using a 50 gauge hypodermic needle. Post injection, rats checked for health immediately post recovery, 1 hour post recovery and 3 hours post recovery and subsequently returned to their home cages. Health was monitored daily for 5 days and then weekly. The experimenter was blinded to the treatment given to each animal. Due to differences in size between the Wistar and WKY rats, it was not possible to be blinded to strain.

4.2.3 Behavioural testing

All rats received 2 habituation sessions to the pain behaviour testing environment to minimise any exploratory behaviour during testing. Baseline measurements were taken prior to injection on day 0 in the morning, and behavioural measurements were subsequently measured from day 3 to day 21 post model-induction, twice weekly. Both weight

bearing asymmetry (WB), and mechanical hind paw withdrawal thresholds (PWTs) for both the paws both ipsilateral and contralateral to the affected joint were assessed.

Healthy rats distribute their weight evenly between limbs and a weight shift onto the contralateral limb is taken as an indicator of pain in the ipsilateral knee joint. WB was assessed using an incapacitance tester (Linton Instrumentation, Diss, UK). A minimum of three measurements were taken where possible, with extra measurements taken when an animals activity levels precluded obtaining consistent measurements.

PWTs were measured using von Frey monofilaments across a range of forces (2, 4, 6, 8, 10, 15 and 26g). The filaments were applied to the plantar surface of each hind paw for 3 seconds or until the paw was withdrawn using criteria similar to that of Chaplan et al (Chaplan, Bach, Pogrel, Chung, & Yaksh, 1994). Each filament was applied in ascending order until 2 out of 3 applications elicited a withdrawal response. The filaments were then applied in descending order until no response was evoked and then then reapplied in ascending order until a response was evoked again. This was taken to be the final PWT.

4.2.4 Locomotion and anxiety testing

The open field and elevated plus maze were used to measure anxiety and locomotor activity in Wistar and WKY rats at day 20 after intra-articular MIA for the open field, and day 27 for the elevated plus maze.

The elevated plus maze is raised from the ground and has four arms: two of these arms have high sides and are enclosed at the end; two of the arms have no sides and are open at the end. In these experiments the rats were placed in the centre of the maze, nose facing into an open arm and allowed free exploration for 10 minutes.

The rats were monitored through a ceiling mounted camera and the rat was tracked using the Ethovision software. Exploration in the closed arms of the maze was taken as an indicator of anxious behaviour whereas exploration in the open arms of the maze was taken as an indicator of lower levels of anxiety. In these experiments the centre point of the rat was used to track the location its location.

A custom made opaque cylindrical arena (90cm diameter) was used to test locomotion in the rats. The rats were placed into the centre of the arena and activity was monitored for a period of 10 minutes. As described for the elevated plus maze, all activity was monitored using the Ethovision software.

4.2.5 Acquisition of MRI

The MRI protocol began with acquisition of an anatomical image, followed by the resting state EPI acquisition, the electrical stimulation EPI scans and finally the naloxone EPI imaging (Fig 4.2).

Imaging was performed on a 30cm bore, Bruker Biospec 7T scanner using a Bruker Avance III console and a rat brain 2 x 2 array coil (Bruker BioSpin, Ettlingen, Germany). Images were acquired with Paravision 5 (Bruker Biospin). Full details provided in general methods (chapter 2).

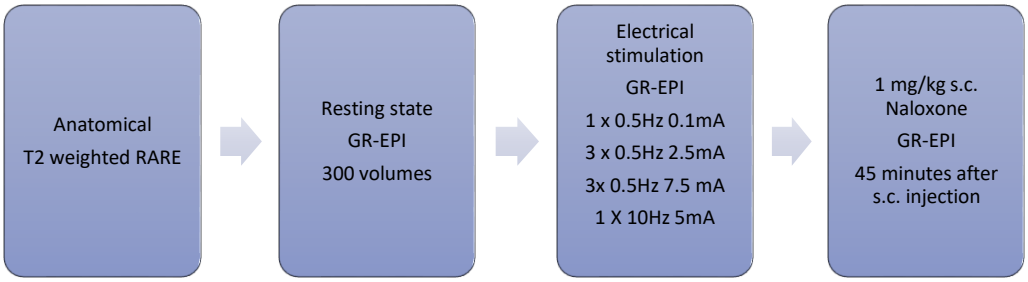

Figure 4.2: Order of scans in each session. Electrical stimulation runs were collected with 10 minutes in between each train of stimulation and each train consisted of 20 stimuli, 2ms in duration.

4.2.6 Resting state fMRI

Images were collected with a gradient-echo echo planar imaging sequence with a TE = 25ms, TR = 1300ms, In-plane spatial resolution 0.46x 046mm^2, slice thickness = 1mm, no interslice gap, Matrix size = 64 x 64 x 14, flip angle 70.8 degrees. 300 volumes were collected in total.

4.2.7 Physiological monitoring

The temperature of the rats was maintained at 37°C +/- 0.5° for the duration of the experiment, and temperature was monitored using a rectal probe. Respiratory rate, heart rate and oxygen saturation were measured with the SAII monitoring system. Arterial blood pressure

(mmHg) was measured from the tail artery with surgeries conducted as previously described (See chapter 2).

4.2.8 Anaesthesia

0.1mg/kg/ml medetomidine (Sedastart, AnimalCare UK) was given through a cannula into the tail vein combined with 0.5% isoflurane in 1l/min oxygen (See chapter 2) for the duration of the experiment.

4.2.9 Analysis

4.2.9.1 Quality control

Quality control was conducted manually. No images required excessive motion correction (threshold for exclusion set at motion of more than 1mm), with an average motion correction of 0.04 mm, in these rats.

3 Wistar rats were excluded because of image distortions that precluded adequate registration of RS-fMRI images to the template image. 1 WKY rat was excluded due to abnormal brain anatomy (Fig 4.3).

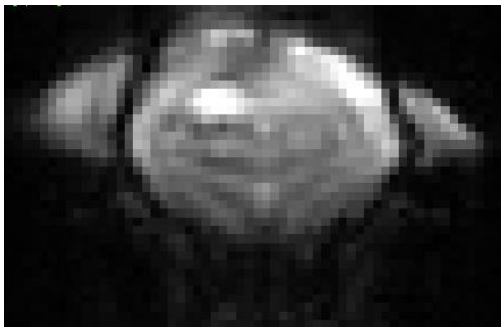

Figure 4.3: Raw image showing distortion to the functional image, caused by the anatomical abnormality, leading to exclusion of this rat from analysis.

4.2.9.2 Pre-processing

Pre-processing was conducted using ITK-SNAP, version 3.2 (Yushkevich *et al*, 2006) and FSL version 6.0.1 (FMRIB, Oxford).

Masks of images were created manually, for both fMRI and anatomical MRI images in ITK-SNAP (Yushkevich *et al*, 2006) and applied using FSLmaths. Subsequent pre-processing was conducted in MELODIC in FSL: functional images underwent MCFLIRT motion correction, interleaved slice timing correction, spatial smoothing to 1mm and individual ICA maps were created for manual denoising of the data (full details described in general methods).

4.2.9.3 Independent component analysis (ICA)

To assess the effect of strain on functional brain connectivity and how functional connectivity may be altered by MIA within each strain, ICA analyses comparing resting state networks (RSNs) were conducted, using MELODIC in FSL version 6.0.1 (FMRIB, Oxford).

4.2.10 Statistics

Differences between groups were investigated using randomise permutation testing (FMRIB, Oxford) and dual regression with FDR post-hoc corrections (Winkler *et al*, 2014). FDR post-hoc corrections were chosen in place of Bonferroni multiple correction as Bonferroni corrections are problematic for use in fMRI, increasing type 2 errors (Lieberman and Cunningham, 2009).

Additional seed based analyses were conducted using FSL (FMRIB, Oxford) to investigate differences in rs-fc from a number of a-priori

chosen seed regions, related to pain processing and related affective processing.

4.2.11 Seed regions:

Seed based analyses were conducted as described in the general methods.

3 seed regions were chosen:

Periaqueductal grey (PAG): The PAG is a cell dense region surrounding the midbrain aqueduct. It is heavily innervated by ascending spinal pathways (Westlund and Willis, 2012).

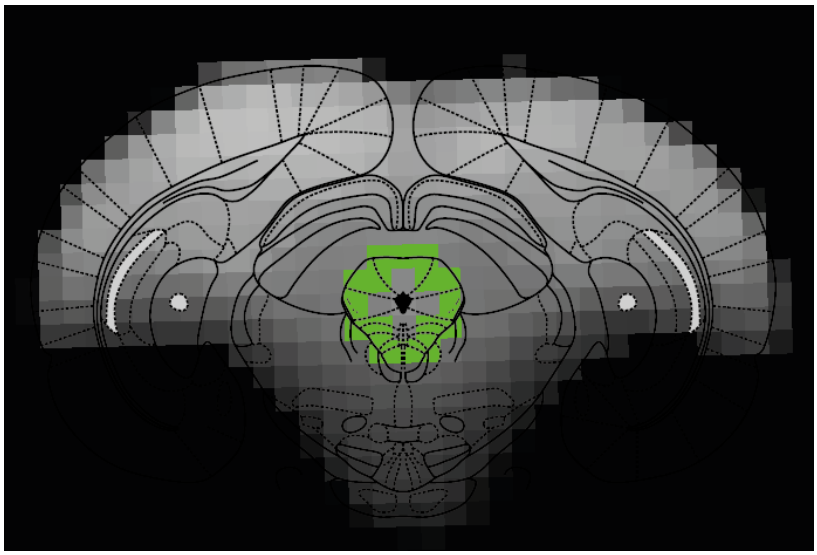

Figure 4.4 Manually drawn PAG seed region, surrounding the aqueduct, on an individual functional image, overlaid onto an atlas for localisation.

VmPFC: Abnormal activity in the VMPFC has been widely reported for a number of mood and anxiety disorders. The VMPFC is thought to suppress negative affect by inhibiting amygdalar output. The region most closely functionally related to the VMPFC in the human is the infralimbic (IL) cortex in the rat brain (Fig 4.5) (Myers-Schulz and Koenigs, 2014).

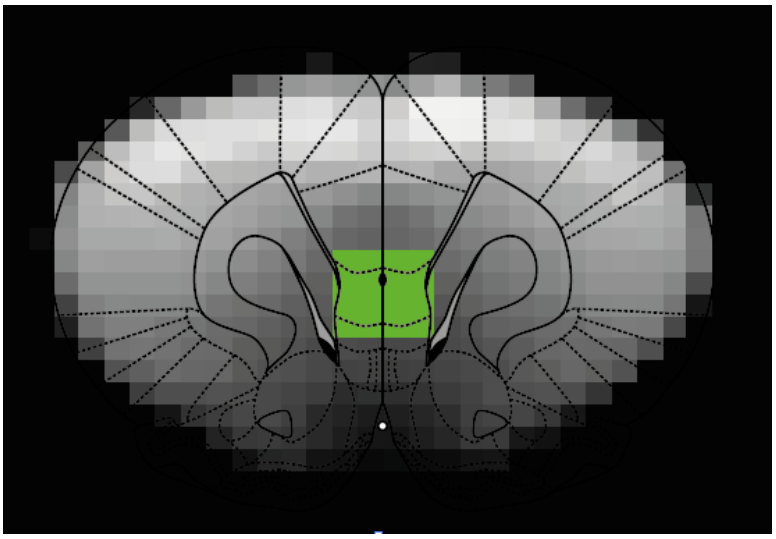

Figure 4.5: Manually drawn IL seed region on an individual functional image, overlaid onto an atlas for localisation

Right Insula: The insula is commonly implicated in mediating anxious behaviour in rodents and is increasingly studied in the chronic pain field (Méndez-Ruette *et al*, 2019).

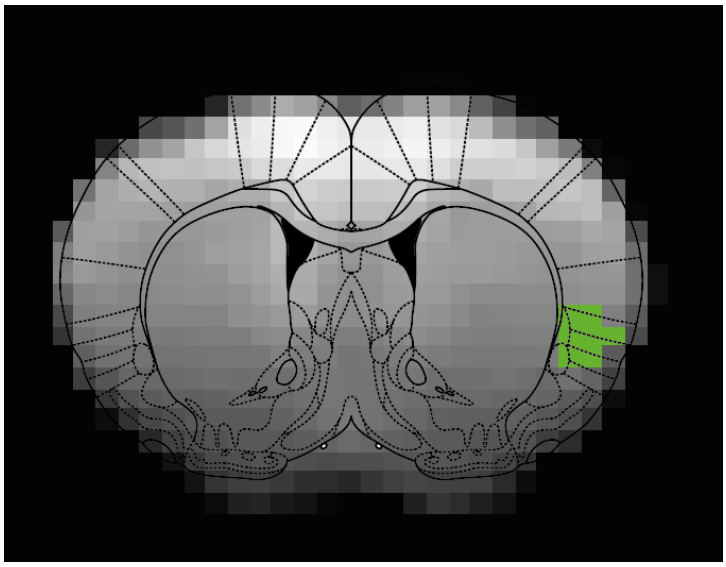

Figure 4.6: Manually drawn insula seed region, on an individual functional image, overlaid onto an atlas for localisation

4.3 Results

4.3.1 The MIA model in Wistar and WKY rats: pain behaviour

Following intra-articular injection of MIA, Wistar rats developed weight bearing asymmetry, with a shift of weight on to the uninjured limb, which was significant on all testing days post injection (Day 28: $p< 0.0001$) In the WKY rats, a shift of weight onto the uninjured limb was also seen and was significant at 14 and 21 days when compared to saline injected rats (Day 21: $p<0.015$, Fig 4.7).

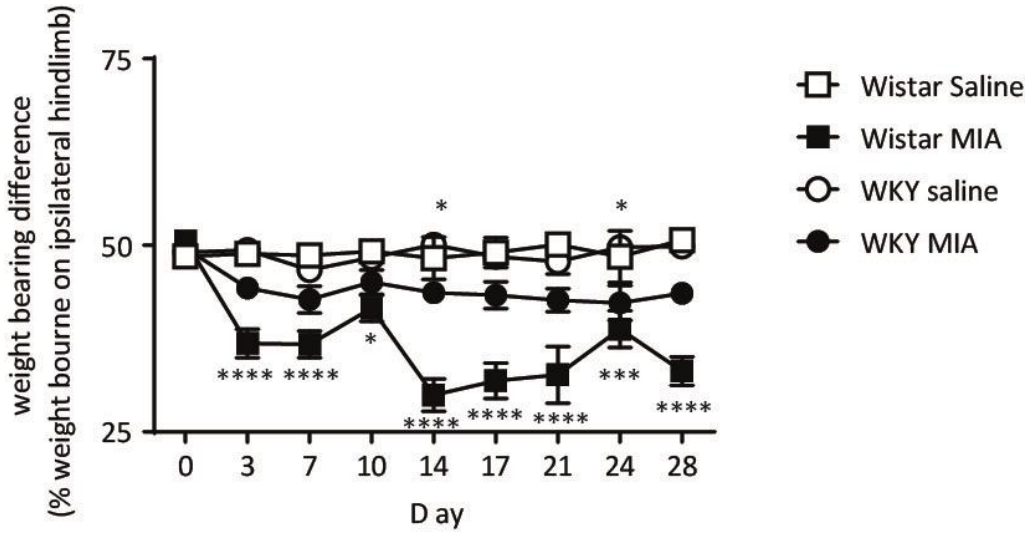

Figure 4.7: WB was measured at regular intervals following intra-articular injection of MIA or saline in Wistar and WKY rats (MIA n= 11 per group, Saline n=10 per group). There was significant WB asymmetry after MIA in both Wistar and WKY MIA treated rats. In Wistar rats this was evident from day 3, compared to their saline injected controls, in WKY rats WB was evident on days 14 and 21. Statistical analysis with ANOVA with Tukey's post hoc comparisons, **** $p<0.0001$, *** $p<0.001$, * $p<0.05$.

In Wistar rats, intra-articular injection of MIA was associated with a decrease in PWTs for the ipsilateral paw, which was significantly different from Wistar rats injected with saline from day 17 post intra-

articular MIA (Day 28: P<0.0001, Fig 4.8). In the WKY rats with intra-articular injection of MIA, the difference in ipsilateral PWTs was not significant when compared to WKY rats injected with saline at any time point. No significant differences were observed within strain between saline and MIA injected rats for contralateral PWTs.

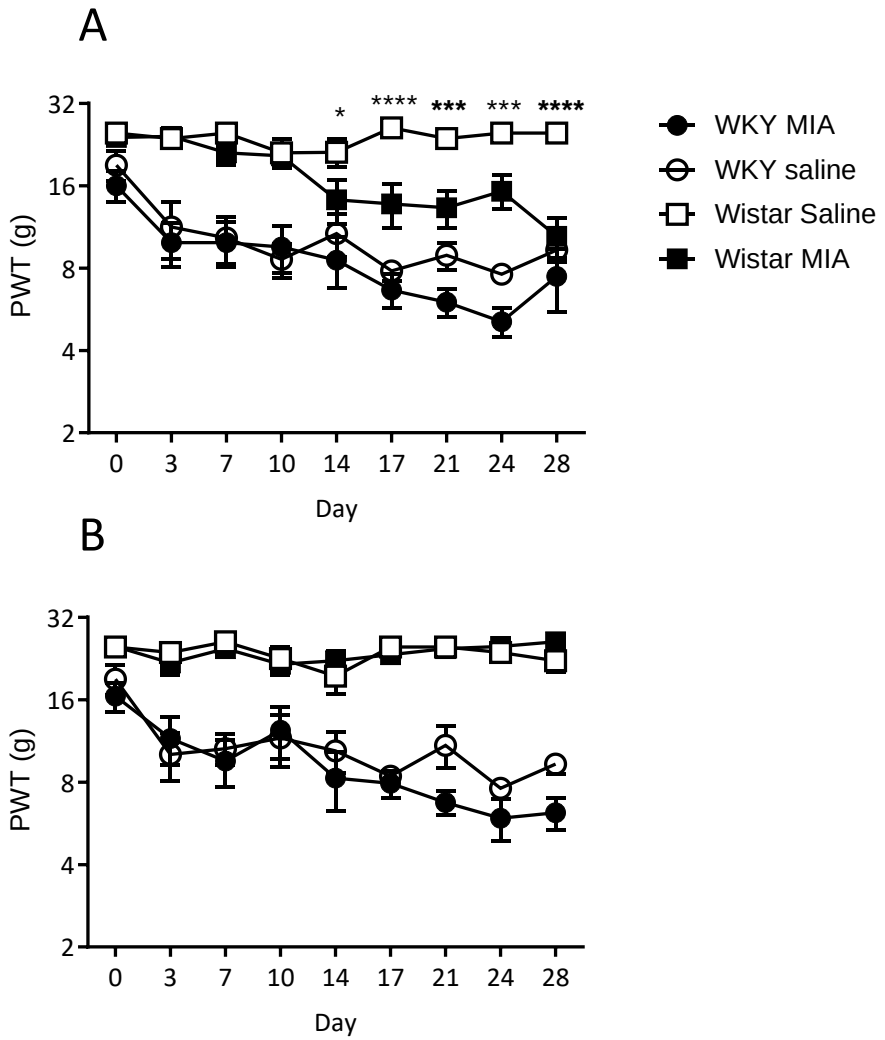

Figure 4.8: Effects of intra-articular injection of MIA or saline on ipsilateral (A) and contralateral (B) PWTs in Wistar and WKY rats (MIA n= 11 per group, Saline n=10 per group). Wistar MIA treated rats exhibited a significant lowering of ipsilateral PWTs from day 17 post MIA injection, and no lowering of contralateral PWTs, compared to saline control injection. The difference in ipsilateral and contralateral PWTs in WKY rats did not reach significance compared to saline control injection. Statistical analysis with two-way ANOVA with Tukey's post hoc * p <0.05, ** p <0.01, *** p <0.001, **** p<0.0001.

4.3.2 Assessment of anxiety levels in the Wistar Kyoto rats.

Time spent in the outer segment of the open arm was taken as a measure of lower anxiety behaviour. WKY rats, irrespective of treatment, spent significantly less time exploring the outermost section of the open arm in the EPM than normal anxiety Wistar controls. No significant differences were seen within strain between those with intra-articular saline and those with intra-articular MIA (Fig 4.9).

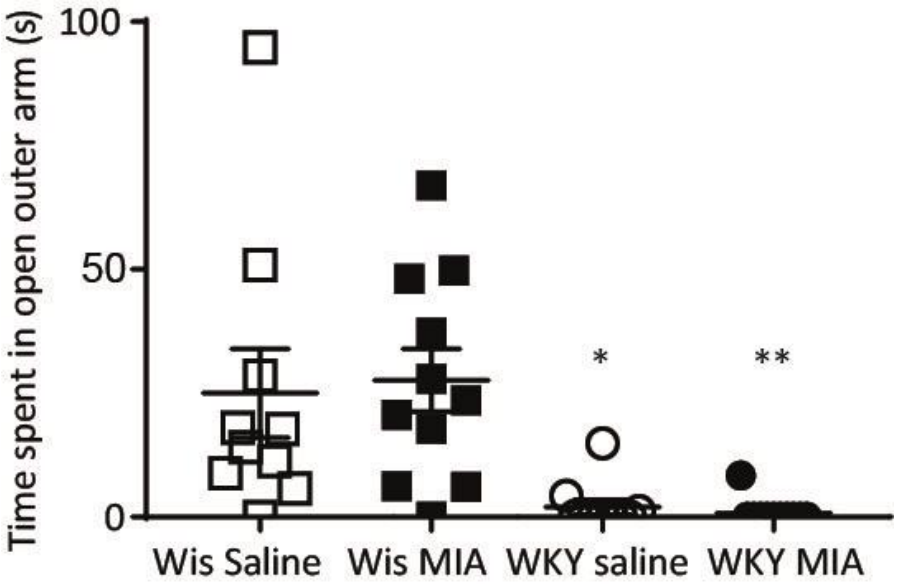

Figure 4.9: Anxiety-like behaviour was assessed in the elevated plus maze at day 27 of the MIA model in MIA injected wistar and WKY rats (n=11) and saline injected wistar and WKY rats (n=10). Comparison between strains revealed significantly less time was spent in the open arm of the maze by WKY rats, irrespective of treatment, when compared to normal anxiety Wistar rats. Statistical analysis with ANOVA ** $p<0.01$, * $p<0.05$.

Time spent in the centre of the open field arena was taken as a measure of lower anxiety-related behaviour. Although there was a significant effect of group, as assessed by one-way ANOVA ($F: 3.35, 38$, $p = 0.04$). Tukey's test for multiple comparisons identified no significant differences

between any groups post hoc. Significant differences were observed for velocity (F: 35.69, 38, p<0.0001) with Tukey's test for multiple comparisons identifying significant differences in velocity between strains, with no within strain differences from MIA (Fig 4.10, p<0.0001).

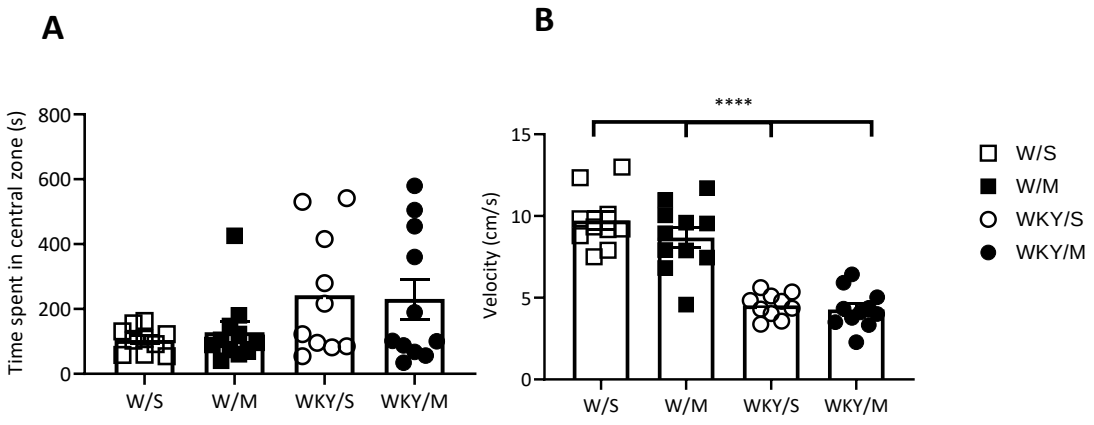

Figure 4.10: Anxiety-like behaviour was assessed in the open field on day 20 of the MIA model, in MIA injected wistar and WKY rats (n=11) and saline injected wistar and WKY rats (n=10). Comparison between strains revealed no significant difference between any group post hoc although there was a significant overall effect of group as identified by one-way ANOVA. Differences in velocity were observed between but not within strains, with WKY rats moving significantly more slowly within the arena. Statistical analysis with one-way ANOVA **** p<0.0001

4.3.3 An exploratory Independent component analysis (ICA) of resting state fMRI after intra-articular MIA

Exploratory ICA was conducted in order to explore differences in resting state networks between the strains and between saline and MIA injected rats. Individual datasets, acquired over 6.5 minutes, were decomposed into 40 spatio-temporal components.

Following intra-articular injection of MIA, a difference in functional connectivity was observed for one component in the Wistar rats. Significantly higher functional connectivity was observed in Wistar rats

with intra-articular MIA, when compared to Wistar controls, between a component of the sensory network (Fig 4.11A) and the dorsomedial PAG (Fig 4.9B, cluster size 10 voxels, maximum cluster intensity p = 0.003). In contrast, no significant differences were observed in WKY rats with intra-articular MIA and WKY control rats for any of the 40 components.

A strain comparison revealed no significant differences between functional connectivity with any of the 40 components between Wistar and WKY rats after FDR correction.

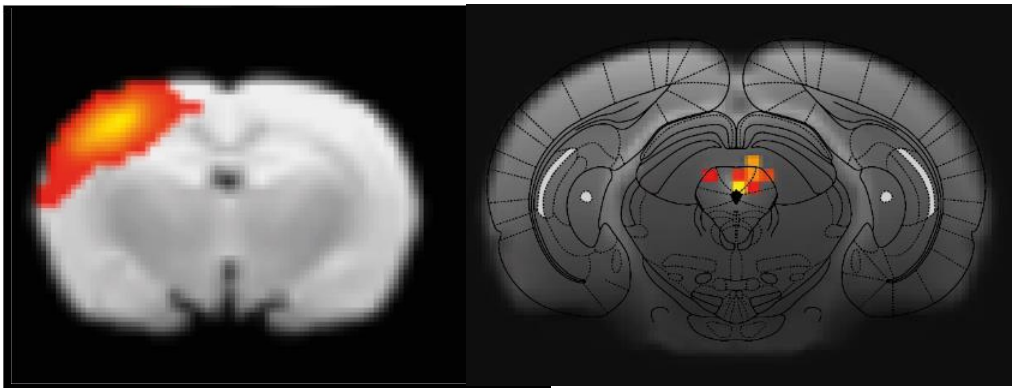

Figure 4.11: A) A spatio-temporal component from the ICA (grouped across all Wistar rats irrespective of treatment), spatially related to sensorimotor areas when overlaid onto an average anatomical image from these rats. B) Increased functional connectivity was observed between the component in A, and the dorsomedial PAG in Wistar rats with intra-articular MIA, when compared to saline injected Wistar rats. Analysis with randomise permutation testing and dual regression, with post-hoc FDR correction at p=0.025.

4.3.4 Seed based analyses

In order to investigate differences in rs-fc, associated with the MIA model and the WKY model of anxiety, seed based analyses were conducted to explore functional connectivity differences from pre-defined, manually created regional masks.

4.3.5 VmPFC (infra-limbic cortex)

A Seed-based analysis from the infra-limbic cortex, between Wistar rats with intra-articular MIA and control rats with intra-articular saline was conducted using FEAT, from a manually created mask. Intra-articular injection of MIA was associated with a lower functional connectivity between the infra-limbic cortex and a cluster of regions, located over the secondary somatosensory cortex and the caudate putamen (Fig 4.12).

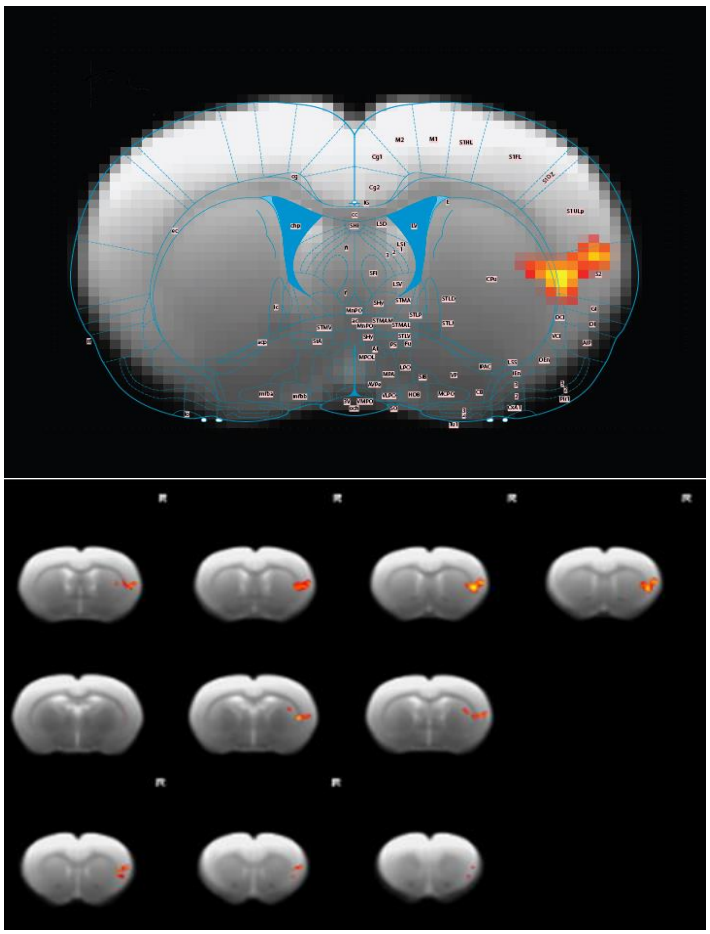

Figure 4.12: A, B) Significantly lower rs-fc was observed in Wistar rats with intra-articular MIA than in saline injected controls, between the infra-limbic cortex and clusters over S2 and caudate putamen. Analysis with FEAT and FDR correction for multiple comparisons.

4.3.6 WB asymmetry was differentially associated with IL-S2 FC in Wistar and WKY rats

A correlation was conducted between WB asymmetry values and Z scores extracted from the significant cluster (caudate putamen/S2) found in the initial VMPFC seed based analysis in the Wistar rats.

A significant correlation between weight bearing asymmetry and Z scores (reflecting the strength of functional connectivity) was observed for Wistar rats after MIA (Fig 4.12 A, r2 = 0.583, p=0.0031), with a decrease in weight borne on the injured limb correlating with increased fc. Interestingly, in contrast to this, a significant negative correlation was seen between fc Z scores and WB values for the WKY rats (Fig 4.12 B, r2 = 0.263, p=0.0248), with a higher weight bearing asymmetry correlating with lower fc.

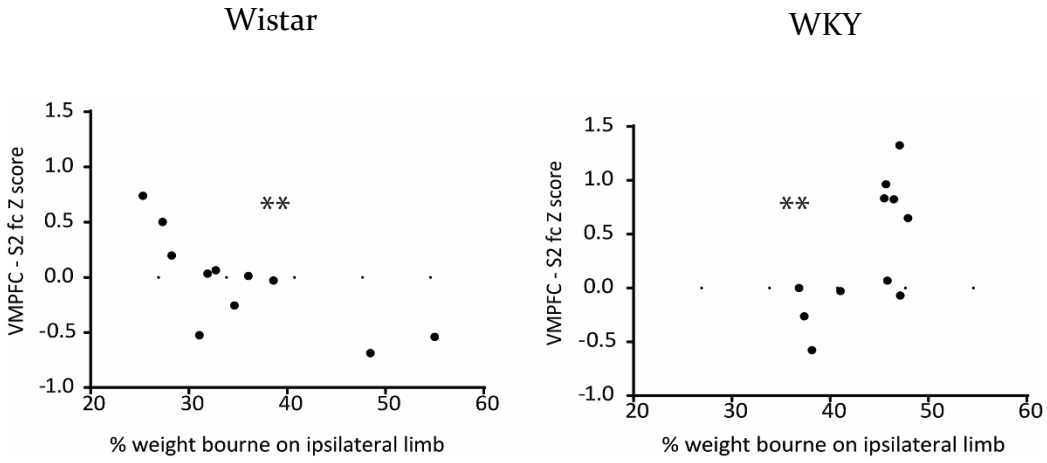

Figure 4.13: Correlation analysis between the FC Z scores *(the strength of the functional connectivity)* extracted from the significant caudate putament/S2 cluster (Fig 4.11) from the infralimibic cortex seed based analysis, with WB. A significant positive correlation was seen in Wistar rats after MIA (n=11) and negative correlation was observed between WB and FC for WKY rats after MIA (n=11). Analysis with Pearson correlation ** P<0.01.

4.3.7 Anxiety was not associated with IL-S2 FC in Wistar or WKY rats

There were no association between time spent in the open arms of the EPM and vmPFC – caudate putamen/S2 Z scores in either Wistar or WKY rats.

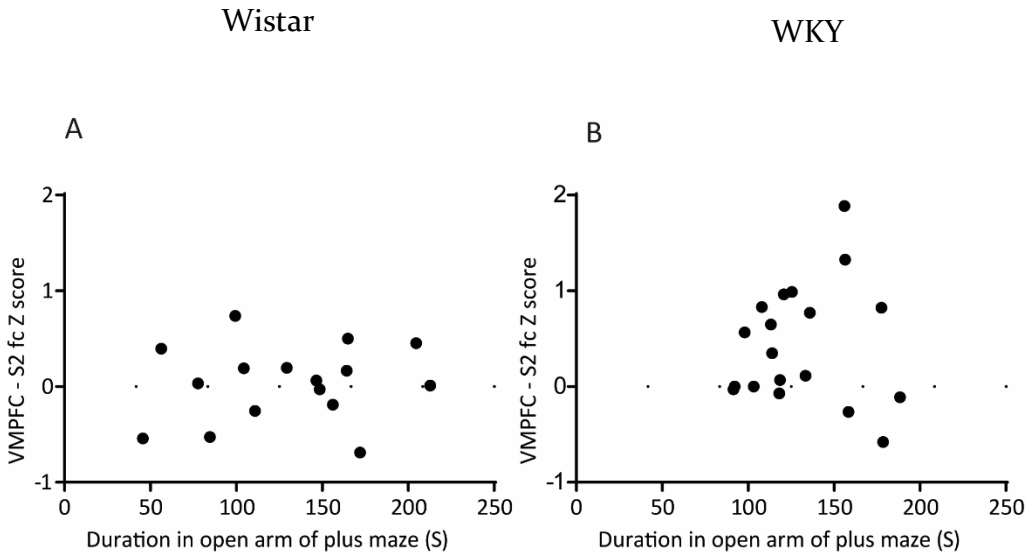

Figure 4.14: Correlation analysis between the FC Z scores extracted from the significant S2 cluster (Fig 4.11) from the infralimibic cortex seed based analysis, with anxiety scores (duration in open arm of plus maze). A significant negative correlation was observed between WB and FC for WKY rats. Analysis with Pearson correlation.

4.3.8 Functional connectivity changes with the Insula

No significant differences in rs-fc were observed from a manually created insula seed region between Wistar rats with intra-articular MIA and Wistar saline injected rats. Similarly, no significant differences in rs-fc

were observed between WKY rats with intra-articular MIA and WKY saline injected rats.

4.3.9 Functional connectivity changes with the PAG

A PAG seed region was manually created and signal intensity values were compared between Wistar rats with intra-articular MIA and saline injected rats (Fig 4.4).

Differences in functional connectivity, using the PAG as a seed region were assessed between the strains. No differences in PAG seed based functional connectivity were seen between Wistar and WKY rats and no difference in PAG seed based functional connectivity was seen between WKY saline and WKY MIA treated rats.

To check that this negative result was not a product of poor placement of the PAG mask, the PAG cluster revealed from the ICA (Fig 4.11 B) was used a seed region. No significant changes in fc from this seed were observed.

4.3.10 BOLD changes after noxious electrical stimulation

Technical difficulties were experienced during the first half of the stimulation runs. When these rats were excluded from the analysis and all remaining functional images were pooled during noxious electrical stimulation at 7.5mA, significant changes in BOLD signal amplitude were observed, only when the statistical threshold was lowered, uncorrected for multiple comparisons and thresholded at p=0.05.

While no differences were observable between groups or strains, stimulation at 7.5mA, 0.5 Hz was able to induce functional brain changes over somatosensory areas, although the biggest cluster of increased BOLD activity was located ipsilaterally, primarily over S1 forelimb (Fig 4.15).

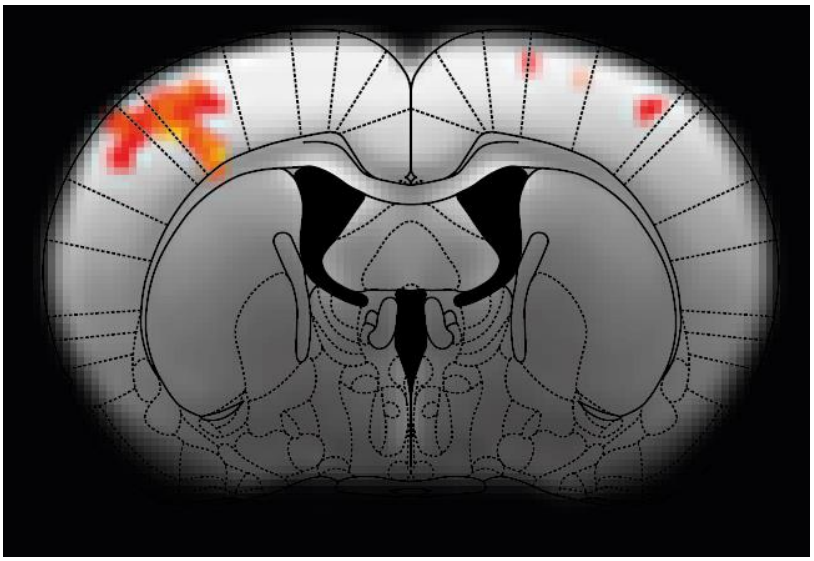

Figure 4.15: When all rats were grouped together (N=22), noxious electrical stimulation at 7.5mA was associated with BOLD signal increases over ipsilateral somatosensory areas, with small areas of activation contralaterally (P=0.05, uncorrected).

4.3.11 Functional connectivity changes after Naloxone

The effects of subcutaneous administration of naloxone in Wistar and WKY rats with and without naloxone were investigated using rs-fMRI.

Comparison of rs-fMRI immediately after naloxone administration (6 minute period) and 30 minutes after administration of naloxone (6 minute period) revealed no significant effect of treatment. Visual inspection of the raw data revealed no issues with data quality acquired.

4.4 Discussion

4.4.1 Resting state fc

In this study, changes in functional connectivity were observed after induction of the MIA model of OA joint pain in normal anxiety rats but not in the high anxiety WKY rats. Although the information that chronic pain is associated with changes in resting state functional connectivity is not new, the evidence base for these changes in the preclinical OA pain field is small. This study is one of few to demonstrate that these changes exist for a model of OA pain, in regions associated with the processing of pain. In addition, how these changes are altered in an OA model of pain in the presence of anxiety, has not yet been studied in the preclinical literature.

The normal anxiety Wistar rats displayed typical pain behaviour in response to the MIA model, with an increase in weight bearing asymmetry and a decrease in ipsilateral PWTs, with progression of the MIA model. For the WKY rats, no differences in functional connectivity were observed in rats that had received intra-articular MIA when compared to their saline injected controls. The behavioural profile of the WKY rats is significantly different to that of the Wistar rats. Both WKY rats injected with MIA and those injected with saline displayed a decrease in PWTs over time, and these were evident for both the ipsilateral and the contralateral paw. In addition, weight bearing differences in the WKY rats are much smaller than those for the Wistar rats. It is possible that *if* fc connectivity differences exist between WKY rats in the presence of MIA, the smaller differences in pain behaviour are reflected in very small differences in resting state activity that would not reach significance.

Interestingly, given the interest in the influence of anxiety and mood on pain, significant differences in functional connectivity with the VMPFC

were seen for the normal anxiety Wistar rats. The higher functional connectivity between the vmPFC and the secondary somatosensory cortex, in the rats experiencing the pain state may suggest that chronic pain could influence the ability of VMPFC to regulate negative emotional responses to pain (Yu *et al.*, 2014).

The lack of a significant difference in fc from the vmPFC and for the ICA for the WKY rats is not surprising. Behaviourally differences between the rats experiencing joint pain and those not experiencing joint pain are similar, with saline treated rats experiencing paw sensitivity that is often not much lower than that of those experiencing joint pain. Speculatively, this lack of a difference could originate from a number of causes. It is possible that the repeated von Frey stimulation is sufficient to cause sensitisation in these rats, or that the stress of behavioural testing increases hypervigilance to stimulation.

However, correlation analysis did reveal differences in functional connectivity, when the Z scores from the connectivity between the vmPFC and the caudate putamen/S2 cluster were correlated with WB asymmetry. A negative correlation was observed in the WKY rats, with higher levels of weight bearing asymmetry correlating with lower VMPFC – caudate putamen/S2 fc.

4.4.2 Naloxone

Subcutaneous naloxone was administered to investigate the effects of the μ opioid antagonist in on BOLD activity in the Wistar and WKY rats. Data from the first 6 minutes after administration of naloxone were compared to a 6 minute time period measured 30 minutes after naloxone administration. No differences in BOLD activity were observed between any of the groups.

4.4.3 Limitations

There were a number of limitations to this study. During the scanning period, experimental error led to an incorrect and suboptimal flip angle being inputted, with a difference of 10 degrees. A significant amount of data had been collected, and visual inspection of the data raised no obvious concerns, with good signal to noise. Although it is probable that this error did not have a significant impact on the results, it is possible that we may have obtained stronger results with a more optimal flip angle.

The literature for preclinical RS-fMRI studies of OA pain is small, with highly discordant results. Although changes in FC have been shown in OA model pain states and in chronic pain of other causes, the results are often not replicable. Reported results include regions that implicated in pain processing but the regions reported differ between studies. This is not unexpected given the number of differences between the studies reported in the literature. Differences in species, strain, anaesthesia, models of chronic pain, nociceptive stimulation, and differences in hardware could all contribute to these discordant findings. Without replicable findings, while it is now clear that there is a difference in functional connectivity after chronic pain, it is not necessarily clear what the nature of this difference is. For these results to be pertinent to the understanding of human OA pain, they need to provide a more detailed account of these changes and how they relate to levels of joint pain, central sensitization, levels of anxiety or other features of chronic pain.

This study was limited to the study of static functional connectivity, averaged over an extended period of time. The degree to which functional connectivity remains static is now heavily debated with evidence to suggest that functional connectivity is more dynamic than previously thought (Preti, Bolton and Van De Ville, 2017). Evidence

supports that changes in the dynamics of functional connectivity are relevant for differences in behavioural tasks, and that the dynamic FC may be relevant for changes in underlying neural circuitry (Jia, Hu and Deshpande, 2014). It is possible that changes in the dynamics of functional connectivity may more accurately reflect the changes that occur during pain and anxiety.

The lack of a functional connectivity between the PAG other regions between groups was surprising. There are a few reasons that this may have occurred. It is possible that it may have been a result of poor placement of the PAG seed region, but the use of the PAG cluster from the ICA (Fig 4.9) as a seed and the confirmation of this negative result, makes this unlikely. ICA and seed based analyses are driven by different underlying statistical theories, making quantitative comparisons between the approaches complicated (Wu *et al*, 2018).

Chapter 5 Opioid sensitivity in a rodent model of osteoarthritis and high anxiety

5.1.1 Introduction

Pain from OA is difficult to treat. Although NSAIDs provide clinically significant pain relief for OA patients (Bannuru *et al*, 2015), they are not suitable for many patients due to the possibility of gastrointestinal or renal adverse side effects, particularly in the elderly or when used long term (Pelletier *et al.*, 2016). Opioid analgesics are commonly prescribed alternative for a number of chronic pain conditions (lower back pain, neuropathic pain). In patients with OA, opioid analgesics are used in cases of more severe pain which are unresponsive to NSAIDS (Pelletier *et al.*, 2016). Although opioids are effective as analgesics, their use in knee or hip OA is not currently supported, with recent findings demonstrating that opioids are not more effective than non-opioid alternatives

In OA patients, when pharmacological treatments are no longer effective, total joint arthroplasties are conducted to remove the affected joint. The majority of patients have a good treatment outcome from total knee arthroplasty (Busse *et al*>, 2018). However, for approximately 20% of patients both chronic pain and disability persists, despite good surgical outcomes based on radiographic appearances of the joint and surgeon assessments (Beswick *et al.*, 2012). In a meta-analysis of hip OA patients, between 14- 36% of OA patients experienced no improvement or worsening of their symptoms (based on the WOMAC arthritis index) 12 months after surgery (Judge et al., 2010), however it is unclear why joint pain persists in some patients after total joint replacement. No clearly defined relationships between clinical variables and health related quality of life (HRQL) have been found, with demographics,

physiological co-morbidities, preoperative health status, type of prosthesis and complications from surgery providing an incomplete explanation of the variability in pain and disability experienced (Jones et al. 2007).

5.1.2 Opioid analgesics: mechanisms of action and side effects

There are many different opioid analgesic drugs, most commonly prescribed are codeine, tramadol, morphine, buprenorphine and oxycodone (Ashaye *et al*, 2018). There are 3 main opioid receptors (μ, δ, and κ), these are inhibitory G protein coupled receptors which are activated by the endogenous opioids endorphin, enkephalin and dynorphin (Hughes *et al.*, 1975; Simantov and Snyder, 1977; Goldstein *et al.*, 1979). Both the beneficial effects and main side-effects mediated by opioid agonists arise from activation of these receptors (Ling *et al.*, 1985; Millan, 1990; Loh *et al.*, 1998; McMahon, 2013). The analgesic effects of the opioids are predominantly mediated by actions at opioid receptors within the central nervous system, both in the spinal cord and in supraspinal centres, primarily at the μ opioid receptors (McMahon, 2013).

Chronic pain conditions can influence opioid receptor function, with evidence for reduced opioid receptor expression in the spinal dorsal horn after peripheral nerve injury (Porecca, 1998). Supraspinally, reduced opioid receptor availability has been demonstrated in the insula, caudate-putamen and motor cortex in a model of neuropathic pain in the rat (Thompson *et al*, 2018). Although these studies demonstrate that chronic pain can alter opioid receptor systems in the central nervous

system, there has been little mechanistic investigation of this in other chronic pain states, such as OA pain.

The use of opioid medications is associated with a number of adverse side effects including dry mouth, nausea, sedation, constipation, dizziness and tiredness, as well as overdose and addiction (Kalso *et al*, 2004; Vowles *et al*, 2015). Although tolerance to some of these side effects occurs, prolonged use of opioids can create additional clinical issues, such as opioid induced hyperalgesia and tolerance to analgesia (Roeckel *et al.*, 2017).

Opioid tolerance is characterised by a reduced responsiveness to opioid agonists, leading to increasing dose requirements to achieve similar analgesic effects. Clinically, doses can escalate quickly and dramatically in chronic pain patients (Buntin-Mushock *et al*, 2005). Opioid induced hyperalgesia manifests as an increase in pain sensitivity following exposure to opioids and is thought to result from alterations in supraspinal sites, leading to descending facilitation of pain from the RVM, through increased expression of dynorphin in the spinal cord (Ossipov *et al.*, 2003).

Given the prevalence of opioid-induced adverse side effects, there is rising criticism of the use of opioid analgesics for non-cancer chronic pain (Von Korff and Deyo, 2004; Veiga *et al*, 2018).

5.1.3 Does negative affect influence outcomes following total joint replacement for OA pain?

A high proportion of chronic pain patients exhibit co-morbid conditions such as depression, generalised anxiety disorder, phobias and panic disorders (McWilliams, Cox and Enns, 2003; McWilliams, Goodwin and Cox, 2004). The proportion of people with OA pain that also have

comorbid anxiety or depression is high with estimates of 17.5% for co-morbid depression (Swain *et al*, 2019) and 16.1% for clinical anxiety conditions (Barnett *et al.*, 2018). Individuals that undergo total joint replacement surgery have higher rates of psychological symptoms than the general population, with only modest improvements post-surgery (Scott, Mathias and Kneebone, 2016) and evidence suggests that psychological co-morbidities, including pain catastrophizing are predictive of chronic post-operative pain after total knee arthroplasty (Forsythe *et al.*, 2008).

There is evidence to suggest that poor outcomes after opioid use prior to total joint replacement surgeries could be related to the poor outcomes linked to psychological co-morbidities. For example, patients who use opioids prior to TKA obtain less pain relief from TKA in the postoperative period (Savannah *et al.*, 2017). Chronic opioid use prior to TKA has additionally been shown as a risk factor for complications and painful and prolonged recovery from surgery (Zywiel *et al.*, 2011). While opioids play an important role in modulating pain responses, they also play an important role in anxiety, fear responses and depression (Winters *et al.*, 2017; Peciña *et al.*, 2018). Differences in opioid analgesia have been shown to vary between sexes as well as with positive/negative affect and pain catastrophizing (Fillingim *et al.*, 2005). Pain catastrophizing is also associated with both individual differences in pain intensity and analgesic use (Jacobsen and Butler, 1996). In these instances, the effectiveness of opioids in providing analgesia and the risk for misuse is altered, with these patients experiencing less analgesia and being at higher risk for misuse (Wasan, Davar, and Jamison 2005; Feingold et al. 2017, 2018). After total joint replacement surgery for knee OA, catastrophizing, a key feature of anxiety disorders, has been shown to be

associated with significantly higher opioid analgesic use (Valdes *et al.*, 2015).

5.1.4 Hypothesis and Aim

There is mounting evidence that the complex interplay between pain and anxiety has detrimental effects on the individual, with OA patients exhibiting greater pain responses and reduced responsiveness to opioid analgesics.

The reduced effectiveness of opioids in patients with OA and anxiety may arise as a result mechanisms of central sensitisation exacerbating pain responses, differences in levels of the endogenous opioids and/or changes in opioid receptor signalling. The duration of time that individuals experience OA pain, differences in the pain experience, and the range of treatments received make it challenging to understand potential causal relationships between pain, anxiety and opioid use. Rat models of OA pain and anxiety allow for more controlled testing of these variables and the ability to robustly explore the effects of pharmacological interventions on OA joint pain.

The aim of the work in this chapter was to investigate whether the changes in the effectiveness of opioids in people with high anxiety and OA pain could be modelled in rats, and then to determine potential underlying mechanisms of any change in opioid receptor function.

To address this aim, the first experiments investigated sensitivity to morphine analgesia between an inbred high anxiety strain of rat and a typical anxiety strain of rat, with and without OA like pathology. In separate groups of rats, the second experiment investigated whether there was evidence for a shift in the endogenous opioid receptor system in rats with high anxiety phenotype and OA pain behaviour. This was

achieved by determining the effects of the μ opioid receptor antagonist naloxone on pain behaviour in the different groups of rats described above. These experiments were undertaken in the well characterised MIA model of OA pain which is described in the general methods. The high anxiety phenotype was modelled in the rat by using an inbred strain, the Wistar Kyoto (WKY) rat, which exhibits well-described anxiety and depressive like behaviours as discussed in the general introduction.

5.2 Methods

The experiments described were conducted in accordance with the Animals (Scientific Procedures) Act 1986 which incorporates Council Directive 2010/63 EU of the European Parliament.

5.2.1 Animals

All rats were kept in conventional open top cages and on a reversed 12 hour dark/artificial light cycle. Holding rooms were maintained at a temperature of 22°C and at a humidity of 55%. Food and water were available ad libitum.

Morphine study: 36 adult male Wistar (Charles River, Margate, UK) and Wistar-Kyoto (Envigo, UK) rats were used for this study (approximately 150g). Rats from each strain (Wistar n=18, WKY n=18) received intra-articular injection of MIA (n=10) or saline (n = 8). The study was conducted in two batches, behavioural testing occurred in groups of 4 or 5, with both strains tested during each session. MIA and saline animals were housed together in groups of 4, within their strains.

Naloxone study: 45 adult male Wistar (Charles River, Margate, UK) and Wistar-Kyoto (Envigo, UK) rats were used for this study (approximately 150g). The rats were split into 4 groups: Wistar saline: (N=10), Wistar MIA (N=12), WKY saline (N=10) and WKY MIA (N=11). Rats were tested in groups of 6, with both strains tested during each session. The study was conducted in two batches, with MIA and saline animals housed together in groups of 4, within their strains.

Exclusions: Some rats were excluded from the study as a whole, or from the naloxone time course. In the naloxone study: 4 rats were excluded from the day 21 naloxone time course due to disruption of the experimental environment resulting in clear effects on pain behaviour. 8 rats were excluded on the basis of joint pathology being inconsistent with the initial treatment received (saline/MIA).

5.2.2 Intra-articular injections

All rats received a singular 50µl intra-articular injection into the left knee, through the infra-patellar ligament under isoflurane anaesthesia (3% 1L/min 02). 20 rats (N=10 per strain) received 1mg/50µl in 0.9% saline of monosodium iodoacetate (MIA) whereas 16 rats (N=8 per strain) received 50µl 0.9% saline using a 50 gauge hypodermic needle.

Post injection, rats were health checked and returned to their home cages after recovery. Health was monitored daily for 3 days and then weekly. The experimenter was blinded to the treatment given to each animal. Due to differences in size between the Wistar and WKY rats, it was not possible to be blinded to strain.

5.2.3 Behavioural testing

All rats received two habituation sessions to the pain behaviour testing environment to minimise any exploratory behaviour during testing. Baseline measurements were taken prior to injection on day 0 in the morning, and behavioural measurements were subsequently measured from day 3 to day 21 post model-induction, twice weekly. Both weight bearing asymmetry (WB), and mechanical hind paw withdrawal thresholds (PWTs) for both the paws both ipsilateral and contralateral to the affected joint were assessed.

Healthy rats distribute their weight evenly between limbs and a weight shift onto the contralateral limb is taken as an indicator of pain in the ipsilateral knee joint. WB was assessed using an incapacitance tester (Linton Instrumentation, Diss, UK). A minimum of three measurements were taken where possible, with extra measurements taken when an animals activity levels precluded obtaining consistent measurements.

PWTs were measured using von Frey monofilaments across a range of forces (2, 4, 6, 8, 10, 15 and 26g). The filaments were applied to the plantar surface of each hind paw for 3 seconds or until the paw was withdrawn using criteria similar to that of Chaplan et al (Chaplan, Bach, Pogrel, Chung, & Yaksh, 1994). Each filament was applied in ascending order until 2 out of 3 applications elicited a withdrawal response. The filaments were then applied in descending order until no response was evoked and then then reapplied in ascending order until a response was evoked again. This was taken to be the final PWT.

5.2.4 Morphine / naloxone dose response study

On day 21 post intra-articular injection of MIA, rats underwent behavioural testing with WB and PWTs. In one group of rats (Wistar N=18, WKY N=18), each rat was then given 3 subcutaneous injections of

either morphine (0.5, 2.0 and 3.5mg/kg/ml, cumulative dose 6 mg/kg/ml) or vehicle in equivalent volumes (0.9% saline), at 60 minute intervals. WB and PWTs were measured at 60 minutes post injection.

In a separate groups of rats (Wistar N=22, WKY N=21) after behavioural testing each rat was given 3 subcutaneous injections of either naloxone (0.1, 0.3, 1mg/kg/ml) or an equivalent volume of vehicle (0.9%s saline) at 60 minute intervals. PWTs only were measured at 15, 30 and 60 minutes post injection.

6.2.5 ELISA measurement of beta-endorphin

In the first subset of rats (N=36), blood samples were collected at day 14, from the tail vein, into heparin containing tubes. The samples were placed on ice for up to an hour and centrifuged for 15 minutes at room temperature at 13,000rpm and the supernatant plasma was collected. Plasma samples were assayed for levels of corticosterone and melatonin using the Abcam corticosterone ELISA kit (Abcam, Cambridge, UK) and a rat melatonin ELISA kit (CUSABIO, Houston, USA). The standards and samples were run in duplicates and the optical density of each well was determined at 450nm.

5.2.6 Knee joint collection for pathology

Ipsilateral and contralateral knee joints were collected whole on day 21 of the model and placed into 4% PFA. Prior to macroscopic scoring (described in methods, chapter 2), collected knee joints were disarticulated.

5.2.7 Statistical analyses

Data were analysed using GraphPad Prism (GraphPad Software Inc., California). All statistics are presented as mean +/- SEM, unless otherwise stated.

Pain behaviour data between the four strain and treatment groups, over multiple time points were analysed with a two-way ANOVA, with Tukey's test for multiple comparisons. Cartilage integrity over the four groups at the final time point was analysed using a one-way ANOVA.

Unpaired t-tests were used to analyse two group, strain comparison data between Wistar and WKY rats. Mann-Whitney tests were used instead, when data were abnormally distributed.

% Analgesia was calculated using the following formula:

((100/baseline measurement) * post-treatment measurement) – baseline measurement

5.3 Results

5.3.1. Assessment of the behavioural phenotype of Wistar Kyoto rats

Prior to commencing the assessment of OA pain responses, it was essential to characterise the behavioural phenotype of the WKY rats compared to controls. There were no significant differences in locomotor activity (velocity) in the open field arena between Wistar rats and WKY rats (Fig 5.1 A). Similarly the total distance covered in the arena was comparable for the two strains of rats (Fig 5.1 B).

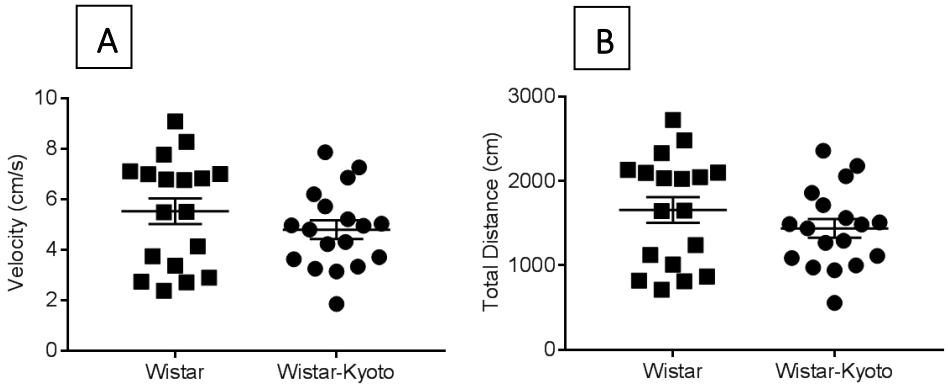

Figures 5.1: Locomotor activity prior to any intervention in Wistar (N=18) per group and WKY rats (N=18). Comparison between strains revealed no difference in (A) velocity (cm/s) and (B) total distance (cm) in the open field arena in WKY rats compared to normal anxiety Wistar rats. Statistical analysis with unpaired t-test.

Prior to any intervention, anxiety like behaviour was also assessed in WKY and Wistar rats. WKY rats exhibited higher levels of anxiety-like behaviour compared to Wistar rats (Fig 5.2). WKY rats spent significantly less time in the centre of the arena ($p = 0.0039$) and crossed the central area of the arena significantly fewer times ($p = 0.0057$) compared to Wistar rats, confirming increased levels of anxiety-like behaviour.

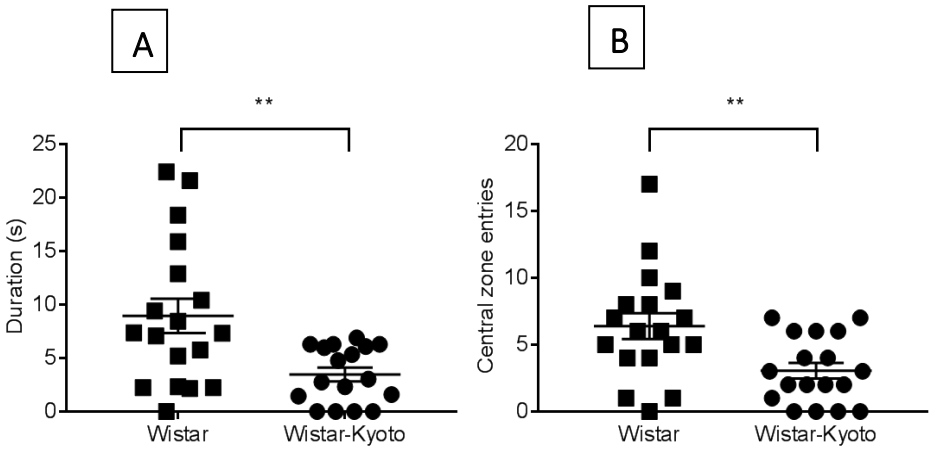

Figures 5.2: Anxiety-like behaviour was measured prior to any intervention in Wistar (N=18) and WKY (N=18) rats. Comparison between strains revealed a significant difference in A) the duration spent in the centre of the open field and B) the number of crossings into the centre zone of the open field arena, indicating higher levels of anxiety-like behaviour in WKY rats compared to Wistar rats. Statistical analysis with unpaired t-test ** $p<0.01$.

In a separate group of rats (N=22), anxiety-like behaviour was measured using the elevated plus maze prior to any intervention (Fig 5.3). WKY rats spent significantly less time exploring the open arm of the plus maze compared to Wistar rats ($p=0.0063$).

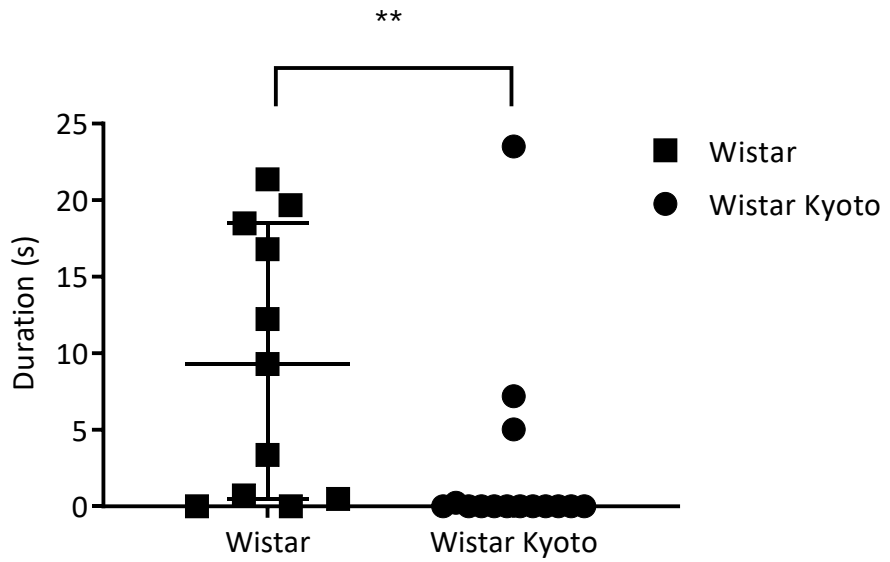

Figure 5.3: Anxiety-like behaviour was assessed in the elevated plus maze prior to any intervention in Wistar rats (n=11) and WKY rats (n=11). Comparison between strains revealed significantly less time was spent in the open arm of the maze by WKY rats when compared to normal anxiety Wistar rats. Statistical analysis with Mann-Whitney ** $p<0.01$.

5.3.2 Baseline pain responses

Prior to intra-articular injection of MIA or saline, Wistar and WKY rats distributed their weight equally between the hind paws (Fig 5.4A, $p = 0.3860$). Similarly, there were no differences between the ipsilateral and contralateral PWTs in Wistar and WKY rats (Fig 5.4B, ipsilateral PWTS: $p= 0.064$).

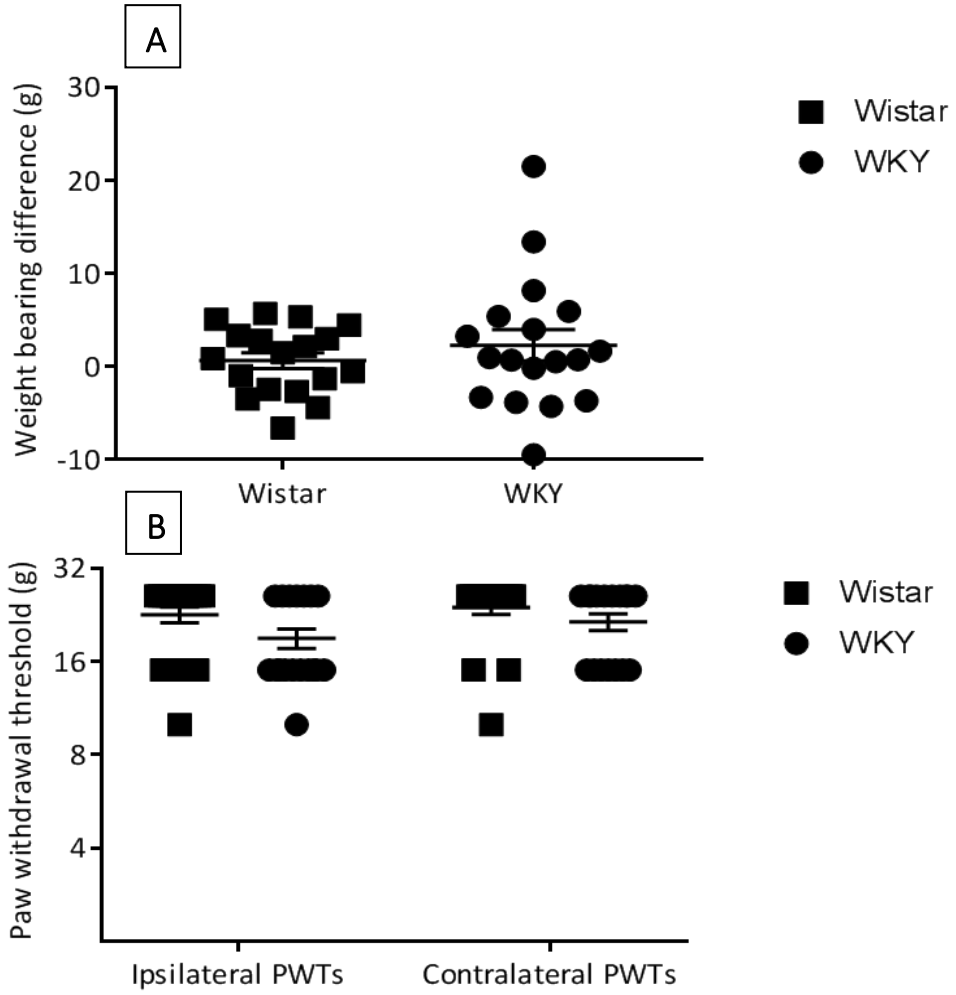

Figure 5.4: Weight bearing and paw withdrawal thresholds were measured prior to any intervention in Wistar (N=18) and WKY (N=18) rats. Strain comparison revealed no significant differences for either measure of pain behaviour. Analysis with unpaired t-test.

5.3.3 The MIA model of OA in Wistar and Wistar Kyoto rats: pain behaviour

Following intra-articular injection of MIA, Wistar rats started to develop weight bearing asymmetry from day 3 post-injection. MIA treated Wistar rats placed less weight on the injected limb, compared to the non-injected limb (Fig 5.5 A) with significant differences evident from day 3 until the end of the study. Similarly, intra-articular injection of MIA in WKY rats was associated with a weight bearing asymmetry compared to saline injected rats (Fig 5.5 B). Comparison between the two strains of rats injected revealed a significantly greater WB asymmetry at day 21 in Wistar MIA rats versus WKY MIA rats (Wistar vs WKY, 39% +/- 1.1% vs 44% +/- 1.0% weight borne on injured limb (Fig 5.5 A)). Apart from this difference; the profile of the pain behaviour was comparable between the two strains of rats.

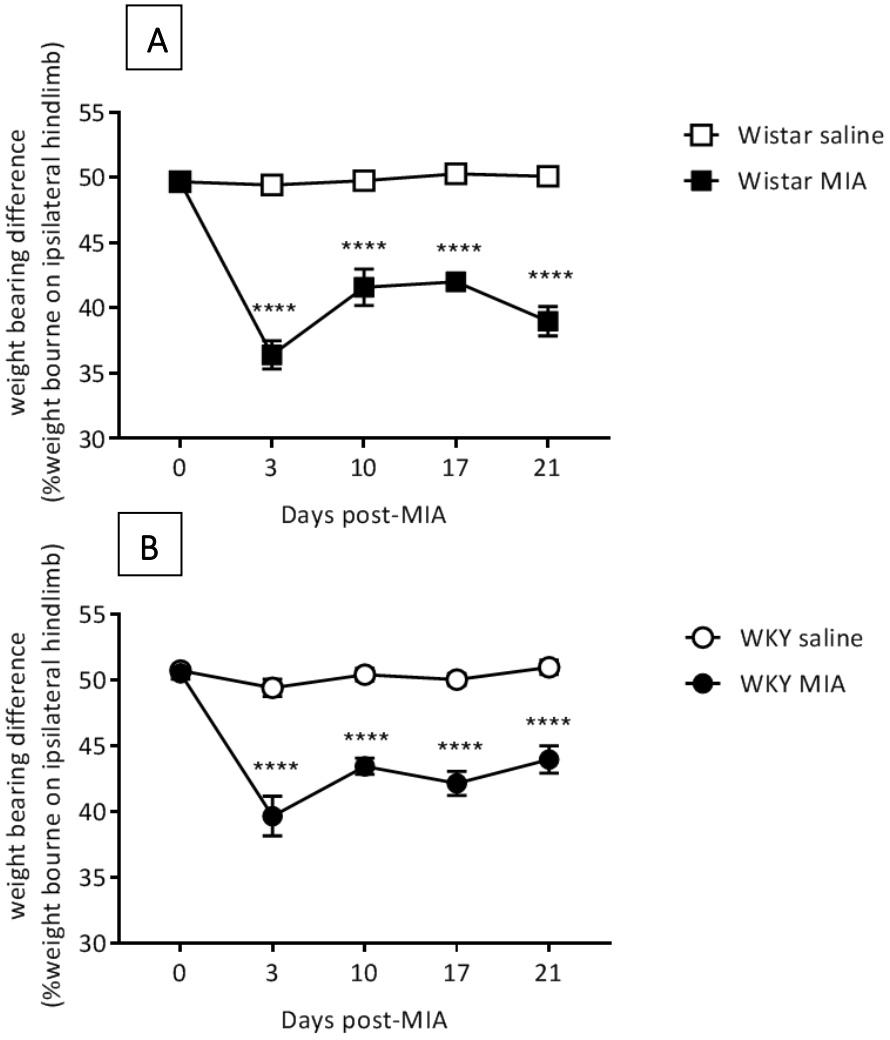

Figure 5.5: WB was measured at regular intervals following intra-articular injection of MIA or saline in Wistar and WKY rats (MIA n= 10 per group, Saline n=8 per group). There was significant WB asymmetry after injection of MIA in both Wistar and WKY MIA treated rats from day 3, compared to their saline injected controls. Wistar MIA injected rats exhibited significantly greater weight bearing asymmetry on day 21 of the model than WKY rats injected with MIA. Statistical analysis with two-way ANOVA, ****p <0.0001

In Wistar rats, intra-articular injection of MIA was associated with a reduction in ipsilateral PWTs. Significant differences compared to saline injected control rats were evident from day 10 until the end of the study (Fig 5.6 A). Similarly, intra-articular injection of MIA was also associated with lowered ipsilateral PWTs in WKY rats, which were significant compared to saline injected rats from day 10 -17 (Fig 5.6 B). Comparison

between the two strains of rats injected with MIA revealed a significantly greater reduction of PWT in WKY rats (8g ± 2.04g) versus Wistar rats (15.7g ± 1.86g) at day 21 (Figs 5.6 A, 5.6 B; Two-way ANOVA revealed a significant interaction between groups (4 groups: strains (Wistar/WKY

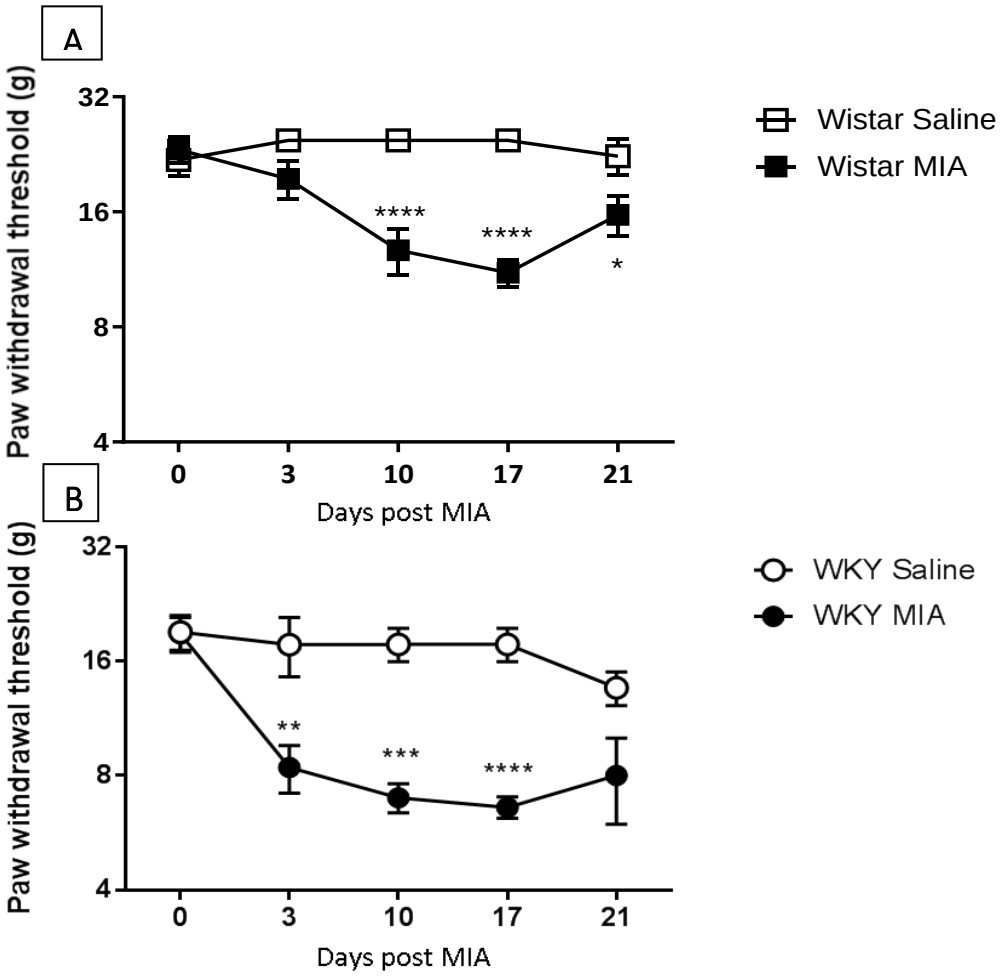

Figure 5.6: Effects of intra-articular injection of MIA or saline on Ipsilateral PWTs in Wistar and WKY rats (MIA n= 10 per group, Saline n=8 per group). Wistar MIA treated rats exhibited a significant lowering of PWTs from day 10 post MIA injection, compared to saline control injection (A). WKY rats exhibited a significant lowering of PWTs from day 3 post MIA injection until day 17 compared to saline control injection (B). Statistical analysis with two-way ANOVA, graphically represented separately **** p <0.0001.

and treatments(MIA/Saline)) and time points ($p < 0.0001$).

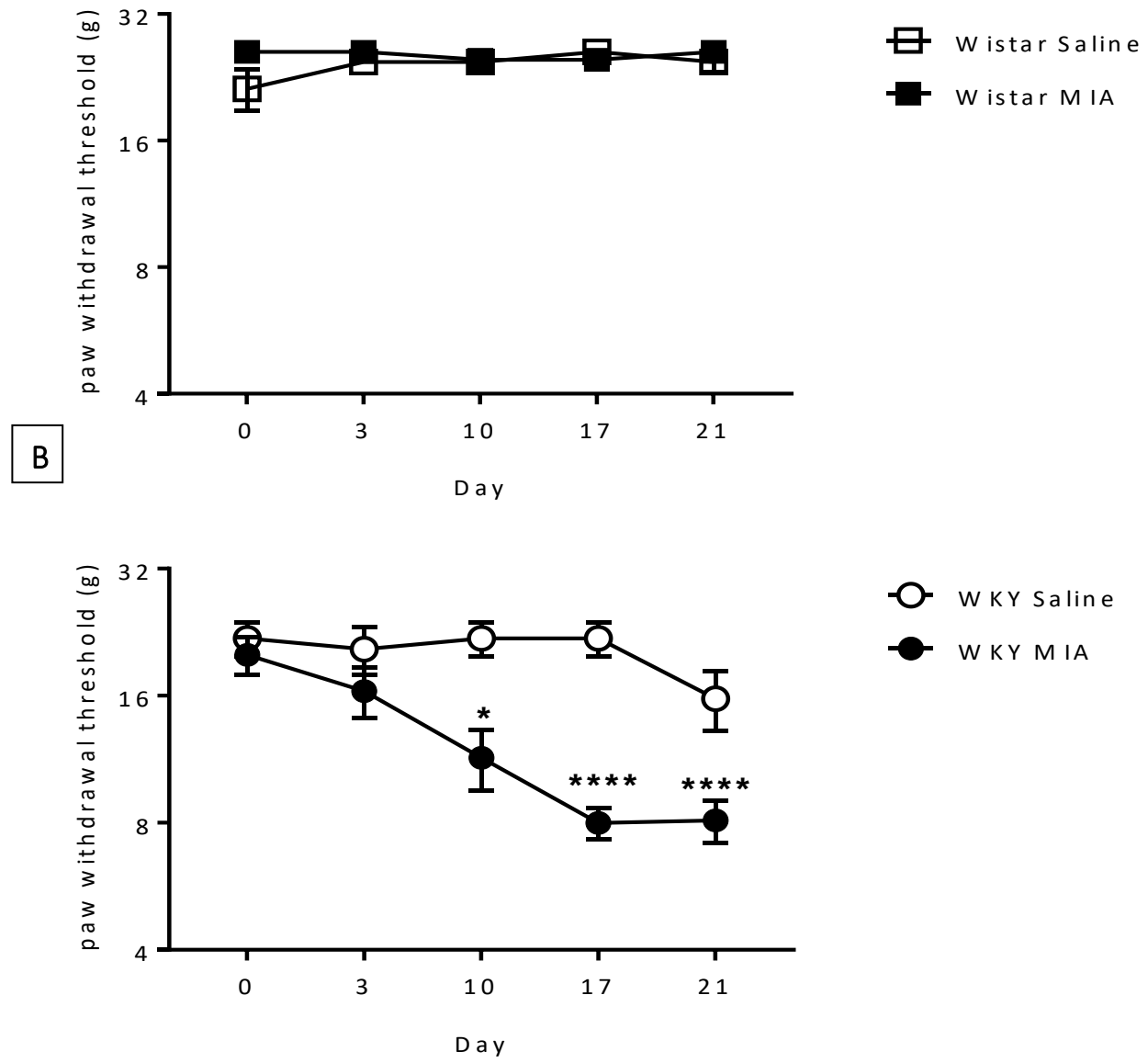

Figure 5.7: Effects of intra-articular injection of MIA or saline on contralateral PWTs in Wistar and WKY rats (MIA n= 10 per group, Saline n=8 per group). Wistar MIA-treated rats did not exhibit significant lowering of PWTs on any day post MIA injection, compared to saline control injection. WKY rats exhibited a significant lowering of PWTs from day 10 post MIA injection until the end of the study compared to saline control injection. Statistical analysis with two-way ANOVA ****$p < 0.0001$ compared to saline controls.

In Wistar rats, intra-articular injection of MIA was not associated with a reduction in contralateral hind paw withdrawal thresholds on any day post MIA injection when compared to saline injected controls (Fig 5.7 A).

In WKY rats, intra-articular injection of MIA was associated with lowered contralateral hind paw withdrawal thresholds compared to saline injected controls (Fig 5.7 B), which were significant from day 10 until the end of the study. Comparison between the two strains of rats injected with MIA revealed a significant difference in PWTs at day 21 in Wistar rats vs WKY rats (Wistar MIA vs WKY MIA, 26g +/- 0g vs 8g +/- 0.9g; Figs 5.7 A, 5.7 B, There was a significant interaction between groups and time points, p <0.0001).

5.3.4 The effects of the MIA model of OA pain on cartilage integrity

In a subset of rats used in the study, the effects of intra-articular injection of MIA (versus saline) on cartilage integrity was determined in Wistar and WKY rats (Fig 5.8). MIA treatment was associated with significant cartilage damage in both strains of rats. A significant effect of treatment (Saline vs MIA) was seen in both strains (P<0.0001) and strain comparison revealed a difference in cartilage damage between Wistar rats and WKY rats injected with MIA (Wistar MIA vs WKY MIA, 22.2 +/- 0.9 vs 17.3 +/-1.7, P=0.0236).

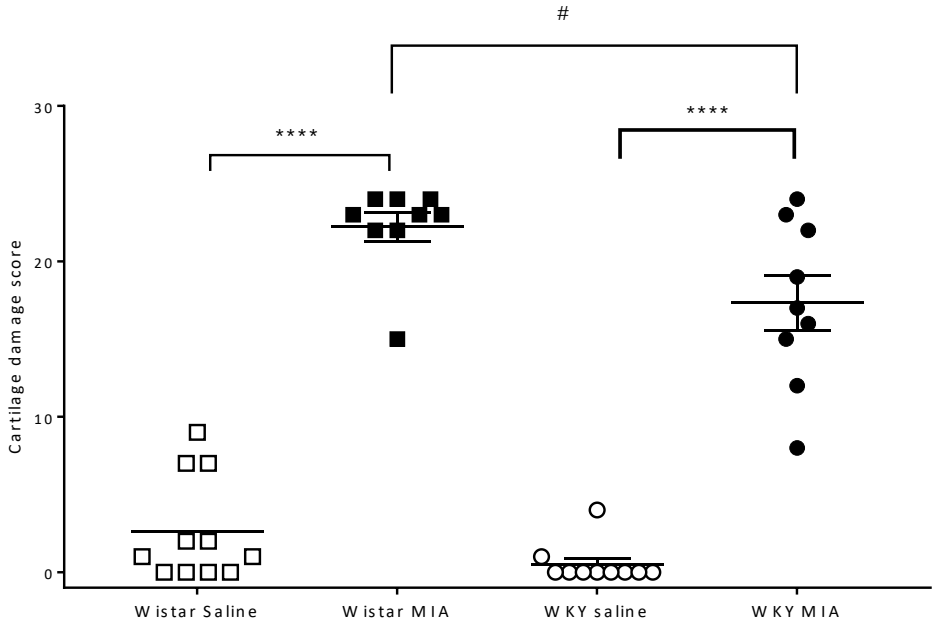

Figure 5.8: Effects of intra-articular injection of MIA versus saline on cartilage damage in Wistar (Saline n=11, MIA n=9) and WKY (MIA n=10, Saline n =9) rats. Both strains of rats exhibited significant cartilage damage following intra-articular injection of MIA compared to saline controls. Statistical analysis with one-way ANOVA, **** p <0.0001 compared to saline controls, # p<0.05 compared to MIA treated Wistar rats.

5.3.5 The effects of morphine on pain behaviour in the MIA model of OA

3.5.1 Weight bearing asymmetry

Rats received subcutaneous injection of morphine on day 21 following intra-articular injection of MIA injection. In Wistar rats, morphine significantly attenuated the existing weight bearing asymmetry compared to pre-drug values (Fig 5.9). In WKY rats, only the highest dose of morphine (6 mg/kg) attenuated weight bearing asymmetry compared to

pre-drug values (Fig 5.9). Two-way ANOVA revealed a significant interaction between group and dose p<0.0001.

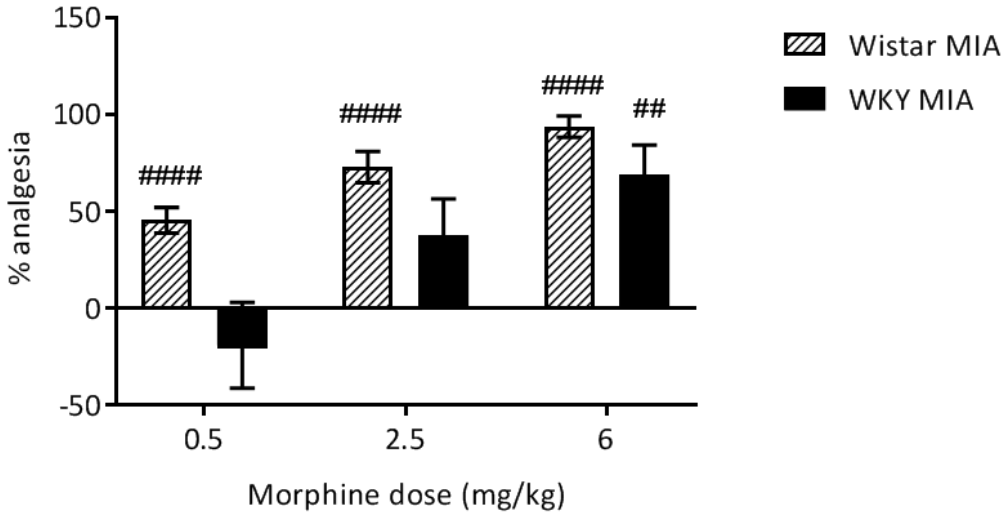

Figure 5.9: Effects of cumulative subcutaneous injection of morphine (0.5, 2.5 and 6mg/kg) on weight bearing asymmetry in Wistar and WKY rats (MIA n= 10 per group) 0.5 and 2.5mg/kg morphine significantly reversed MIA induced weight bearing asymmetry in Wistar rats, but not in WKY rats. The highest dose of morphine produced comparable inhibition of weight bearing asymmetry in the two strains of rats. Statistical analysis with Two-way ANOVA, ##p<0.01, ####p<0.0001, compared to pre-drug weight bearing values on day 21.

3.5.2 Paw withdrawal thresholds

In Wistar rats, morphine attenuated reductions in ipsilateral PWTs in the MIA model of OA pain (Fig 5.10 A). In WKY rats, only the highest dose of morphine (6mg/kg) significantly attenuated the lowered PWTs in the MIA model of OA pain (Fig 5.10 A).

As described earlier, following intra-articular injection of MIA WKY rats also exhibited lowered contralateral PWTs. The highest dose of morphine

(6mg/kg) significantly attenuated the lowered contralateral PWTs in WKY rats, whereas no reversal was possible for Wistar rats, as contralateral PWTs were not lowered (Fig 5.10 B).

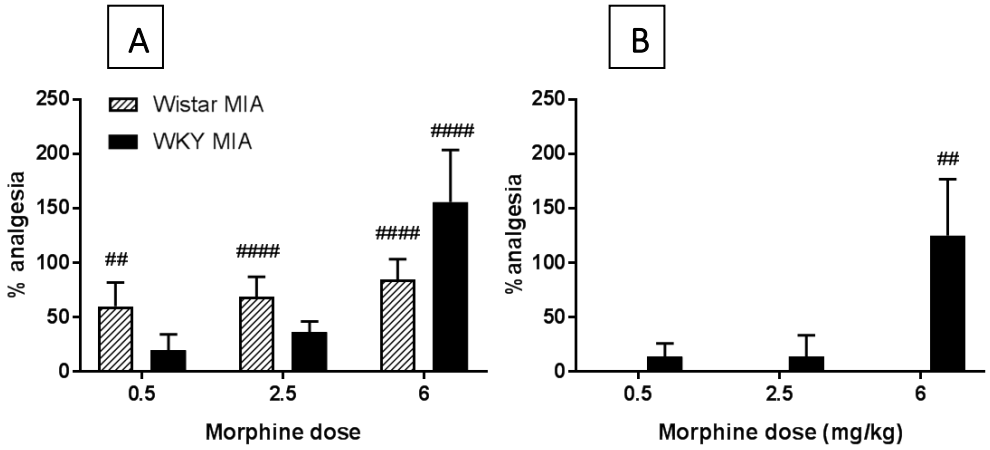

Figure 5.10: Effects of cumulative subcutaneous morphine (0.5, 2.5 and 6mg/kg) on PWTs in MIA treated Wistar and WKY rats (N= 10 per group). A) 0.5 and 2.5mg/kg morphine significantly reversed lowered ipsilateral PWTs in MIA treated Wistar rats, but not in MIA treated WKY rats. 6mg/kg morphine produced comparable reversal of lowered PWTs in the two strains of rats. B) 6mg/kg morphine reversed lowered contralateral PWTs in WKY rats. Statistical analysis with ANOVA, ## $p<0.01$, #### $p<0.0001$, compared to day 21 baseline PWTs.

5.3.6 Effects of the opioid receptor antagonist naloxone on pain behaviour in the MIA model of OA

To understand better whether opioid receptor signalling was altered in the WKY rats, and the impact of the MIA model of OA pain, I investigated the effects of blocking the μ opioid receptor with a selective antagonist. In separate groups of Wistar and WKY rats, the effects of the opioid receptor antagonist naloxone on pain behaviour was studied. Only PWTs were measured due to the time constraints posed by its short duration of action.

In the control Wistar rats (intra-articular injection of saline), naloxone did not alter PWTs whereas PWTs were lowered in the MIA treated Wistar rats, (Fig 5.11 A).

There was a significant difference in the effect of naloxone treatment between the saline and MIA treated Wistar rats (0.1mg/kg: p=0.0037). Interestingly, in WKY rats, naloxone treatment resulted in significantly lower PWTs in both the control group which received intra-articular injection of saline and the group that received injection of MIA (Fig 5.11 A). There was no significant difference in the effects of naloxone between saline and MIA treated WKY rats (1mg/kg p = 0.99).

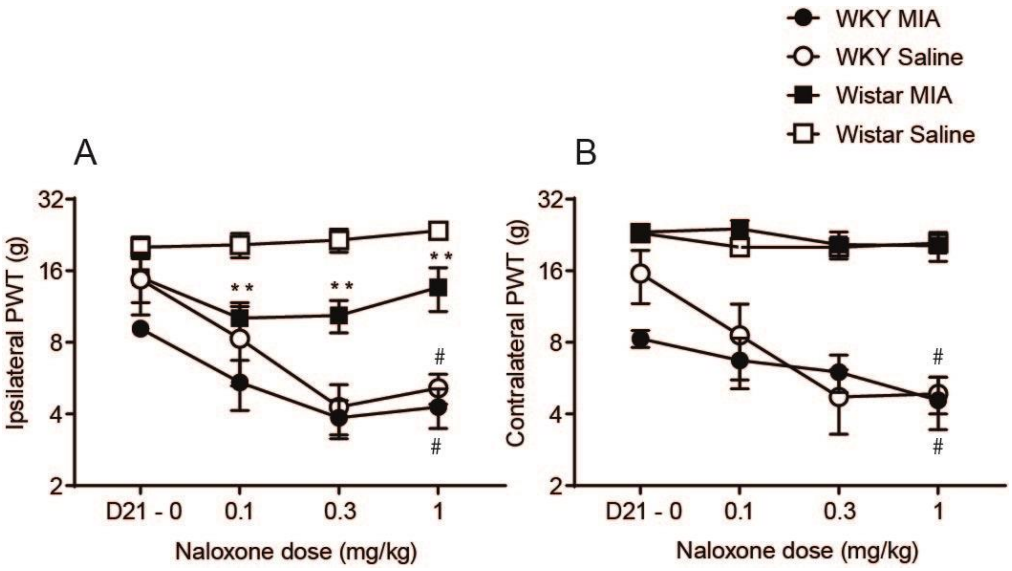

Figures 5.11: Effects of subcutaneous naloxone (0.1, 0.3 and 1mg/kg) on PWTs in Wistar (MIA=8, Saline n = 11) and WKY rats (MIA n= 7, Saline n=7). **A)** 0.1, 0.3 & 1mg/kg subcutaneous naloxone produced significantly lowered ipsilateral PWTs in Wistar MIA rats when compared to saline injected controls. In WKY rats, ipsilateral PWTs were lowered significantly after administration of naloxone, but lowering of ipsilateral PWTs was not significantly different at any dose between MIA and saline injected rats. **B)** Contralateral PWTs in Wistar rats, irrespective of MIA, were not lowered by naloxone. In WKY rats, contralateral PWTs were lowered after subcutaneous naloxone, irrespective of MIA.
Analysis with ANOVA, **p<0.01 compared to saline injected controls. Analysis with wilcoxon rank test, # p<0.05 compared to day 21 baseline

Naloxone treatment did not alter the contralateral PWTs in either group of Wistar rats (Fig 5.11 B). Interestingly in WKY rats, naloxone treatment resulted in significantly lower PWTs in both the control group which received intra-articular injection of saline and the group that received injection of MIA (Fig 5.11 B). There was no significant difference between the effects of naloxone on contralateral PWTs between saline and MIA treated WKY rats (1mg/kg p=0.99).

5.3.7 Plasma levels of β endorphin

To investigate whether circulating levels of endogenous opioid peptides could have influenced the loss of analgesia at low doses of morphine, levels of β-endorphin in plasma were measured by ELISA in separate groups of WKY and Wistar rats (without intra-articular injection of MIA). Plasma levels of β endorphin were comparable between Wistar and WKY rats, although there was a trend towards increased levels in the WKY group (Fig 5.12).

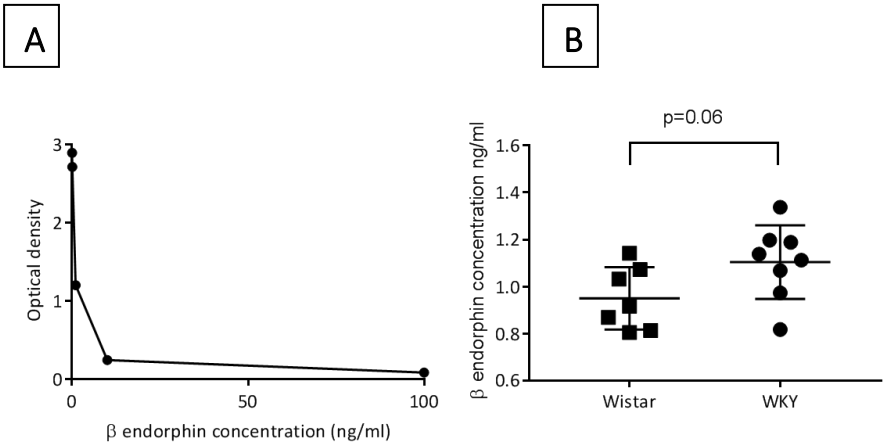

Figure 5.12: β endorphin ELISA in plasma in naïve Wistar (n=8) and WKY (N=7) rats. **A**) Standard curve for β endorphin concentration. **B**) Strain comparison revealed no significant difference in β endorphin concentration between Wistar and WKY rats. Statistical analysis with unpaired t-test.

5.4 Discussion

OA pain is difficult to treat and is often accompanied by anxiety, depression or other disorders encompassing features of negative affect (Judge *et al*, 2010). Changes in the endogenous opioid system are strongly implicated in both chronic pain and anxiety, with high levels of opioid receptors expressed in supraspinal regions associated with both pain and mood disorders (Winters *et al.*, 2017).

5.4.1 The effect of intra-articular MIA on pain behaviour in the WKY rats

In these studies, differences in pain responses were seen between the WKY rats, which were used as the genetic model of anxiety vulnerability, and the typical anxiety Wistar rats.

In both strains, a significant difference in weight bearing asymmetry was seen between rats after intra-articular injection of MIA and their saline injected controls. Although both strains of rats experienced weight bearing asymmetry from day 3 post-MIA, weight bearing asymmetry was significantly greater in the Wistar rats at the end of the study, compared to WKY MIA-treated rats. This difference in weight bearing asymmetry may in part, be explained by differences in cartilage damage, given that cartilage damage scores were significantly higher in MIA-treated Wistar rats. However, both strains of rats exhibited significant cartilage damage in comparison to their saline injected controls. Weight differences between the strains may also contribute to some of this difference, with WKY rats weighing approximately 80g less than Wistar at day 21 post intra-articular MIA injection.

Both Wistar and WKY rats exhibited a significant lowering of ipsilateral PWTs in comparison to their saline injected controls. However, strain comparison revealed that WKY rats exhibited significantly lower ipsilateral paw withdrawal thresholds than the normal anxiety Wistar rats with MIA, pointing to an increase in mechanical allodynia and central sensitisation in MIA treated WKY rats. These results are in keeping with the literature in human OA patients, which show that a subset of OA patients, around 30%, are likely to display central sensitisation, although the cause of this is unclear (Lluch *et al*, 2014).

5.4.2 The effect of the opioid analgesic morphine on pain behaviour in the WKY rats after MIA

The second aim of this study was to investigate the response of the high anxiety WKY rats to the analgesic effects of the opioid agonist morphine. The analgesic effects of morphine were investigated in response to both weight bearing asymmetry and mechanical hind paw stimulation.

Normal anxiety Wistar rats exhibited a significant reduction in weight bearing asymmetry and an increase in paw withdrawal thresholds at each dose of morphine. In comparison, WKY rats exhibited a reduced responsiveness to morphine, with significant decreases in WB asymmetry and increases in ipsilateral and contralateral PWTs only evident at the highest dose of morphine. However, analgesic responses to morphine were comparable between the strains of rats treated with MIA for the high dose of 6 mg/kg. These differences in opioid sensitivity are consistent with observations in chronic lower back pain patients with comorbid anxiety, who experience diminished analgesia from morphine (Wasan, Davar and Jamison, 2005b). In the preclinical literature, the reduced efficacy of morphine in WKY rats has recently also been demonstrated in the CFA model of chronic pain (Hestehave *et al.*, 2019),

demonstrating that this effect is present across pain states. In my studies, although clear differences in the response to morphine were seen between the normal anxiety Wistar rats and the high anxiety WKY rats MIA-treated rats, it is unclear how these differences related to underlying differences in endogenous opioid receptor function.

The second study therefore investigated the effects of the opioid antagonist naloxone, which has highest binding affinity for μ opioid receptors, to probe whether the differential responses to morphine reflect underlying differences in the endogenous μ opioid system. In response to naloxone, Wistar MIA rats exhibited an additional decrease in already lowered PWTs in comparison to their saline injected controls. This suggests that for the normal anxiety Wistar rats, there is an effect of intra-articular MIA on endogenous opioid tone, which can be revealed by blocking the μ opioid receptor pharmacologically. In the high anxiety WKY rats, naloxone lowered both ipsilateral and contralateral PWTs irrespective of intra-articular injection of MIA. This suggests the presence of greater endogenous opioid tone in the high anxiety WKY rats in the absence of a pain state, which may reflect differences in μ opioid receptor function due to anxiety. Despite this suggestion of greater endogenous opioid tone in WKY rats per se, induction of the model of OA pain still led to greater decreases PWTs and the contralateral pain phenotype. This suggests that the nociceptive drive is far higher in the WKY rats following induction the MIA model of OA pain, despite joint pathology being less than that seen in the Wistar rats.

To probe further the potential differences in endogenous opioid tone, levels of plasma β-endorphin were measured. Although there was no statistically significant difference between WKY and Wistar rats, however there was a trend towards higher plasma levels of β-endorphin in WKY rats. It is plausible that this study was underpowered and with more time

and larger group sizes that this difference would have reached significance.

To date few studies has investigated links between the levels of endogenous opioids and the analgesic efficacy of morphine. While differences in β-endorphin levels have not been shown to predict analgesic responsiveness to morphine in normal populations, some effect has been shown in chronic pain patients, with higher levels of β-endorphin in plasma suggesting lower responsiveness to morphine analgesia (Bruehl *et al*, 2017). It is therefore possible that in the high anxiety WKY strain, lowered responsiveness to morphine reflects differences in endogenous μ opioid peptides. It is also important to consider that differences in μ opioid peptides may be specific to regions of the brain that are high in opioids, or in the spinal cord and that measuring circulating levels of opioid peptides may not accurately reflect these underlying changes.

5.4.3 Limitations

There were some practical limitations with these studies. There were some differences in pain behaviour after intra-articular injection of MIA shown in this chapter in the WKY rats, to the pain behaviour obtained from WKY rats in other studies. In this study, there was a significant degree of training in behavioural techniques, resulting in rats undergoing behavioural testing from more than one experimenter. It is likely that there are some differences between experimenters for behavioural data. Another limitation stems from the use of a genetic model to model anxiety vulnerability. While the WKY rats have been consistently shown to have increased levels of baseline anxiety, it is also unclear whether there are other physiological differences that might influence their responses to opioids, and whether there are pharmacokinetic differences

that influence the WKY response to morphine/naloxone independently of their levels of anxiety. The use of behavioural measures as an outcome, whilst functionally relevant, limits further interpretation of the underlying mechanisms leading to alterations in opioidergic function. Future studies to define these mechanisms would need to focus on potential molecular changes such as alterations in phosphorylation of the receptor.

5.4.4 Conclusions

The understanding of how responses to opioids differ and the impact that co-morbid conditions such as anxiety can have on pain responses and responses to analgesic treatment is highly relevant. Given the high prescription rates of opioids in an attempt to provide analgesia from musculoskeletal disorders and the high risk of adverse side effects, it is important to more carefully consider when and who opioid analgesics might provide appropriate treatment for OA pain. With the rise of research into precision medicine, exploring individual responses to opioids and risk factors could be particularly relevant for analgesia for chronic OA pain.

Chapter 6 Investigation of changes in neuronal activity after noxious stimulation in the MIA model of OA pain

6.1 Background

Although fMRI is an excellent technique for the investigation of whole brain haemodynamic changes, it provides a surrogate signal for neuronal activity that can be challenging to interpret. Neurovascular coupling, the mechanistic link between neuronal activity and subsequent increases in cerebral blood flow (CBF), is complex and it is not always clear how neuronal activity and the BOLD signal relate (Logothetis, 2008). Electrophysiological methods can provide complementary information which is more directly related to neuronal activity. The increased temporal resolution of electrophysiological techniques such as EEG and ECoG.

6.1.1 ECoG

Electrocorticography (ECoG), is an electrophysiological technique used to measure neuronal activity (Buzsáki, Anastassiou and Koch, 2012). The electrocorticogram (the signal measured during ECoG) is measured from the surface of the brain as opposed to the scalp as is the case in EEG. This signal is constituted of electric current contributions from a range of active cellular processes. Any excitable membrane can contribute to this signal, including spines, dendrites, somas, axons, axon terminals or transmembrane currents. (Buzsáki, Anastassiou and Koch, 2012). The signal measured by ECoG primarily originates in the superficial layers of

the cortex, while deeper structures require electrodes to be inserted into the brain (Buzsáki, Anastassiou and Koch, 2012).

ECoG can be used to investigate two different features of neuronal activity: Event related potentials and oscillations. Event related potentials (ERPs) are alterations in voltage that are time-locked to a stimulus; for somatosensory stimuli these are referred to as somatosensory evoked potentials (SEPs). Although investigation of SEPs has formed a small part of the electrophysiological pain literature, stimulation by infrared lasers has been shown to elicit ERPs that are visible in the electroencephalogram (Mouraux, Guérit and Plaghki, 2003). In humans however, studies of nociceptive stimulation are complicated by the multi-faceted nature of the pain experience. It is not clear for example, whether ERPs represent pain after stimulation or attentional orienting to salient stimuli (Iannetti *et al*>, 2008).

Few studies have investigated ECoG power changes in response to nociceptive stimulation in rodents and this literature has focused primarily on neonatal development. In neonates, baseline power over the somatosensory cortex has been shown to increase with age, with a shift from power in the delta to theta frequency band in week 3 of life. SEPs have been shown to be present in response to electrical stimulation at all ages, but SEPs in response to hind paw incision were not evident until week 3 (P Chang *et al.*, 2016). Comparisons of neonates and adults have shown an altered frequency distribution after noxious thermal stimulation, with differences in theta power only evident in adult rats (Devonshire, Greenspon and Hathway, 2015).

ECoG can also be used to explore the frequency spectra of this extra-cellular electrical signal over a period of time. Oscillations have been heavily implicated in the processing of pain (Ploner, Sorg and Gross, 2017). Frequencies can be divided into bands, ranging from delta (0-4Hz), theta (4-7Hz), Alpha (8-13Hz), beta (14-29Hz) and Gamma (30-

100Hz). The frequency bands in this chapter were chosen to be consistent with a previous publication from the research group, but these bands are typical in EEG/ECoG (Devonshire, Greenspon and Hathway, 2015). Changes in the power of neuronal responses in all frequency bands have been shown to change after painful stimulation (See refs in Ploner, Sorg and Gross, 2017).

Increases in stimulus intensity have been demonstrated to link to changes in oscillatory activity, with decreased power in the alpha and beta frequency bands and increased power in the gamma frequency band (Tiemann *et al*, 2015; Nickel *et al*, 2017). These differences were shown to be regionally specific: decreases in alpha and beta band power were measured over the somatosensory cortex and increases in gamma power were measured over the prefrontal cortex. It is not clear precisely what underlying processes or mechanisms these differences reflect. Neuronal oscillations and synchronisation are however, thought to underlie flexible communication between and within areas, and changes in oscillations are present in a number of neuropsychiatric disorders (Uhlhaas, 2011).

In contrast, Bunk and colleagues showed that stimulus intensity only explained power in the delta frequency band, and that psychological measures of pain intensity better predicted oscillatory activity in alpha, beta and theta frequency bands, although the gamma band was not studied (Bunk *et al*, 2018).

These results highlight the discordant nature of the literature. Differences in electrode setup, stimulus modality and intensity, analysis techniques are all likely to affect results (Bunk *et al*, 2018). However, these results *do* suggest that differences in stimulus intensity and subjective ratings of pain intensity can influence oscillatory activity in the brain and that these differences are dependent on where the signal is measured from.

6.1.2 Chronic pain

There is little evidence for alterations in neuronal activity in chronic pain conditions. In human chronic lower back patients, a positive association was shown between pain intensity and gamma and beta oscillations in the prefrontal cortex (May *et al.*, 2019).

In mice, Leblanc and colleagues showed an increase in cortical power over S1 and the prefrontal cortex in awake, and freely behaving mice in neuropathic, inflammatory and acute pain. In addition to general increases in power, they also found increases in coherence between S1 and the PFC at later but not early stages of neuropathic pain (LeBlanc *et al.*, 2016).

6.1.3 Rationale:

Differences in functional connectivity were demonstrated using fMRI in Chapter 4 in the MIA model, in normal anxiety Wistar rats. It is challenging to investigate differences with fMRI in rats in response to noxious stimulation, due to the time scale of data acquired and practical issues such as access to the animal. Although recording of neuronal activity after noxious stimulation comprises the majority of spinal electrophysiology literature in OA pain, little work has investigated supraspinal differences to date.

6.1.4 Aims and hypothesis:

To investigate difference in SEPs and oscillations in the MIA model of OA pain, during noxious mechanical, electrical and thermal stimulation to the hind paw. I hypothesised that SEPs and oscillatory power would be increased after intra-articular MIA and that this would likely occur in the delta and theta frequency bands.

6.2 Methods

6.2.1 Animals

A total of 12 adult male Sprague-Dawley rats were used for these experiments weighing 250-300g (Charles River, Margate, UK). This study was conducted in accordance with the UK home office Animals (Scientific Procedures) Act (1986).

Exclusions: Stimulation runs were primarily excluded due to technical issues with recording software or in case of death under anaesthesia (n=2). One rat was excluded when outliers reached statistical significance using the Grubbs outlier test in Prism.

6.2.2 Intra-articular injections

All rats received a singular 50µl intra-articular injection of either 1mg MIA or 0.9% saline using a 50 gauge hypodermic needle (See General Methods for full description). The experimenter was blinded to the treatment given to each animal.

6.2.3 Behavioural testing

All rats received two habituation sessions to the pain behaviour testing environment to minimise any exploratory behaviour during testing. Baseline measurements were taken prior to injection on day 0 in the morning, and behavioural measurements were subsequently measured from day 3 to day 21 post model-induction, twice weekly. Both weight bearing asymmetry (WB), and mechanical hind paw withdrawal thresholds (PWTs) for both the paws both ipsilateral and contralateral to the affected joint were assessed.

6.2.4 ECoG surgeries

All surgeries were conducted under isoflurane anaesthesia. The rats were induced at 3% isoflurane delivered in 1l/min oxygen, which was reduced to 2 ½ - 2% isoflurane for the duration of the surgery. The tail artery was cannulated for measurement of blood pressure (mmHg) using an MR compatible blood pressure transducer (Samba sensors, Gothenburg, Sweden) and fine flexible tubing. The tail vein was chosen for cannulation for intravenous (IV) administration of medetomidine (Sedastart, Produlab Pharma, The Netherlands) and a continuous infusion of medetomidine was subsequently delivered using a continuous infusion pump, with the rate varying according to the weight of the animal. Core body temperature was monitored using a rectal probe and controlled using a thermostatic heating mat (Harvard Apparatus, Edenbridge, UK).

A craniotomy was performed and 12 small holes were drilled into the skull. Electrodes were placed into the holes for ECoG recording (see full description in general methods).

6.2.5 Stimulation

6.2.5.1 Mechanical

Mechanical stimulation was conducted first. Mechanical stimulations were given using von Frey hairs, applied to the plantar surface of each hind paw, in trains of 3, with 1 stimulation given per minute in an ascending order (2g-26g). Stimulations were first conducted on the ipsilateral paw in full, and then on the contralateral paw.

6.2.5.2 Thermal

Thermal stimulation was delivered 10 minutes after the end of mechanical stimulation. Thermal stimulation was applied to the plantar surface of each hind paw, in trains of 3, with 1 stimulation given per 3 minutes. Non-noxious stimulation was applied first, at 30 degrees c followed by noxious stimulation at 55 degrees c. Stimulations were first conducted on the ipsilateral paw in full, and then on the contralateral paw.

6.2.5.3 Electrical

Pins were placed intradermally into the hind paw for electrical stimulation. The first train of stimulation given was innocuous: 1 train of 20 stimulations at 0.1mA, with 2ms duration. Each noxious train was given 3 times, with 20 stimulations per train at 2.5mA and 7.5mA, 2ms duration. 15 minutes were left between stimulation trains.

6.2.6 Anaesthesia

All rats were transferred from isoflurane (for induction and surgery) to medetomidine and isoflurane anaesthesia (0.05 – 0.1mg/kg + 0.5% isoflurane, see General Methods for full description).

6.2.7 Analysis

ECoG data were processed using MATLAB 2016b (MathWorks, Massachusetts) and analysed using GraphPad Prism (GraphPad, California) with a RM one way ANOVA and Tukey's multiple comparisons. Fast Fourier Transform (FFT) functions were applied to the 20s post stimulation period to analyse EEG frequency composition.

6.3. Results

6.3.1 SEPs are evident after noxious electrical stimulation

Individual ECoG traces were manually inspected to ensure the presence of a SEP. SEPs were not observed during stimulation at 0.1mA (Fig 6.1, A), but were clear at both 2.5mA (Fig 6.1, B) and 7.5mA (Fig 6.1, C).

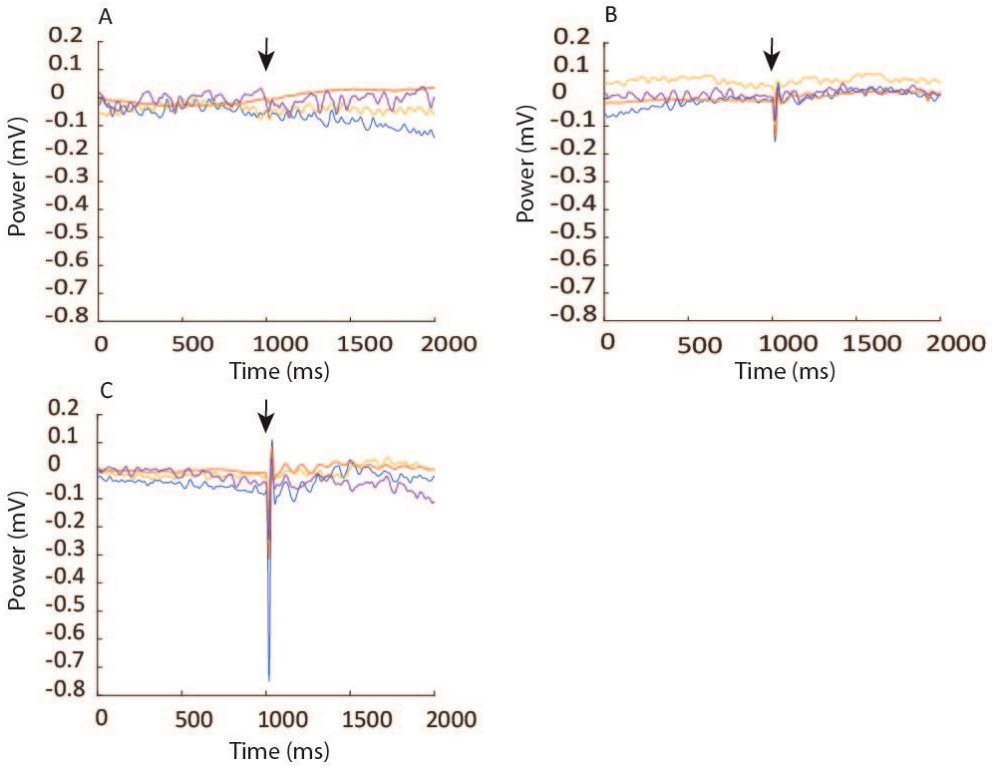

Figure 6.1: Raw traces from the saline group of SD rats after intra-articular MIA (N=4). Each line represents the data from an individual rat and stimulation times are shown with an arrow: Electrical stimulation occurred at the midpoint of the trace (1000ms) at 0.1mA (A), 2.5mA (B) and 7.5mA (C). The data were averaged over stimulus trains (20 stimuli) and over repetitions of trains for 2.5mA and 7.5mA (3 trains).

6.3.2 Differences in SEPs are evident after intra-articular MIA.

The depolarisation amplitude values were extracted from the SEP recorded over the somatosensory cortex using MATLAB 2018a (MathWorks, Massachusetts). Significant differences were seen in depolarisation power between rats with intra-articular MIA and saline injected controls at 7.5mA (Fig 6.2, p=0.03).

Within the group of MIA treated rats, significant differences were observed between 2.5mA and 7.5mA (p=0.015) and 0.1mA and 7.5mA (p=0.005) whereas no significant differences were seen in the group of saline injected rats with increasing electrical stimulation amplitude.

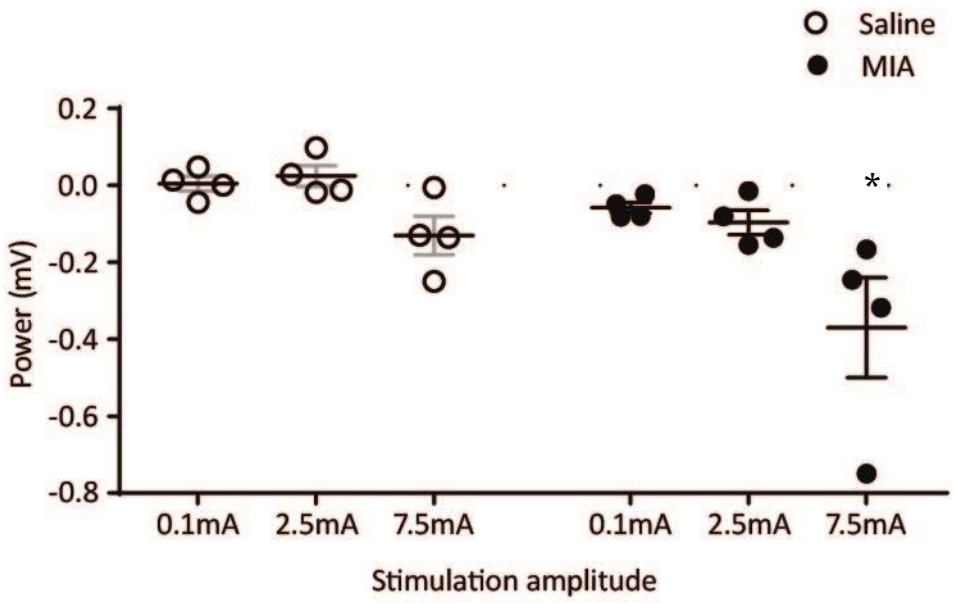

Figure 6.2: Depolarisation values after electrical stimulation at 0.1mA, 2.5mA and 7.5mA. Significant differences were observed between rats after intra-articular MIA (n=4) and saline controls (n=4) at 7.5mA noxious electrical stimulation. Data analysed with 2 way ANOVA and Tukey's multiple comparsions. * $p<0.05$.

6.3.3 Noxious thermal stimulation

Noxious thermal stimulation applied to the ipsilateral hind paw at 50°c (1 train of 3 stimuli) produced no post-stimulus alterations in power in any frequency band when compared to pre-stimulus power (Fig 6.3).

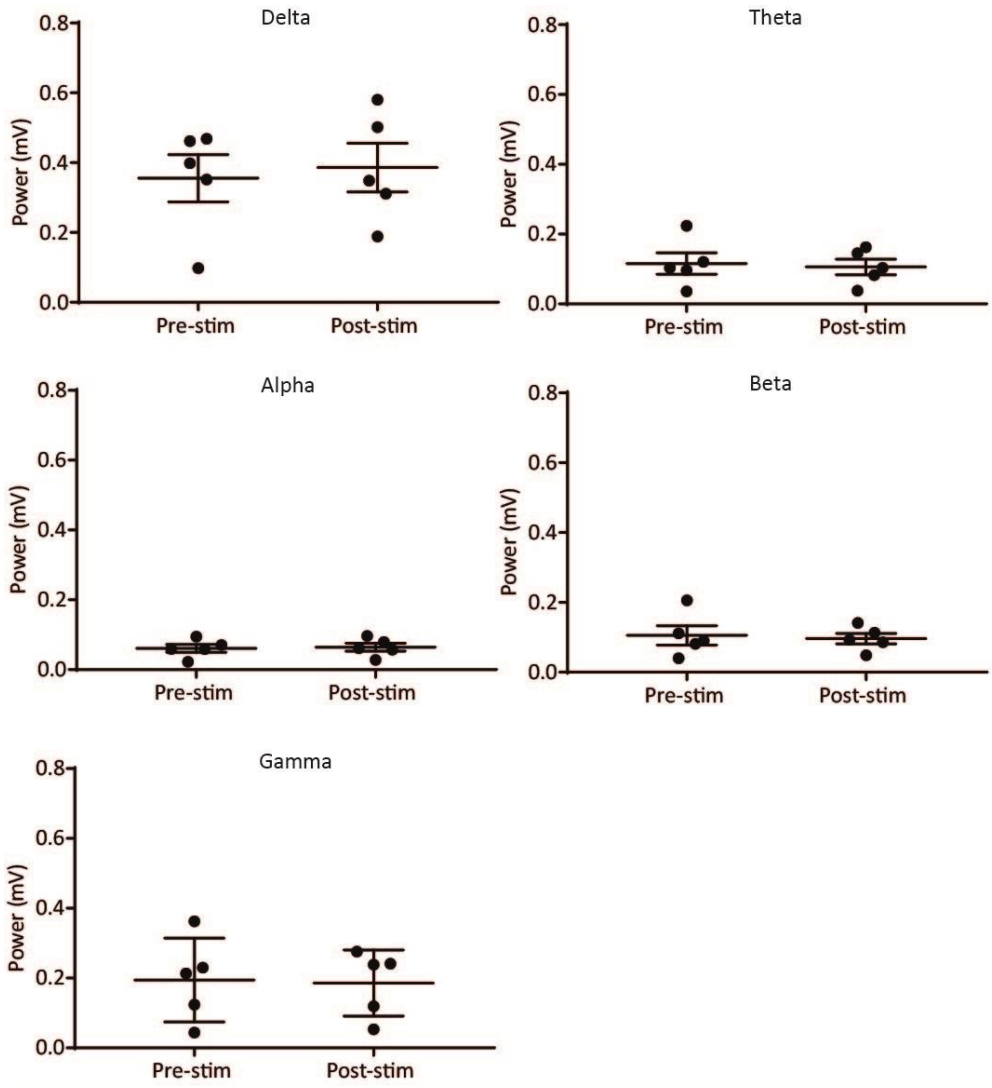

Figure 6.3: Power in each frequency band after stimulation at 50°c applied to the ipsilateral hindpaw in rats after intra-articular MIA (n=5). No differences were seen in power before and after stimulation in any frequency band. Data were analysed with t-tests.

6.3.4 Mechanical:

Mechanical stimulation did not reliably evoke SEPs and traces were subject to high levels of experimental noise. The noise was present in every frequency band and therefore could not be reliably removed (Fig 6.4).

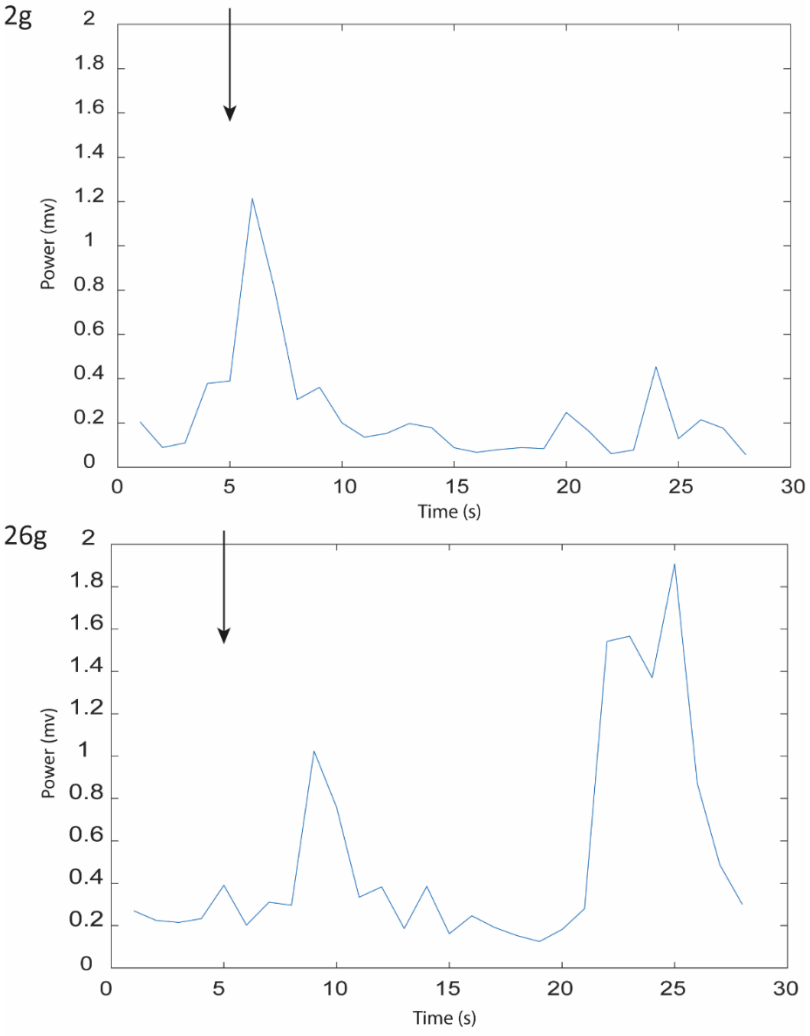

Figure 6.4: Individual ECoG trace during mechanical stimulation at 2g (A) and 26g (B). For stimulation at 2g an increase in power, directly after stimulation was observed in all frequency bands (indicated by the arrow). This increase in power was not observed for stimulation at 26g and a significant incidence of noise is observed between 20s and 28s.

6.4 Discussion

In this study, differences in SEPs and post stimulus frequencies of neuronal activity were investigated using a variety of noxious stimuli. These differences have not been demonstrated in the MIA model of OA pain, and provide additional support for results indicating functional brain changes during the MIA model.

Over the somatosensory cortex, significant increases in the depolarisation phase of the SEP were observed after noxious electrical stimulation, when compared to non-noxious electrical stimulation, in rats that had received intra-articular MIA (Fig 6.2). This effect was not present in rats with intra-articular saline, suggesting that MIA may lead to alterations in neuronal activity after noxious stimulation of the hind paw. There is little evidence for differences in SEPs after chronic pain in humans or animals at the brain level but there is some evidence for the link between SEPs and the experience of pain (Benromano *et al.*, 2017).

Analysis of the frequency of oscillations did not show any difference in any particular frequency band in the thermal stimulation and was challenging due to the removal of environmental noise. Although these results are not in line with the literature, in which differences are frequently shown after painful stimulation (See refs in Ploner, Sorg and Gross, 2017), there are practical reasons why these differences were not observed, including environmental noise and the new equipment setup.

6.4.1 Noise

A significant amount of noise, of unknown origin, was experienced during data collection. The noise was challenging to reduce, and despite grounding of the animal and shielding of electrodes persisted throughout the experiments.

The SEPs from electrical stimulation were the most robust out of all forms of stimulation, and were largely unaffected by this noise. Electrical stimuli were electronically controlled, and delivered 20 times per train, with multiple trains for the noxious stimuli. The high number of stimuli delivered, as well as the reliable triggering of the stimuli, may have mitigated the effects of any environmental noise.

Both the mechanical and the thermal stimulation were delivered by a pneumatic device, which relied on consistent air pressure in order to provide an accurate interval between initiations of the stimulus and when the stimulus was delivered. Both mechanical and thermal stimuli were only delivered 3 times per train, giving fewer stimuli over which to average, when compared to electrical stimulation.

The noise during thermal stimulation was less troublesome than the noise that occurred during mechanical stimulation and was therefore less challenging to remove. Mechanical stimulation required more manual input, and while the pneumatic device was used to press the von-Frey hair into the hind paw, it was necessary to manually change hairs between trains of stimuli, hold the pneumatic device in place while also pressing the button to trigger the stimulation. Movement seemed to increase noise, suggesting that it was not electrical in origin and the increase in movement for the mechanical stimulation may have led to the decrease in data quality.

6.4.2 Anaesthesia

Anaesthesia acts supraspinally to induce a loss of consciousness and is therefore likely to have affected the frequency spectra of the data acquired. Jang and colleagues showed that medetomidine when combined with ketamine alters the spectral profile of the signal, with increased power in the lower frequency bands, from delta to alpha (Ja*ng*

et al, 2009). Under medetomidine, wakening from anaesthesia has been demonstrated to be correlated with an increase in the beta/delta ratio, with increased wakefulness leading to decreases in delta power (Pawela *et al.*, 2009). In this study, power was highest in the delta frequency band, and this likely was a product of anaesthesia. Although the use of anaesthesia in these experiments is helpful, for comparison to the data collected with fMRI, it is important to remember the influence that anaesthesia has on neuronal activity and how this may limit comparison with human EEG studies or studies of non-anaesthetised and freely behaving rodents (LeBlanc *et al.*, 2016).

6.4.3 Somatosensory cortex

A major limitation of this study is that it allows for little interpretation of the mechanisms that might lead to increased SEPs in the somatosensory cortex. The increase in electrical activity is broadly in line with the literature. Increases in S1 activity have been shown in central pain syndrome (CPS), both for spontaneous activity and in response to noxious stimulation (Quiton *et al*, 2010). While this suggests that neuronal activity is altered in S1 during a chronic pain state, it reveals little about how and why these alterations develop and whether it is even relevant for the identification of a pain state, or whether it can be reduced by analgesics.

In addition, the analysis of this data was fairly basic, providing a rudimentary picture of changes in neuronal activity. Although the regional study of increases and decreases in power is interesting, ECoG can also be used to explore differences in synchrony between regions, which are thought to possibly play a more important role in pain perception than oscillations in any one region alone (Apkarian and Chialvo 2006).

Chapter 7 General Discussion

This thesis set out to investigate functional connectivity changes in response to the MIA model of OA pain, and whether anxiety-like behaviour mediated this relationship. Functional connectivity differences were observed following induction of the MIA model of OA pain and correlation analysis revealed that the relationship between pain behaviour and functional connectivity from the vmPFC to S2/caudate putamen was altered in the high anxiety WKY strain of rats.

The regions identified in the functional connectivity analysis have established involvement in the opioidergic descending control of pain. Behaviourally, in the WKY rats, an increase in mechanical hypersensitivity was observed and responses to morphine were attenuated, with increased endogenous opioidergic tone.

7.1 Altered pain profiles in the WKY rat

Interestingly, following induction of the MIA model of OA pain, the WKY rats showed a different pain profile to the normal anxiety Wistar rats, with increased mechanical sensitivity to the hind paw, which was evident for both ipsilateral and contralateral hind paws. Weight bearing asymmetry, an indicator of joint pain was somewhat lower in WKY rats, possibly reflecting an impact of the lower body weight of the WKY rats, the contralateral pain phenotype experienced, or an unknown and unintended difference in this inbred strain.

Mechanical hind paw sensitivity was also increased in the control WKY rats (intra-articular injection of saline), suggesting that there was an underlying strain effect. Again, it is unclear whether this was an effect of heightened anxiety levels or whether it occurred as a consequence of an

unknown genetic difference in the WKY rats, or in response to repeated mechanical behavioural testing.

The behavioural differences between the WKY/Wistar strains are not unexpected but are important to bear in mind when interpreting behavioural differences. Strain differences in pain behaviour are common, and have been demonstrated even in the typical outbred controls strains between Sprague-Dawley and Wistar rats: SD rats have been shown to exhibit increased paw sensitivity when compared to Wistar rats on the lateral part of the hind paw (Vukojević, Lovrić-Kojundžić and Sapunar, 2007), despite the fact that SD rats are outbred from the Wistar. In addition to differences between strains, for many paradigms, differences between vendors have also been reported (Paré and Kluczynski, 1997). In the CFA model of pain and inflammation, differences have been observed for hyperalgesia and spinal preprodynorphin mRNA in a number of commonly used rat strains (Zha*ng et al*, 2003). These differences complicate the interpretations that can be made from models using inbred strain.

7.2 Feasibility testing for fMRI

In order to investigate functional connectivity in the rat, it was necessary to test anaesthetic regimes described in the rodent fMRI literature to ensure that any effects of anaesthesia on the BOLD signal or underlying neuronal activity were minimised. It was also necessary to check the suitability of these methods for the study of nociception. This work showed that an anaesthetic regime of medetomidine combined with a small amount (0.5%) isoflurane provided a stable plane of anaesthesia without a burst-suppression firing pattern, which allowed nociceptive brain activity to be observed with both ECoG and fMRI. ICA revealed functional networks with preserved inter-hemispheric functional connectivity, leading to the conclusion that this anaesthetic combination

could be used to investigate functional connectivity changes in the MIA model of OA pain. The results from the testing of the anaesthetic regime were in line with expectations, and were comparable to those from anaesthetic regime comparison studies for functional connectivity (Grandjean *et al*, 2014; Bukhari *et al*, 2017; Paasonen *et al*, 2018).

After the preparatory work, I applied fMRI to the primary question of this PhD: How does anxiety influence functional connectivity changes in the MIA model of OA pain? In order to investigate the influence of anxiety on OA pain, the inbred WKY rats were used to model endogenous anxiety, and 1mg intra-articular MIA was used to model OA pain in the knee joint.

7.3 Functional connectivity changes after induction of the model of OA pain

Functional connectivity changes were observed following intra-articular MIA compared to saline treated rats. In the first study, the exploratory ICA analysis revealed significantly increased functional connectivity between somatosensory regions and the PAG in Wistar rats but not WKY rats. The seed based analyses used a priori chosen regions that are commonly implicated in pain processing: vmPFC; amygdala; anterior insula. The seed based analysis revealed lowered functional connectivity between the vmPFC and a cluster that included the secondary somatosensory cortex and the caudate putamen in Wistar rats after intra-articular MIA. Again this finding was only seen in the Wistar rats and not the WKY rats, suggesting a loss of this connectivity in the higher anxiety strain of rats. Based on the chronic pain neuroimaging literature, I expected a difference in functional connectivity between the amygdala and anterior insula seeds, however this was not observed (Yu *et al.*, 2014; Cottam *et al.*, 2018).

7.4 Altered effects of opioid analgesia in high anxiety rats

There is mounting clinical evidence that individuals with OA pain and high anxiety use higher levels of opioid analgesics (Valdes *et al.*, 2015). Using behavioural pharmacology, responsiveness to morphine was investigated in Wistar and WKY rats after induction of the MIA model of OA pain. Lowered responsiveness to morphine was observed at day 21 of the MIA model in WKY rats, with only the highest dose of morphine providing a significant degree of analgesia, both for weight bearing asymmetry and PWTs. To investigate whether this coincided with changes in μ opioid receptor function, responses to the μ opioid antagonist naloxone were investigated after intra-articular MIA in both strains. Administration of naloxone led to a reduction in PWTs in all WKY rats irrespective of hind paw, or of administration of MIA, whereas in the Wistar rats, naloxone reduced PWTs only in rats that had received intra-articular MIA. This suggests that in normal anxiety rats, alterations to μ opioid receptor function occur in response to joint pain, but that in the WKY rats, increased endogenous opioid tone may be present irrespective of the model of pain and this tone cannot be further increased by the induction of a model of pain.

7.5 Functional connectivity changes after MIA

The functional connectivity results (chapter 5) were in line with the preclinical imaging literature (Abaei *et al*, 2016; Spisák *et al*, 2017). In the only previous fMRI study of the MIA model, an increase in BOLD activity was observed in the PAG after intra-articular administration of capsaicin. In my work, the PAG was the only region that ICA analysis revealed to have an increase in functional connectivity after intra-articular injection of MIA in Wistar rats. The work in this thesis has extended the previous

findings, demonstrating that the PAG has altered *resting state* functional connectivity with a component localised to the somatosensory cortex. This suggests that alterations in functional connectivity with the PAG, a key region in the descending control of pain, are not only altered in response to additional nociceptive stimulation, but are also evident in spontaneous fluctuations in BOLD activity. Although the finding of functional connectivity differences in preclinical pain models is not new, results in the literature are highly discordant and difficult to interpret, beyond the suggestion that ongoing pain causes alterations in functional connectivity, in and between regions related to the processing of pain (Abaei *et al.*, 2016; Spisák *et al.*, 2017).

In order to take the functional connectivity results from this study further, behavioural scores were correlated with functional connectivity strength. The correlations between weight bearing asymmetry and functional connectivity strength from the vmPFC were particularly interesting.

The difference in the direction of the relationship between the strains, for the correlation between weight bearing asymmetry values and the strength of the connectivity between the vmPFC and the S2 cluster indicated a possible key difference in pain modulation between the strains. This difference is challenging to interpret but could reflect differences in brain networks involved in emotional regulation of pain.

The infralimbic cortex, the best estimate of an analogue for the vmPFC in the rat, forms a network with limbic regions, such as the basolateral amygdala, thalamus and hippocampus (Bloodgood *et al.*, 2018). A major subcortical target of L5 neurons in the mPFC is the PAG, which is involved in descending inhibition of pain (Cheriyan and Sheets, 2018). The infralimbic cortex has been implicated in emotional regulation, which is highly relevant, given the influence of negative affect on OA pain, particularly with regard to opioid analgesia (Yu *et al.*, 2014; Valdes

et al., 2015). Speculatively, increased functional connectivity from the infralimbic cortex could reflect increased activity in response to emotional regulation in the presence of chronic pain. The negative correlation between the infralimbic cortex and the S2 cluster in the WKY strain of rats could reflect some dysfunction of emotional regulation, related to heightened anxiety levels, leading to the increased pain responses.

7.6 Opioids

Although μ opioid receptors are widely distributed in the brain, there is a high density of μ receptors in both the PFC and the PAG, regions identified in the functional connectivity studies in this thesis.

Given the increased focus on opioids in the chronic pain literature, particularly with regard to anxiety and negative affect, it was interesting to observe the lowered responsiveness to morphine analgesia in the WKY rats combined with the model of OA pain. Human work largely relies on self-report and on statistics of opioid usage, which can make it challenging to separate the effects of opioid effectiveness from opioid seeking behaviour and opioid prescribing behaviour. The mechanisms underlying changes in μ opioid receptor function are still not well understood, but in my thesis, heightened anxiety was linked to a lowered effectiveness of morphine, independent of opioid seeking/prescribing behaviour, in conjunction with alterations in functional connectivity. This work is highly relevant, given the rise of opioid prescribing and the wider opioid epidemic, and the socioeconomic burden of treating chronic pain.

7.7 Interpretation of functional connectivity results

A critical question about the neuroimaging findings, both from the fMRI functional connectivity and ECoG work, is what the significance of these findings actually is, and what these findings mean for pain. Resting state functional connectivity changes reflect changes in spontaneous BOLD activity in the brain, which is an indirect measure of neuronal activity. Functional connectivity changes have been shown for almost every condition or symptom that involves the central nervous system, however it is unclear what these changes actually reflect mechanistically (Cowdrey *et al.*, 2014; Mulders *et al.*, 2015; Hull *et al.*, 2017).

Functional connectivity, at its core, refers to the statistical correlation of activity between regions, which does not provide any information about the directionality of the information flow, or whether these changes reflect adaptive or maladaptive processes in response to the condition. If functional connectivity changes occur in conjunction with changes in behaviour, it is also not clear exactly how they relate to illness/experience/responses to treatment, only that they are assumed to relate to that behaviour.

Functional connectivity has, however, been shown to be related to structural connectivity which can be measured with diffusion weighted MRI, a technique which uses diffusion of water molecules to generate contrast for structural brain differences. In a review of studies that investigated both functional and structural connectivity, 27 out of 28 studies showed a positive structure-function relationship (Straathof *et al*, 2019), suggesting that structural connectivity likely underpins functional connectivity.

7.8 Reproducibility and translatability of research

In this thesis, a difference in pain behaviour following intra-articular MIA was observed between batches of WKY rats used in the imaging work (chapter 4) and the opioid pharmacology studies (chapter 5). There were some experimental differences between the two chapters which may account for some of this difference. In particular, some of the pain behaviour in Chapter 5 was split between myself and another researcher for practical reasons and the work was undertaken during different periods of the year. Behavioural pain testing has a subjective element and has been shown to be variable between experimenters and changes in the local environment. In particular, a study of rats and mice demonstrated that exposure to men was able to induce a stress response, thereby creating an additional analgesic response (Sorge *et al*, 2014). Stress induced analgesia is a well-known phenomenon, and is an important consideration in studies of pain, particularly when combined with anxiety (See review: Butler and Finn, 2009). Stress induced analgesia was not tested in this thesis, and therefore may be a factor leading to differences between experiments due to different researcher involvement, differences between batches of rats per se and environmental differences due to the period of the study. Nevertheless, all experiments were designed so that complete controls were included for all studies allowing appropriate comparisons between groups.

In this PhD, behavioural testing was conducted twice weekly, not only for the behavioural pharmacology work but also for the fMRI study. In the rodent neuroimaging literature, behaviour has not been consistently measured. In particular, in a study of migraine pain, pain was accepted with little validation above signs such as inflammation (Spisak, 2017). In situations where pain behaviour is not assessed, it is unclear how changes in the BOLD response actually relate to the pain experience and to what degree central sensitisation or hyperalgesia are present.

A criticism often levelled at rodent methods of nociceptive testing is that behavioural changes due to the experience of pain are not necessarily equivalent across species, and certainly, the behaviours that are indicative of pain in the human may not be applicable in the rat or the mouse and vice versa (Mao, 2012). The reliance on evoked measures of pain behaviour is thought to be problematic, as clinically, pain is self-reported in the human and is generally described as spontaneous in nature, in absence of overt stimulation (Mao, 2012). The use of neuroimaging to investigate functional connectivity, in conjunction with behavioural measurements, aids translatability by providing additional brain measures and not solely relying on evoked pain behaviour.

Variations also exist between models of OA pain, in terms of the resulting joint damage, timescale, and degree of pain/pain phenotype experienced. In these studies the MIA model of OA pain was chosen in order to provide a reproducible pain phenotype, as this was the primary outcome (Combe, Bramwell and Field, 2004). However, this was at the expense of valid modelling of OA pathology in the joint (Teeple *et al.*, 2013). However, animal models are important for the standardisation of genetic and environmental backgrounds and facilitate the characterisation of anatomy, neurochemistry and allow for electrophysiology and tissue collection that would not be possible in humans (Mogil, Davis and Derbyshire, 2010).

7.9 Future directions

The work in this thesis has demonstrated that the investigation of the mechanisms underlying the influence of anxiety on chronic pain although clinically important, is technically challenging. The fMRI work provided a preliminary base from which to ask some detailed questions about functional connectivity in OA pain. This thesis used a number of

different techniques to examine behavioural changes in response to opioids and opioid antagonists, BOLD responses and neuronal responses, in vivo. Although these approaches point to behavioural differences in response to pain, responses to morphine analgesia and differences in endogenous opioids, and changes in functional connectivity, interpretation of the underlying mechanisms from these techniques is limited.

The work in this thesis suggests that functional connectivity changes occur in response to OA pain, and that anxiety can alter this relationship. There are several interesting questions that arise from my work.

Work in this thesis measured functional connectivity at the endpoint of the MIA model of OA pain. An interesting addition to this work would be to investigate when in the MIA model these changes take place, with longitudinal imaging before intra-articular MIA, at an early time point and at a late time point of the model. One of the primary advantages of MRI is its non-invasive nature, making it particularly suitable for longitudinal imaging. Longitudinal imaging would also facilitate the investigation of individual differences in pain responses, which could be important for the treatment of pain. It would be clinically interesting to determine whether anxiety levels or pain sensitivity at early time points predict subsequent changes supraspinal functional connectivity and whether changes in functional connectivity could be related to differences in pain phenotypes and could provide a preliminary neuroimaging biomarker. A neuroimaging biomarker: a measureable pattern of brain activity predictive of some outcome, for example pain, or a certain pain phenotype, would complement behavioural measures of pain and provide biological targets for interventions (Reddan and Wager, 2018).

It is clear from the literature reviewed in this thesis that the findings from the fMRI pain research field are incredibly heterogeneous. Although

regions that are known to be involved in pain processing are likely always implicated in pain imaging studies, the lack of replicability of fMRI studies is a major issue. The discordance in findings of the preclinical pain imaging literature, and neuroimaging literature as a whole, emphasises the need for the differences in functional connectivity identified in the model of OA pain in the rat in this thesis to be confirmed in future studies (Poldrac*k et al*, 2017). Another important approach is to use complementary imaging modalities for provide supporting evidence of the mechanisms changes presented herein. For example, PET imaging would facilitate the understanding of the potential changes in opioid receptor function in the model of OA pain, or the potential impact of co-morbid anxiety. The use of manganese-enhanced MRI approaches is an alternative powerful approach to overcome the problematic effects of anaesthesia on the BOLD signal (Devonshire *et al.*, 2017).

While the work in this PhD showed some promising results in terms of general changes that occur in CNS connectivity associated with chronic pain and anxiety, advances in mechanistic understanding were more limited. Future work to identify the underlying mechanistic changes in opioid receptor function would be valuable for the understanding of the effects of pain and anxiety on the experience and treatment of pain. With imaging, it could be useful to investigate the effect of morphine on BOLD activity in these two strains of rats, potentially providing some localisation of supraspinal opioidergic differences.

Future work should focus on the use of molecular techniques to determine changes in the density, distribution and functional coupling of opioid receptors. Although the μ opioid receptor was the most translationally relevant opioid receptor for my thesis, κ opioid receptors have also been implicated in stress and chronic pain (Navratilova *et al.*, 2019), and future studies could investigate their roles further.

Conclusion

This thesis set out to investigate functional connectivity changes in response to the MIA model of OA pain, and whether endogenous anxiety mediated this relationship.

Functional connectivity differences were observed following induction of the MIA model of OA pain and correlation analysis revealed that the relationship between pain behaviour and functional connectivity from the vmPFC to the caudate putamen/S2 was altered in the high anxiety WKY strain of rats, possibly reflecting dysfunction of the vmPFC in emotional regulation in response to pain.

The regions identified in the functional connectivity analysis have established involvement in the opioidergic descending control of pain, and differences were not evident in regions not involved in pain processing.

Behaviourally, in the WKY rats, responses to morphine were attenuated, with increased opioidergic tone, suggesting that some of the differences in the sensitivity to morphine may reflect differences in the endogenous opioid system. These changes are important to understand, given the rise of the opioid epidemic and the difficulties in the treatment of chronic pain, particularly in light of the worsening effect of negative affect both on treatment and also on the severity of pain.

While this study provided new evidence of the influence of anxiety on functional brain changes in the MIA model of OA pain, further work is required to replicate the new functional connectivity data and focus on molecular mechanisms underpinning the altered function of the opioidergic system.

References

• *OTC medicines: breakdown of sales value 2017-2018 | UK Statistic* (no date). Available at: https://www.statista.com/statistics/415963/over-the-counter-otc-medicine-breakdown-of-sales-in-great-britain/ (Accessed: 22 May 2019).

Abaei, M. *et al.* (2016) 'Neural correlates of hyperalgesia in the monosodium iodoacetate model of osteoarthritis pain', *Molecular Pain*, 12, pp. 1–12. doi: 10.1177/1744806916642445.

ACR Diagnostic Guidelines (no date). Available at: https://www.hopkinsarthritis.org/physician-corner/education/arthritis-education-diagnostic-guidelines/#class_knee (Accessed: 13 June 2019).

Akaike, A. *et al.* (1978) 'Analgesia induced by microinjection of morphine into, and electrical stimulation of, the nucleus reticularis paragigantocellularis of rat medulla oblongata.', *Neuropharmacology*, 17(9), pp. 775–8. Available at: http://www.ncbi.nlm.nih.gov/pubmed/692832 (Accessed: 27 May 2019).

An, X. *et al.* (1998) 'Prefrontal cortical projections to longitudinal columns in the midbrain periaqueductal gray in macaque monkeys', *Journal of Comparative Neurology*, 401(4), pp. 455–479. doi: 10.1002/(SICI)1096-9861(19981130)401:4<455::AID-CNE3>3.0.CO;2-6.

Antal, M. *et al.* (1996) 'Direct evidence of an extensive GABAergic innervation of the spinal dorsal horn by fibres descending from the rostral ventromedial medulla', *Neuroscience*, 73(2), pp. 509–518. doi: 10.1016/0306-4522(96)00063-2.

Apkarian, A. V. *et al.* (2005) 'Human brain mechanisms of pain perception and regulation in health and disease', *European Journal of Pain*. John Wiley & Sons, Ltd, 9(4), pp. 463–484. doi:

10.1016/j.ejpain.2004.11.001.

Apkarian, A. V. (2015) *The brain adapting with pain: Contribution of neuroimaging technology to pain mechanisms*, *The Brain Adapting with Pain: Contribution of Neuroimaging Technology to Pain Mechanisms*. Available at: https://www.scopus.com/inward/record.uri?eid=2-s2.0-84979877966&partnerID=40&md5=a362c7257a99097c9c6db3a9dfecec3d (Accessed: 14 June 2016).

Apkarian, A. V. and Chialvo, D. R. (2006) 'The shadows of pain', *Pain*, August, pp. 221–222. doi: 10.1016/j.pain.2006.04.028.

Apkarian, A. V *et al.* (1992) 'Persistent pain inhibits contralateral somatosensory cortical activity in humans.', *Neuroscience letters*, 140(2), pp. 141–7. Available at: http://www.ncbi.nlm.nih.gov/pubmed/1501770 (Accessed: 5 June 2019).

Ashaye, T. *et al.* (2018) 'Opioid prescribing for chronic musculoskeletal pain in UK primary care: results from a cohort analysis of the COPERS trial.', *BMJ open*. British Medical Journal Publishing Group, 8(6), p. e019491. doi: 10.1136/bmjopen-2017-019491.

Bajic, D. *et al.* (2017) 'Identifying Rodent Resting-State Brain Networks with Independent Component Analysis', *Frontiers in Neuroscience*, 11(December). doi: 10.3389/fnins.2017.00685.

Baliki, M. N. *et al.* (2008) 'Beyond Feeling: Chronic Pain Hurts the Brain, Disrupting the Default-Mode Network Dynamics', *Journal of Neuroscience*, 28(6), pp. 1398–1403. doi: 10.1523/JNEUROSCI.4123-07.2008.

Baliki, Marwan N *et al.* (2014) 'Functional reorganization of the default mode network across chronic pain conditions', *PLoS ONE*, 9(9). doi: 10.1371/journal.pone.0106133.

Baliki, M N *et al.* (2014) 'Resting-sate functional reorganization of the rat limbic system following neuropathic injury.', *Scientific reports*, 4, p. 6186.

doi: 10.1038/srep06186.

Bannuru, R. R. *et al.* (2015) 'Comparative effectiveness of pharmacologic interventions for knee osteoarthritis: A systematic review and network meta-analysis', *Annals of Internal Medicine*, 162(1), pp. 46–54. doi: 10.7326/M14-1231.

Barnett, L. A. *et al.* (2018) 'Relationship of anxiety with joint pain and its management: A population survey.', *Musculoskeletal care*, 16(3), pp. 353–362. doi: 10.1002/msc.1243.

Barthas, F. *et al.* (2015) 'The anterior cingulate cortex is a critical hub for pain-induced depression', *Biological Psychiatry*. Elsevier, 77(3), pp. 236–245. doi: 10.1016/j.biopsych.2014.08.004.

Beckmann, C. F. *et al.* (1995) 'Decomposing FMRI data using ICA', *Magnetic Resonance Imaging*, 1(1995), pp. 1–16.

Behroozi, M. *et al.* (no date) 'In Vivo Measurement of T 1 and T 2 Relaxation Times in Awake Pigeon and Rat Brains at 7T'. doi: 10.1002/mrm.26722.

Benromano, T. *et al.* (2017) 'Increased evoked potentials and behavioral indices in response to pain among individuals with intellectual disability', *Pain Medicine (United States)*. Oxford University Press, 18(9), pp. 1715–1730. doi: 10.1093/pm/pnw349.

Beswick, a. D. *et al.* (2012) 'What proportion of patients report long-term pain after total hip or knee replacement for osteoarthritis? A systematic review of prospective studies in unselected patients', *BMJ Open*, 2(1), pp. e000435–e000435. doi: 10.1136/bmjopen-2011-000435.

Bingel, U. *et al.* (2004) 'Somatotopic organization of human somatosensory cortices for pain: A single trial fMRI study', *NeuroImage*, 23(1), pp. 224–232. doi: 10.1016/j.neuroimage.2004.05.021.

Birn, R. M. *et al.* (2006) 'Separating respiratory-variation-related fluctuations from neuronal-activity-related fluctuations in fMRI', *NeuroImage*, 31(4), pp. 1536–1548. doi: 10.1016/j.neuroimage.2006.02.048.

Biswal, B. *et al.* (1995) 'Functional connectivity in the motor cortex of resting human brain using echo-planar MRI.', *Magnetic resonance in medicine*, 34(4), pp. 537–41. Available at: http://www.ncbi.nlm.nih.gov/pubmed/8524021 (Accessed: 26 April 2019).

Bloodgood, D. W. *et al.* (2018) 'Fear extinction requires infralimbic cortex projections to the basolateral amygdala', *Translational Psychiatry*. Nature Publishing Group, 8(1). doi: 10.1038/s41398-018-0106-x.

Borras, M. C. *et al.* (2004) 'FMRI Measurement of CNS Responses to Naloxone Infusion and Subsequent Mild Noxious Thermal Stimuli in Healthy Volunteers', *Journal of Neurophysiology*, 91(6), pp. 2723–2733. doi: 10.1152/jn.00249.2003.

Borsook, D. *et al.* (2016) 'Reward deficiency and anti-reward in pain chronification', *Neuroscience and Biobehavioral Reviews*. Elsevier Ltd, pp. 282–297. doi: 10.1016/j.neubiorev.2016.05.033.

Bove, G. M. and Swenson, R. S. (2006) 'Nociceptors and Peripheral Sources of Pain', in *Pain Management*. Elsevier Inc., pp. 1081–1092. doi: 10.1016/B978-0-7216-0334-6.50133-3.

Bove, S. . *et al.* (2003) 'Weight bearing as a measure of disease progression and efficacy of anti-inflammatory compounds in a model of monosodium iodoacetate-induced osteoarthritis', *Osteoarthritis and Cartilage*. W.B. Saunders, 11(11), pp. 821–830. doi: 10.1016/S1063-4584(03)00163-8.

Bowker, R. M., Westlund, K. N. and Coulter, J. D. (1981) 'Origins of serotonergic projections to the spinal cord in rat: An immunocytochemical-retrograde transport study', *Brain Research*, 226(1–

2), pp. 187–199. doi: 10.1016/0006-8993(81)91092-1.

Breivik, H. *et al.* (2006) 'Survey of chronic pain in Europe: Prevalence, impact on daily life, and treatment', *European Journal of Pain*, 10(4), pp. 287–287. doi: 10.1016/j.ejpain.2005.06.009.

Brooks, J. C. W. *et al.* (2005) 'Somatotopic organisation of the human insula to painful heat studied with high resolution functional imaging', *NeuroImage*, 27(1), pp. 201–209. doi: 10.1016/j.neuroimage.2005.03.041.

Bruehl, S. *et al.* (2017) 'Do Resting Plasma β-Endorphin Levels Predict Responses to Opioid Analgesics?', *The Clinical Journal of Pain*, 33(1), pp. 12–20. doi: 10.1097/AJP.0000000000000389.

Bukhari, Q. *et al.* (2017) 'Resting state fMRI in mice reveals anesthesia specific signatures of brain functional networks and their interactions', *Frontiers in Neural Circuits*. Frontiers Research Foundation, 11. doi: 10.3389/fncir.2017.00005.

Bunk, S. F. *et al.* (2018) 'Does EEG activity during painful stimulation mirror more closely the noxious stimulus intensity or the subjective pain sensation?', *Somatosensory & Motor Research*. Informa UK Limited, 35(3–4), pp. 192–198. doi: 10.1080/08990220.2018.1521790.

Buntin-Mushock, C. *et al.* (2005) 'Age-dependent opioid escalation in chronic pain patients', *Anesthesia and Analgesia*, pp. 1740–1745. doi: 10.1213/01.ANE.0000152191.29311.9B.

Bushnell, M. C. *et al.* (1999) 'Pain perception: Is there a role for primary somatosensory cortex?', *Proceedings of the National Academy of Sciences*. National Academy of Sciences, 96(14), pp. 7705–7709. doi: 10.1073/PNAS.96.14.7705.

Buskila, D. and Cohen, H. (2007) 'Comorbidity of fibromyalgia and psychiatric disorders', *Current Pain and Headache Reports*, pp. 333–338. doi: 10.1007/s11916-007-0214-4.

Busse, J. W. *et al.* (2018) 'Opioids for Chronic Noncancer Pain', *Jama*, 320(23), p. 2448. doi: 10.1001/jama.2018.18472.

Butler, R. K. and Finn, D. P. (2009) 'Stress-induced analgesia', *Progress in Neurobiology*, pp. 184–202. doi: 10.1016/j.pneurobio.2009.04.003.

Buzsáki, G., Anastassiou, C. A. and Koch, C. (2012) 'The origin of extracellular fields and currents--EEG, ECoG, LFP and spikes.', *Nature reviews. Neuroscience*. NIH Public Access, 13(6), pp. 407–20. doi: 10.1038/nrn3241.

Carrillo, M. *et al.* (2019) 'Emotional Mirror Neurons in the Rat's Anterior Cingulate Cortex', *Current Biology*. Cell Press, 29(8), pp. 1301-1312.e6. doi: 10.1016/J.CUB.2019.03.024.

La Cesa, S. *et al.* (2014) 'FMRI pain activation in the periaqueductal gray in healthy volunteers during the cold pressor test', *Magnetic Resonance Imaging*, 32(3), pp. 236–240. doi: 10.1016/j.mri.2013.12.003.

Chang, C. T., Jiang, B. Y. and Chen, C. C. (2019) 'Ion channels involved in substance P-mediated nociception and antinociception', *International Journal of Molecular Sciences*. MDPI AG, p. 1596. doi: 10.3390/ijms20071596.

Chang, Pei-ching *et al.* (2016) 'Novel method for functional brain imaging in awake minimally restrained rats', *Journal of Neurophysiology*, 116(1), pp. 61–80. doi: 10.1152/jn.01078.2015.

Chang, P *et al.* (2016) 'The Development of Nociceptive Network Activity in the Somatosensory Cortex of Freely Moving Rat Pups.', *Cerebral cortex (New York, N.Y. : 1991)*, 26(12), pp. 4513–4523. doi: 10.1093/cercor/bhw330.

Chaplan, S. R. *et al.* (1994) 'Quantitative assessment of tactile allodynia in the rat paw', *Journal of Neuroscience Methods*, 53(1), pp. 55–63. doi: 10.1016/0165-0270(94)90144-9.

Chaves, J. F. and Brown, J. M. (1987) 'Spontaneous cognitive strategies for the control of clinical pain and stress', *Journal of Behavioral Medicine*. Kluwer Academic Publishers-Plenum Publishers, 10(3), pp. 263–276. doi: 10.1007/BF00846540.

Chehadi, O. *et al.* (2017) 'Gray matter alteration associated with pain catastrophizing in patients 6 months after lumbar disk surgery: a voxel-based morphometry study.', *Pain reports*. Wolters Kluwer Health, 2(5), p. e617. doi: 10.1097/PR9.0000000000000617.

Cheriyan, J. and Sheets, P. L. (2018) 'Altered excitability and local connectivity of mPFC-PAG neurons in a mouse model of neuropathic pain', *Journal of Neuroscience*. Society for Neuroscience, 38(20), pp. 4829–4839. doi: 10.1523/JNEUROSCI.2731-17.2018.

Comb, M. *et al.* (1982) 'Primary structure of the human Met- And Leu-enkephalin precursor and its mRNA', *Nature*. Nature Publishing Group, 295(5851), pp. 663–666. doi: 10.1038/295663a0.

Combe, R., Bramwell, S. and Field, M. J. (2004) 'The monosodium iodoacetate model of osteoarthritis: A model of chronic nociceptive pain in rats?', *Neuroscience Letters*. doi: 10.1016/j.neulet.2004.08.023.

Cooper, S. J. (1975) 'Anaesthetisation of prefrontal cortex and response to noxious stimulation', *Nature*. Nature Publishing Group, 254(5499), pp. 439–440. doi: 10.1038/254439a0.

Correa-Sales, C., Rabin, B. C. and Maze, M. (1992) 'A hypnotic response to dexmedetomidine, an alpha 2 agonist, is mediated in the locus coeruleus in rats.', *Anesthesiology*, 76(6), pp. 948–52. doi: 10.1097/00000542-199206000-00013.

Cottam, W. J. *et al.* (2018) 'Altered Connectivity of the Right Anterior Insula Drives the Pain Connectome Changes in Chronic Knee Osteoarthritis', *Pain*, 159(5), p. 1. doi: 10.1097/j.pain.0000000000001209.

Cowdrey, F. A. *et al.* (2014) 'Increased resting state functional connectivity in the default mode network in recovered anorexia nervosa', *Human Brain Mapping*, 35(2), pp. 483–491. doi: 10.1002/hbm.22202.

Critchley, H. *et al.* (2007) 'Neural Activity Relating to Generation and Representation of Galvanic Skin Conductance Responses: A Functional Magnetic Resonance Imaging Study', *Journal of Neuroscience*. Society for Neuroscience, 20(8), pp. 3033–3040. doi: 20024039.

Cubukcu, D., Sarsan, A. and Alkan, H. (2012) 'Relationships between Pain, Function and Radiographic Findings in Osteoarthritis of the Knee: A Cross-Sectional Study.', *Arthritis*. Hindawi Limited, 2012, p. 984060. doi: 10.1155/2012/984060.

Damoiseaux, J. S. *et al.* (2006) 'Consistent resting-state networks across healthy subjects', *Proceedings of the National Academy of Sciences*. National Acad Sciences, 103(37), pp. 13848–13853. doi: 10.1073/pnas.0601417103.

Daniel Kalthoff and Matthias Hoen (no date) *No Title*. Available at: https://www.bruker.com/fileadmin/user_upload/8-PDF-Docs/MagneticResonance/MRI/brochures/functional_Connectivity.pdf (Accessed: 27 June 2020).

Davis, M. *et al.* (2010) 'Phasic vs Sustained Fear in Rats and Humans: Role of the Extended Amygdala in Fear vs Anxiety', *Neuropsychopharmacology*, 35(1), pp. 105–135. doi: 10.1038/npp.2009.109.

Deligianni, F. *et al.* (2014) 'Relating resting-state fMRI and EEG whole-brain connectomes across frequency bands', *Frontiers in Neuroscience*. Frontiers, 8, p. 258. doi: 10.3389/fnins.2014.00258.

Deuis, J. R., Dvorakova, L. S. and Vetter, I. (2017) 'Methods used to evaluate pain behaviors in rodents', *Frontiers in Molecular Neuroscience*. Frontiers Media S.A. doi: 10.3389/fnmol.2017.00284.

Devonshire, I. M. *et al.* (2015) 'A quantification of the relationship between neuronal responses in the rat rostral ventromedial medulla and noxious stimulation-evoked withdrawal reflexes', *European Journal of Neuroscience*. Blackwell Publishing Ltd, 42(1), pp. 1726–1737. doi: 10.1111/ejn.12942.

Devonshire, I. M. *et al.* (2017) 'Manganese-enhanced magnetic resonance imaging depicts brain activity in models of acute and chronic pain: A new window to study experimental spontaneous pain?', *NeuroImage*, 157, pp. 500–510. doi: 10.1016/j.neuroimage.2017.06.034.

Devonshire, I. M., Greenspon, C. M. and Hathway, G. J. (2015) 'Developmental alterations in noxious-evoked EEG activity recorded from rat primary somatosensory cortex', *Neuroscience*. Elsevier Ltd, 305, pp. 343–350. doi: 10.1016/j.neuroscience.2015.08.004.

Dixon, W. J. (1980) 'Efficient Analysis of Experimental Observations', *Annual Review of Pharmacology and Toxicology*, 20(1), pp. 441–462. doi: 10.1146/annurev.pa.20.040180.002301.

Dray, A. (1995) *Inflammatory mediators of pain*, *British Journal of Anaesthesia*. doi: 10.1093/bja/75.2.125.

Dunckley, P. *et al.* (2005) 'Cortical processing of visceral and somatic stimulation: Differentiating pain intensity from unpleasantness', *Neuroscience*. Pergamon, 133(2), pp. 533–542. doi: 10.1016/J.NEUROSCIENCE.2005.02.041.

Elliott, J. E. (1997) 'Organochlorine contaminants in seabird eggs from the Queen Charlotte Islands', *Occasional Paper of the Canadian Wildlife Service*, (93), pp. 137–146. doi: 10.1016/j.biopsych.2005.02.021.

Englund, M., Guermazi, A. and Lohmander, S. L. (2009) 'The Role of the Meniscus in Knee Osteoarthritis: a Cause or Consequence?', *Radiologic Clinics of North America*, pp. 703–712. doi: 10.1016/j.rcl.2009.03.003.

Ernst, R. R. and Anderson, W. A. (1966) 'Application of Fourier Transform Spectroscopy to Magnetic Resonance', *Review of Scientific Instruments*, 37(1), pp. 93–102. doi: 10.1063/1.1719961.

Faull, R. L. and Villiger, J. W. (1987) 'Opiate receptors in the human spinal cord: a detailed anatomical study comparing the autoradiographic localization of [3H]diprenorphine binding sites with the laminar pattern of substance P, myelin and nissl staining.', *Neuroscience*, 20(2), pp. 395–407. Available at: http://www.ncbi.nlm.nih.gov/pubmed/2438589 (Accessed: 21 May 2019).

Fayaz, A. *et al.* (2016) 'Prevalence of chronic pain in the UK: a systematic review and meta-analysis of population studies.', *BMJ open*. British Medical Journal Publishing Group, 6(6), p. e010364. doi: 10.1136/bmjopen-2015-010364.

Feingold, D. *et al.* (2017) 'Depression and anxiety among chronic pain patients receiving prescription opioids and medical marijuana', *Journal of Affective Disorders*. Elsevier B.V., 218(October 2016), pp. 1–7. doi: 10.1016/j.jad.2017.04.026.

Feingold, D. *et al.* (2018) 'Journal of A ff ective Disorders The association between severity of depression and prescription opioid misuse among chronic pain patients with and without anxiety : A cross- sectional study', *Journal of Affective Disorders*. Elsevier B.V., 235(March), pp. 293–302. doi: 10.1016/j.jad.2018.04.058.

Ferguson, S. a. and Cada, A. M. (2004) 'Spatial learning/memory and social and nonsocial behaviors in the Spontaneously Hypertensive, Wistar-Kyoto and Sprague-Dawley rat strains', *Pharmacology Biochemistry and Behavior*, 77(3), pp. 583–594. doi: 10.1016/j.pbb.2003.12.014.

Fields, H. (1991) 'Neurotransmitters In Nociceptive Modulatory Circuits', *Annual Review of Neuroscience*. Annual Reviews, 14(1), pp. 219–245. doi:

10.1146/annurev.neuro.14.1.219.

Fields, H. L. *et al.* (1983) 'The activity of neurons in the rostral medulla of the rat during withdrawal from noxious heat', *Journal of Neuroscience*, 3(12), pp. 2545–2552. doi: 10.1523/jneurosci.03-12-02545.1983.

Fillingim, R. B. *et al.* (2005) 'Sex-related psychological predictors of baseline pain perception and analgesic responses to pentazocine', *Biological Psychology*, 69(1 SPEC. ISS.), pp. 97–112. doi: 10.1016/j.biopsycho.2004.11.008.

Finan, P. H. *et al.* (2013) 'Discordance between pain and radiographic severity in knee osteoarthritis: Findings from quantitative sensory testing of central sensitization', *Arthritis and Rheumatism*, 65(2), pp. 363–372. doi: 10.1002/art.34646.

Flecknell, P. *et al.* (2015) 'Preanesthesia, Anesthesia, Analgesia, and Euthanasia', *Laboratory Animal Medicine*. Academic Press, pp. 1135–1200. doi: 10.1016/B978-0-12-409527-4.00024-9.

Forsythe, M. E. *et al.* (2008) 'Prospective relation between catastrophizing and residual pain following knee arthroplasty: Two-year follow-up', *Pain Research and Management*. Hindawi Limited, 13(4), pp. 335–341. doi: 10.1155/2008/730951.

Goldstein, A. *et al.* (1979) 'Dynorphin-(1-13), an extraordinarily potent opioid peptide.', *Proceedings of the National Academy of Sciences of the United States of America*. National Academy of Sciences, 76(12), pp. 6666–70. doi: 10.1073/pnas.76.12.6666.

Gracely, R. H. *et al.* (2004) 'Pain catastrophizing and neural responses to pain among persons with fibromyalgia', *Brain*, 127(4), pp. 835–843. doi: 10.1093/brain/awh098.

Graeff, F. G. *et al.* (1993) 'Role of the amygdala and periaqueductal gray in anxiety and panic', *Behavioural Brain Research*, 58(1–2), pp. 123–131. doi:

10.1016/0166-4328(93)90097-A.

Grandjean, J. *et al.* (2014) 'Optimization of anesthesia protocol for resting-state fMRI in mice based on differential effects of anesthetics on functional connectivity patterns', *NeuroImage*. Elsevier Inc., 102(P2), pp. 838–847. doi: 10.1016/j.neuroimage.2014.08.043.

Griffa, A. *et al.* (2013) 'Structural connectomics in brain diseases', *NeuroImage*. Academic Press, 80, pp. 515–526. doi: 10.1016/j.neuroimage.2013.04.056.

Griffanti, L. *et al.* (2017) 'Hand classification of fMRI ICA noise components', *NeuroImage*, 154(June 2016), pp. 188–205. doi: 10.1016/j.neuroimage.2016.12.036.

Guingamp, C. *et al.* (1997) *A Dose-Response Study of Loss of Mobility, Morphology, and Biochemistry*, *ARTHRITIS & RHEUMATISM*. Available at: https://onlinelibrary.wiley.com/doi/pdf/10.1002/art.1780400917 (Accessed: 16 April 2019).

Guy, G. P. *et al.* (2017) 'Vital Signs: Changes in Opioid Prescribing in the United States, 2006-2015.', *MMWR. Morbidity and mortality weekly report*. Centers for Disease Control and Prevention, 66(26), pp. 697–704. doi: 10.15585/mmwr.mm6626a4.

Hadler, N. M. (1992) 'Knee pain is the malady - Not osteoarthritis', *Annals of Internal Medicine*, pp. 598–599. doi: 10.7326/0003-4819-116-7-598.

Hagmann, P. *et al.* (2008) 'Mapping the Structural Core of Human Cerebral Cortex', *PLoS Biology*. Edited by K. J. Friston. Public Library of Science, 6(7), p. e159. doi: 10.1371/journal.pbio.0060159.

Hahn, A. *et al.* (2013) 'Comparing neural response to painful electrical stimulation with functional MRI at 3 and 7 T', *NeuroImage*. Academic Press, 82, pp. 336–343. doi: 10.1016/J.NEUROIMAGE.2013.06.010.

Hayes, D. J. *et al.* (2017) 'Affective Circuitry Alterations in Patients with Trigeminal Neuralgia', *Frontiers in Neuroanatomy*, 11, p. 73. doi: 10.3389/fnana.2017.00073.

Haywood, A. R., Hathway, G. J. and Chapman, V. (2018) 'Differential contributions of peripheral and central mechanisms to pain in a rodent model of osteoarthritis', *Scientific Reports*. Nature Publishing Group, 8(1). doi: 10.1038/s41598-018-25581-8.

Hestehave, S. *et al.* (2019) 'The analgesic efficacy of morphine varies with rat strain and experimental pain model: implications for target validation efforts in pain drug discovery', *European Journal of Pain (United Kingdom)*. Blackwell Publishing Ltd, 23(3), pp. 539–554. doi: 10.1002/ejp.1327.

Hill, C. L. *et al.* (2007) 'Synovitis detected on magnetic resonance imaging and its relation to pain and cartilage loss in knee osteoarthritis.', *Annals of the rheumatic diseases*. BMJ Publishing Group, 66(12), pp. 1599–603. doi: 10.1136/ard.2006.067470.

Hope, P. J., Fleetwood-Walker, S. M. and Mitchell, R. (1990) 'Distinct antinociceptive actions mediated by different opioid receptors in the region of lamina I and laminae III-V of the dorsal horn of the rat.', *British journal of pharmacology*. Wiley-Blackwell, 101(2), pp. 477–83. doi: 10.1111/j.1476-5381.1990.tb12733.x.

Hoshiyama, Y. *et al.* (2015) 'Chondrocyte clusters adjacent to sites of cartilage degeneration have characteristics of progenitor cells.', *Journal of orthopaedic research : official publication of the Orthopaedic Research Society*. NIH Public Access, 33(4), pp. 548–55. doi: 10.1002/jor.22782.

Hoyer, C. *et al.* (2014) 'Advantages and Challenges of Small Animal Magnetic Resonance Imaging as a Translational Tool', *Neuropsychobiology*. Karger Publishers, 69(4), pp. 187–201. doi: 10.1159/000360859.

Hubbard, C. S. *et al.* (2014) 'Altered Brain Structure and Function Correlate with Disease Severity and Pain Catastrophizing in Migraine Patients.', *eNeuro*. Society for Neuroscience, 1(1), p. e20.14. doi: 10.1523/ENEURO.0006-14.2014.

Hughes, J. *et al.* (1975) 'Identification of two related pentapeptides from the brain with potent opiate agonist activity', *Nature*. Nature Publishing Group, 258(5536), pp. 577–579. doi: 10.1038/258577a0.

Hull, J. V. *et al.* (2017) 'Resting-state functional connectivity in autism spectrum disorders: A review', *Frontiers in Psychiatry*. Frontiers Media S.A. doi: 10.3389/fpsyt.2016.00205.

Iannetti, G. D. *et al.* (2008) 'Determinants of laser-evoked EEG responses: Pain perception or stimulus saliency?', *Journal of Neurophysiology*, 100(2), pp. 815–828. doi: 10.1152/jn.00097.2008.

Iannetti, G. D. and Mouraux, a. (2010) 'From the neuromatrix to the pain matrix (and back)', *Experimental Brain Research*, 205(1), pp. 1–12. doi: 10.1007/s00221-010-2340-1.

Jacobsen, P. B. and Butler, R. W. (1996) 'Relation of cognitive coping and catastrophizing to acute pain and analgesic use following breast cancer surgery', *Journal of Behavioral Medicine*, 19(1), pp. 17–29. doi: 10.1007/BF01858172.

Jang, H. S. *et al.* (2009) 'Evaluation of t e anaesthetic effects of medetomidine and ketamine in rats and their reversal with atipamezole', *Veterinary Anaesthesia and Analgesia*. Blackwell Publishing Ltd, 36(4), pp. 319–327. doi: 10.1111/j.1467-2995.2009.00463.x.

Jenkinson, M. *et al.* (2002) 'Improved optimization for the robust and accurate linear registration and motion correction of brain images', *NeuroImage*, 17(2), pp. 825–841. doi: 10.1016/S1053-8119(02)91132-8.

Jia, H., Hu, X. and Deshpande, G. (2014) 'Behavioral Relevance of the

Dynamics of the Functional Brain Connectome', *Brain Connectivity*, 4(9), pp. 741–759. doi: 10.1089/brain.2014.0300.

Jiang, L. *et al.* (2012) 'Body mass index and susceptibility to knee osteoarthritis: A systematic review and meta-analysis', *Joint Bone Spine*. Elsevier Masson, 79(3), pp. 291–297. doi: 10.1016/J.JBSPIN.2011.05.015.

Johnson, V. L. and Hunter, D. J. (2014) 'The epidemiology of osteoarthritis', *Best Practice & Research Clinical Rheumatology*. Baillière Tindall, 28(1), pp. 5–15. doi: 10.1016/J.BERH.2014.01.004.

Jonckers, E. *et al.* (2015) 'The power of using functional fMRI on small rodents to study brain pharmacology and disease', *Frontiers in Pharmacology*, pp. 1–19. doi: 10.3389/fphar.2015.00231.

Jones, A. K. P. *et al.* (1991) 'Cortical and subcortical localization of response to pain in man using positron emission tomography', *Proceedings of the Royal Society B: Biological Sciences*, 244(1309), pp. 39–44. doi: 10.1098/rspb.1991.0048.

Jones, C. A. *et al.* (2007) 'Total Joint Arthroplasties: Current Concepts of Patient Outcomes after Surgery', *Rheumatic Disease Clinics of North America*, 33(1), pp. 71–86. doi: 10.1016/j.rdc.2006.12.008.

Judge, A. *et al.* (2010) 'Patient-reported outcomes one year after primary hip replacement in a European collaborative cohort', *Arthritis Care and Research*, 62(4), pp. 480–488. doi: 10.1002/acr.20038.

Kalbhen, D. A. (1987) 'Chemical model of osteoarthritis--a pharmacological evaluation.', *The Journal of rheumatology*, 14 Spec No, pp. 130–1. Available at: http://www.ncbi.nlm.nih.gov/pubmed/3625668 (Accessed: 24 June 2019).

Kalso, E. *et al.* (2004) 'Opioids in chronic non-cancer pain: Systematic review of efficacy and safety', *Pain*, 112(3), pp. 372–380. doi: 10.1016/j.pain.2004.09.019.

Karuppal, R. (2017) 'Current concepts in the articular cartilage repair and regeneration', *Journal of Orthopaedics*. Reed Elsevier India Pvt. Ltd., pp. A1–A3. doi: 10.1016/j.jor.2017.05.001.

Koechlin, E., Ody, C. and Kouneiher, F. (2003) 'The Architecture of Cognitive Control in the Human Prefrontal Cortex', *Science*, 302(5648), pp. 1181–1185. doi: 10.1126/science.1088545.

Von Korff, M. and Deyo, R. A. (2004) 'Potent opioids for chronic musculoskeletal pain: Flying blind?', *Pain*, 109(3), pp. 207–209. doi: 10.1016/j.pain.2004.02.019.

van der Kraan, P. M. and van den Berg, W. B. (2012) 'Chondrocyte hypertrophy and osteoarthritis: role in initiation and progression of cartilage degeneration?', *Osteoarthritis and Cartilage*. W.B. Saunders, 20(3), pp. 223–232. doi: 10.1016/J.JOCA.2011.12.003.

Kucyi, A. and Davis, K. D. (2017) 'The Neural Code for Pain: From Single-Cell Electrophysiology to the Dynamic Pain Connectome', *The Neuroscientist*, 23(4), pp. 397–414. doi: 10.1177/1073858416667716.

Laeger, I. *et al.* (2012) 'Amygdala responsiveness to emotional words is modulated by subclinical anxiety and depression', *Behavioural Brain Research*. Elsevier, 233(2), pp. 508–516. doi: 10.1016/J.BBR.2012.05.036.

Lange, A. K. *et al.* (2007) 'Degenerative meniscus tears and mobility impairment in women with knee osteoarthritis', *Osteoarthritis and Cartilage*. W.B. Saunders, 15(6), pp. 701–708. doi: 10.1016/J.JOCA.2006.11.004.

Latremoliere, A. and Woolf, C. J. (2009a) 'Central sensitization: a generator of pain hypersensitivity by central neural plasticity.', *The journal of pain : official journal of the American Pain Society*. NIH Public Access, 10(9), pp. 895–926. doi: 10.1016/j.jpain.2009.06.012.

Latremoliere, A. and Woolf, C. J. (2009b) 'Central sensitization: a

generator of pain hypersensitivity by central neural plasticity.', *The journal of pain : official journal of the American Pain Society*, 10(9), pp. 895–926. doi: 10.1016/j.jpain.2009.06.012.

Leal, P. C. *et al.* (2017) 'Trait vs. state anxiety in different threatening situations', *Trends in Psychiatry and Psychotherapy*. Associação de Psiquiatria do Rio Grande do Sul, 39(3), pp. 147–157. doi: 10.1590/2237-6089-2016-0044.

LeBlanc, B. W. *et al.* (2016) 'Electroencephalographic signatures of pain and analgesia in rats', *Pain*. Lippincott Williams and Wilkins, 157(10), pp. 2330–2340. doi: 10.1097/j.pain.0000000000000652.

Li, A. L. *et al.* (2016) 'Stimulation of the ventral tegmental area increased nociceptive thresholds and decreased spinal dorsal horn neuronal activity in rat', *Experimental Brain Research*. Springer Berlin Heidelberg, 234(6), pp. 1505–1514. doi: 10.1007/s00221-016-4558-z.

Li, Yanhui *et al.* (2017) 'Role of the Lateral Habenula in Pain-Associated Depression.', *Frontiers in behavioral neuroscience*, 11, p. 31. doi: 10.3389/fnbeh.2017.00031.

Liao, W. *et al.* (2010) 'NeuroImage Selective aberrant functional connectivity of resting state networks in social anxiety disorder', *NeuroImage*. Elsevier Inc., 52(4), pp. 1549–1558. doi: 10.1016/j.neuroimage.2010.05.010.

Lieberman, M. D. and Cunningham, W. A. (2009) 'Type I and Type II error concerns in fMRI research: Re-balancing the scale', *Social Cognitive and Affective Neuroscience*, 4(4), pp. 423–428. doi: 10.1093/scan/nsp052.

Ling, G. S. *et al.* (1985) 'Separation of opioid analgesia from respiratory depression: evidence for different receptor mechanisms.', *Journal of Pharmacology and Experimental Therapeutics*, 232(1).

Lluch, E. *et al.* (2014) 'Evidence for central sensitization in patients with

osteoarthritis pain: A systematic literature review', *European Journal of Pain*, 18(10), pp. 1367–1375. doi: 10.1002/j.1532-2149.2014.499.x.

Logothetis, N. K. (2008) 'What we can do and what we cannot do with fMRI', *Nature*. Nature Publishing Group, pp. 869–878. doi: 10.1038/nature06976.

Loh, H. H. *et al.* (1998) 'mu Opioid receptor knockout in mice: effects on ligand-induced analgesia and morphine lethality.', *Brain research. Molecular brain research*, 54(2), pp. 321–6. Available at: http://www.ncbi.nlm.nih.gov/pubmed/9555078 (Accessed: 2 June 2019).

Lueptow, L. M., Fakira, A. K. and Bobeck, E. N. (2018) 'The Contribution of the Descending Pain Modulatory Pathway in Opioid Tolerance', *Frontiers in Neuroscience*. Frontiers, 12, p. 886. doi: 10.3389/fnins.2018.00886.

Ma, V. Y., Chan, L. and Carruthers, K. J. (2014) 'Incidence, prevalence, costs, and impact on disability of common conditions requiring rehabilitation in the united states: Stroke, spinal cord injury, traumatic brain injury, multiple sclerosis, osteoarthritis, rheumatoid arthritis, limb loss, and back pa', *Archives of Physical Medicine and Rehabilitation*. Elsevier Ltd, 95(5), pp. 986-995.e1. doi: 10.1016/j.apmr.2013.10.032.

Malfait, A. M., Little, C. B. and McDougall, J. J. (2013) 'A commentary on modelling osteoarthritis pain in small animals', *Osteoarthritis and Cartilage*. W.B. Saunders, 21(9), pp. 1316–1326. doi: 10.1016/J.JOCA.2013.06.003.

Malfliet, A. *et al.* (2017) 'Brain changes associated with cognitive and emotional factors in chronic pain: A systematic review', *European Journal of Pain*. John Wiley & Sons, Ltd, 21(5), pp. 769–786. doi: 10.1002/ejp.1003.

Man, G. S. and Mologhianu, G. (2014) 'Osteoarthritis pathogenesis - a complex process that involves the entire joint.', *Journal of medicine and*

life. Carol Davila - University Press, 7(1), pp. 37–41. Available at: http://www.ncbi.nlm.nih.gov/pubmed/24653755 (Accessed: 16 October 2019).

Mao, J. (2012) 'Current challenges in translational pain research', *Trends in Pharmacological Sciences*, pp. 568–573. doi: 10.1016/j.tips.2012.08.001.

Marker, C. L. and Pomonis, J. D. (2012) 'The Monosodium Iodoacetate Model of Osteoarthritis Pain in the Rat', in. Humana Press, pp. 239–248. doi: 10.1007/978-1-61779-561-9_18.

Masamoto, K. *et al.* (2007) 'Relationship between neural, vascular, and BOLD signals in isoflurane-anesthetized rat somatosensory cortex', *Cerebral Cortex*, 17(4), pp. 942–950. doi: 10.1093/cercor/bhl005.

Mathiessen, A. and Conaghan, P. G. (2017) 'Synovitis in osteoarthritis: current understanding with therapeutic implications.', *Arthritis research & therapy*. BioMed Central, 19(1), p. 18. doi: 10.1186/s13075-017-1229-9.

May, E. S. *et al.* (2019) 'Prefrontal gamma oscillations reflect ongoing pain intensity in chronic back pain patients.', *Human brain mapping*, 40(1), pp. 293–305. doi: 10.1002/hbm.24373.

Mayer, D. J. and Price, D. D. (1976) 'Central nervous system mechanisms of analgesia.', *Pain*, 2(4), pp. 379–404. Available at: http://www.ncbi.nlm.nih.gov/pubmed/195254 (Accessed: 1 June 2019).

McAuley, J. D. *et al.* (2009) 'Wistar-Kyoto rats as an animal model of anxiety vulnerability: Support for a hypervigilance hypothesis', *Behavioural Brain Research*, 204(1), pp. 162–168. doi: 10.1016/j.bbr.2009.05.036.

McHugh, R. K. *et al.* (2019) 'Pain catastrophizing and distress intolerance: prediction of pain and emotional stress reactivity', *Journal of Behavioral Medicine*. Springer US, pp. 1–7. doi: 10.1007/s10865-019-00086-5.

McHugh, R. K. and Otto, M. W. (2012) 'Refining the Measurement of Distress Intolerance', *Behavior Therapy*, 43(3), pp. 641–651. doi: 10.1016/j.beth.2011.12.001.

McMahon, S. B. (Stephen B. . (2013) *Wall and Melzack's textbook of pain*.

McWilliams, L. A., Cox, B. J. and Enns, M. W. (2003) 'Mood and anxiety disorders associated with chronic pain: An examination in a nationally representative sample', *Pain*, 106(1–2), pp. 127–133. doi: 10.1016/S0304-3959(03)00301-4.

McWilliams, L. A., Goodwin, R. D. and Cox, B. J. (2004) 'Depression and anxiety associated with three pain conditions: Results from a nationally representative sample', *Pain*, 111(1–2), pp. 77–83. doi: 10.1016/j.pain.2004.06.002.

Megat, S. *et al.* (2018) 'A critical role for dopamine D5 receptors in pain chronicity in male mice', *Journal of Neuroscience*. Society for Neuroscience, 38(2), pp. 379–397. doi: 10.1523/JNEUROSCI.2110-17.2017.

MENDELL, L. M. and WALL, P. D. (1965) 'Responses of Single Dorsal Cord Cells to Peripheral Cutaneous Unmyelinated Fibres', *Nature*. Nature Publishing Group, 206(4979), pp. 97–99. doi: 10.1038/206097a0.

Méndez-Ruette, M. *et al.* (2019) 'The Role of the Rodent Insula in Anxiety', *Frontiers in Physiology*. Frontiers, 10, p. 330. doi: 10.3389/fphys.2019.00330.

Meyer, R. A. *et al.* (1991) 'Mechanically insensitive afferents (MIAs) in cutaneous nerves of monkey', *Brain Research*, 561(2), pp. 252–261. doi: 10.1016/0006-8993(91)91601-V.

Micale, V. and Drago, F. (2018) 'Endocannabinoid system, stress and HPA axis', *European Journal of Pharmacology*. Elsevier B.V., 834, pp. 230–239. doi: 10.1016/j.ejphar.2018.07.039.

Millan, M. J. (1990) 'κ-Opioid receptors and analgesia', *Trends in Pharmacological Sciences*. Elsevier Current Trends, 11(2), pp. 70–76. doi: 10.1016/0165-6147(90)90321-X.

Millan, M. J. (2002) 'Descending control of pain', *Progress in Neurobiology*. Pergamon, 66(6), pp. 355–474. doi: 10.1016/S0301-0082(02)00009-6.

Mogil, J. S., Davis, K. D. and Derbyshire, S. W. (2010) 'The necessity of animal models in pain research', *Pain*, pp. 12–17. doi: 10.1016/j.pain.2010.07.015.

Moriwaki, A. *et al.* (1996) 'mu Opiate receptor immunoreactivity in rat central nervous system.', *Neurochemical research*, 21(11), pp. 1315–31. Available at: http://www.ncbi.nlm.nih.gov/pubmed/8947922 (Accessed: 23 June 2019).

Morrison, I. *et al.* (2004) 'Vicarious responses to pain in anterior cingulate cortex: Is empathy a multisensory issue?', *Cognitive, Affective, & Behavioral Neuroscience*. Springer-Verlag, 4(2), pp. 270–278. doi: 10.3758/CABN.4.2.270.

Morton, D. L., Sandhu, J. S. and Jones, A. K. (2016) 'Brain imaging of pain: state of the art.', *Journal of pain research*. Dove Press, 9, pp. 613–24. doi: 10.2147/JPR.S60433.

Moulton, E. A. *et al.* (2012) 'BOLD Responses in Somatosensory Cortices Better Reflect Heat Sensation than Pain', *Journal of Neuroscience*, 32(17), pp. 6024–6031. doi: 10.1523/jneurosci.0006-12.2012.

Mouraux, A., Guérit, J. M. and Plaghki, L. (2003) 'Non-phase locked electroencephalogram (EEG) responses to CO2 laser skin stimulations may reflect central interactions between A∂- and C-fibre afferent volleys', *Clinical Neurophysiology*. Elsevier Ireland Ltd, 114(4), pp. 710–722. doi: 10.1016/S1388-2457(03)00027-0.

Mulders, P. C. *et al.* (2015) 'Resting-state functional connectivity in major depressive disorder: A review', *Neuroscience and Biobehavioral Reviews*. Elsevier Ltd, pp. 330–344. doi: 10.1016/j.neubiorev.2015.07.014.

Myers-Schulz, B. and Koenigs, M. (2014) 'Functional anatomy of ventromedial prefrontal cortex: Implications for mood and anxiety disorders', *Molecular psychiatry*, 17(2), pp. 132–141. doi: 10.1038/mp.2011.88.Functional.

Nakanishi, S. *et al.* (1979) 'Nucleotide sequence of cloned cDNA for bovine corticotropin-β-lipotropin precursor', *Nature*. Nature Publishing Group, 278(5703), pp. 423–427. doi: 10.1038/278423a0.

Nam, H. *et al.* (2014) 'Learned helplessness and social avoidance in the Wistar-Kyoto rat', *Frontiers in Behavioral Neuroscience*. Frontiers Research Foundation, 8(APR). doi: 10.3389/fnbeh.2014.00109.

Napadow, V., Sclocco, R. and Henderson, L. A. (2019) 'Brainstem neuroimaging of nociception and pain circuitries', *PAIN Reports*, 4(4), p. e745. doi: 10.1097/PR9.0000000000000745.

Navratilova, E. *et al.* (2019) 'Kappa opioid signaling in the central nucleus of the amygdala promotes disinhibition and aversiveness of chronic neuropathic pain', *Pain*. Lippincott Williams and Wilkins, 160(4), pp. 824–832. doi: 10.1097/j.pain.0000000000001458.

Nees, F. *et al.* (2019) 'Hypothalamic-pituitary-adrenal axis feedback sensitivity in different states of back pain', *Psychoneuroendocrinology*. Pergamon, 101, pp. 60–66. doi: 10.1016/J.PSYNEUEN.2018.10.026.

Nickel, M. M. *et al.* (2017) 'Brain oscillations differentially encode noxious stimulus intensity and pain intensity', *NeuroImage*. Academic Press Inc., 148, pp. 141–147. doi: 10.1016/j.neuroimage.2017.01.011.

Ong, W.-Y., Stohler, C. S. and Herr, D. R. (2019) 'Role of the Prefrontal Cortex in Pain Processing', *Molecular Neurobiology*. Springer US, 56(2),

pp. 1137–1166. doi: 10.1007/s12035-018-1130-9.

Ossipov, M. H. *et al.* (2003) 'Induction of pain facilitation by sustained opioid exposure: Relationship to opioid antinociceptive tolerance', in *Life Sciences*. Elsevier Inc., pp. 783–800. doi: 10.1016/S0024-3205(03)00410-7.

Ossipov, M. H., Dussor, G. O. and Porreca, F. (2010) 'Central modulation of pain.', *The Journal of clinical investigation*. American Society for Clinical Investigation, 120(11), pp. 3779–87. doi: 10.1172/JCI43766.

Paasonen, J. *et al.* (2018) 'Functional connectivity under six anesthesia protocols and the awake condition in rat brain', *NeuroImage*, 172(January), pp. 9–20. doi: 10.1016/j.neuroimage.2018.01.014.

Pare, D. and Duvarci, S. (2012) 'Amygdala microcircuits mediating fear expression and extinction', *Current Opinion in Neurobiology*, pp. 717–723. doi: 10.1016/j.conb.2012.02.014.

Paré, W. P. and Kluczynski, J. (1997) 'Differences in the stress response of Wistar-Kyoto (WKY) rats from different vendors', *Physiology and Behavior*. Elsevier Inc., 62(3), pp. 643–648. doi: 10.1016/S0031-9384(97)00191-1.

Pawela, C. P. *et al.* (2009) 'A protocol for use of medetomidine anesthesia in rats for extended studies using task-induced BOLD contrast and resting-state functional connectivity', *NeuroImage*, 46(4), pp. 1137–1147. doi: 10.1016/j.neuroimage.2009.03.004.

Paxinos, G. (2014) *The Rat Nervous System: Fourth Edition*, *The Rat Nervous System: Fourth Edition*. Elsevier Inc. doi: 10.1016/C2009-0-02419-2.

Peciña, M. *et al.* (2018) 'Endogenous opioid system dysregulation in depression: implications for new therapeutic approaches', *Molecular Psychiatry*. Nature Publishing Group, p. 1. doi: 10.1038/s41380-018-0117-2.

Pelletier, J.-P. *et al.* (2016) 'Efficacy and safety of oral NSAIDs and analgesics in the management of osteoarthritis: Evidence from real-life setting trials and surveys', *Seminars in Arthritis and Rheumatism*. W.B. Saunders, 45(4), pp. S22–S27. doi: 10.1016/J.SEMARTHRIT.2015.11.009.

Pert, C. B. and Snyder, S. H. (1973) 'Opiate receptor: demonstration in nervous tissue.', *Science (New York, N.Y.)*, 179(4077), pp. 1011–4. Available at: http://www.ncbi.nlm.nih.gov/pubmed/4687585 (Accessed: 26 May 2019).

Piampring, P. (2016) 'Problems with complete dentures and related factors in patients in Rajavithi hospital from 2007 to 2012', *Journal of the Medical Association of Thailand*, 99, pp. S182–S187. doi: 10.1016/j.neuroimage.2006.01.015.

Ploner, M. *et al.* (2017) 'Differential Organization of Touch and Pain in Human Primary Somatosensory Cortex', *Journal of Neurophysiology*. American Physiological SocietyBethesda, MD, 83(3), pp. 1770–1776. doi: 10.1152/jn.2000.83.3.1770.

Ploner, M., Sorg, C. and Gross, J. (2017) 'Brain Rhythms of Pain', *Trends in Cognitive Sciences*. Elsevier Ltd, pp. 100–110. doi: 10.1016/j.tics.2016.12.001.

Poldrack, R. A. *et al.* (2017) 'Scanning the horizon: Towards transparent and reproducible neuroimaging research', *Nature Reviews Neuroscience*. Nature Publishing Group, 18(2), pp. 115–126. doi: 10.1038/nrn.2016.167.

Preti, M. G., Bolton, T. A. and Van De Ville, D. (2017) 'The dynamic functional connectome: State-of-the-art and perspectives', *NeuroImage*. Academic Press Inc., 160, pp. 41–54. doi: 10.1016/j.neuroimage.2016.12.061.

Quartana, P. J., Campbell, C. M. and Edwards, R. R. (2009) 'Pain catastrophizing : a critical review', *Expert Rev Neurother*, 9(5), pp. 745–758. doi: 10.1586/ERN.09.34.Pain.

Quiton, R. L. *et al.* (2010) 'Abnormal activity of primary somatosensory

cortex in central pain syndrome', *Journal of Neurophysiology*, 104(3), pp. 1717–1725. doi: 10.1152/jn.00161.2010.

Raichle, M. E. *et al.* (2001) 'A default mode of brain function.', *Proceedings of the National Academy of Sciences of the United States of America*, 98(2), pp. 676–82. doi: 10.1073/pnas.98.2.676.

Rainville, P. *et al.* (1997) 'Pain affect encoded in human anterior cingulate but not somatosensory cortex.', *Science (New York, N.Y.)*. American Association for the Advancement of Science, 277(5328), pp. 968–71. doi: 10.1126/science.277.5328.968.

Rasmussen, N. A. and Farr, L. A. (2009) 'Beta-endorphin response to an acute pain stimulus', *Journal of Neuroscience Methods*. Elsevier, 177(2), pp. 285–288. doi: 10.1016/J.JNEUMETH.2008.10.013.

Rea, P. and Rea, P. (2015) 'Chapter 8 – Spinal Tracts – Ascending/Sensory Pathways', in *Essential Clinical Anatomy of the Nervous System*, pp. 133–160. doi: 10.1016/B978-0-12-802030-2.00008-X.

Reddan, M. C. and Wager, T. D. (2018) 'Modeling Pain Using fMRI: From Regions to Biomarkers', *Neuroscience Bulletin*. Springer, pp. 208–215. doi: 10.1007/s12264-017-0150-1.

Reynolds, D. V (1969) 'Surgery in the rat during electrical analgesia induced by focal brain stimulation.', *Science (New York, N.Y.)*, 164(3878), pp. 444–5. Available at: http://www.ncbi.nlm.nih.gov/pubmed/4887743 (Accessed: 1 June 2019).

Rice, A. S. C., Smith, B. H. and Blyth, F. M. (2016) 'Pain and the global burden of disease', *Pain*. Lippincott Williams and Wilkins, 157(4), pp. 791–796. doi: 10.1097/j.pain.0000000000000454.

Riordan, E. A. and Little, C. (2014) 'Pathogenesis of post-traumatic OA with a view to intervention', *Best Practice & Research Clinical Rheumatology*. Baillière Tindall, 28(1), pp. 17–30. doi:

10.1016/J.BERH.2014.02.001.

Rizvi, T. A. *et al.* (1991) 'Connections between the central nucleus of the amygdala and the midbrain periaqueductal gray: Topography and reciprocity', *The Journal of Comparative Neurology*, 303(1), pp. 121–131. doi: 10.1002/cne.903030111.

Robbins, T. W. (1996) 'Dissociating executive functions of the prefrontal cortex', *Philosophical Transactions of the Royal Society B: Biological Sciences*. Royal Society, 351(1346), pp. 1463–1471. doi: 10.1098/rstb.1996.0131.

Roeckel, L.-A. *et al.* (2017) 'Morphine-induced hyperalgesia involves mu opioid receptors and the metabolite morphine-3-glucuronide', *Scientific Reports*. Nature Publishing Group, 7(1), p. 10406. doi: 10.1038/s41598-017-11120-4.

Russell, M. D. *et al.* (2018) 'Reduced anterior cingulate grey matter volume in painful hand osteoarthritis', *Rheumatology International*, 38(8), pp. 1429–1435. doi: 10.1007/s00296-018-4085-2.

Sandell, L. J. and Aigner, T. (2001) 'Articular cartilage and changes in Arthritis: Cell biology of osteoarthritis', *Arthritis Research*. BioMed Central, 3(2), p. 107. doi: 10.1186/ar148.

Dos Santos Pinheiro, E. S. *et al.* (2016) 'Electroencephalographic patterns in chronic pain: A systematic review of the literature', *PLoS ONE*. Public Library of Science. doi: 10.1371/journal.pone.0149085.

Savannah, S. *et al.* (2017) 'Impact of preoperative opioid use on total knee arthroplasty outcomes', *Journal of Bone and Joint Surgery - American Volume*, pp. 803–808. doi: 10.2106/JBJS.16.01200.

Scanzello, C. R. and Goldring, S. R. (2012) 'The role of synovitis in osteoarthritis pathogenesis.', *Bone*. NIH Public Access, 51(2), pp. 249–57. doi: 10.1016/j.bone.2012.02.012.

Scott, J. E., Mathias, J. L. and Kneebone, A. C. (2016) 'Depression and anxiety after total joint replacement among older adults: a meta-analysis.', *Aging & mental health*, 20(12), pp. 1243–1254. doi: 10.1080/13607863.2015.1072801.

Servatius, R. J. *et al.* (2008) 'Rapid avoidance acquisition in Wistar-Kyoto rats', *Behavioural Brain Research*, 192(2), pp. 191–197. doi: 10.1016/j.bbr.2008.04.006.

Shin, L. M. and Liberzon, I. (2010) 'The neurocircuitry of fear, stress, and anxiety disorders', *Neuropsychopharmacology*. Nature Publishing Group, 35(1), pp. 169–191. doi: 10.1038/npp.2009.83.

Da Silva, J. T. and Seminowicz, D. A. (2019) 'Neuroimaging of pain in animal models', *PAIN Reports*, 4(4), p. e732. doi: 10.1097/PR9.0000000000000732.

Simantov, R. and Snyder, S. H. (1977) 'Opiate receptor binding in the pituitary gland', *Brain Research*. Elsevier, 124(1), pp. 178–184. doi: 10.1016/0006-8993(77)90877-0.

Sinclair, M. D. (2003) 'A review of the physiological effects of α2-agonists related to the clinical use of medetomidine in small animal practice', *Canadian Veterinary Journal*, pp. 885–897.

Snyder, A. Z. and Raichle, M. E. (2013) 'A Brief History of the Resting State: the Washington University Perspective', *NeuroImage*, 62(2), pp. 902–910. doi: 10.1016/j.neuroimage.2012.01.044.A.

Sorge, R. E. *et al.* (2014) 'Olfactory exposure to males, including men, causes stress and related analgesia in rodents', *Nature Methods*. Nature Publishing Group, 11(6), pp. 629–632. doi: 10.1038/nmeth.2935.

Spanos, N. P. *et al.* (1979) 'The effects of hypnotic susceptibility, suggestions for analgesia, and the utilization of cognitive strategies on the reduction of pain', *Journal of Abnormal Psychology*, 88(3), pp. 282–

292. doi: 10.1037/0021-843X.88.3.282.

Spisák, T. *et al.* (2017) 'Central sensitization-related changes of effective and functional connectivity in the rat inflammatory trigeminal pain model', *Neuroscience*. Pergamon, 344, pp. 133–147. doi: 10.1016/J.NEUROSCIENCE.2016.12.018.

Srikanth, V. K. *et al.* (2005) 'A meta-analysis of sex differences prevalence, incidence and severity of osteoarthritis', *Osteoarthritis and Cartilage*. W.B. Saunders, 13(9), pp. 769–781. doi: 10.1016/J.JOCA.2005.04.014.

Steinhaus, M. E., Christ, A. B. and Cross, M. B. (2017) 'Total Knee Arthroplasty for Knee Osteoarthritis: Support for a Foregone Conclusion?', *HSS Journal ®*, 13(2), pp. 207–210. doi: 10.1007/s11420-017-9558-4.

Steriade, M. *et al.* (1993) 'The slow (< 1 Hz) oscillation in reticular thalamic and thalamocortical neurons: scenario of sleep rhythm generation in interacting thalamic and neocortical networks.', *The Journal of neuroscience : the official journal of the Society for Neuroscience*, 13(8), pp. 3284–99. Available at: http://www.ncbi.nlm.nih.gov/pubmed/8340808 (Accessed: 26 April 2019).

Steriade, M., Amzica, F. and Contreras, D. (1994) 'Cortical and thalamic cellular correlates of electroencephalographic burst-suppression', *Electroencephalography and Clinical Neurophysiology*, 90(1), pp. 1–16. doi: 10.1016/0013-4694(94)90108-2.

Straathof, M. *et al.* (2019) 'A systematic review on the quantitative relationship between structural and functional network connectivity strength in mammalian brains', *Journal of Cerebral Blood Flow and Metabolism*. SAGE Publications Ltd, pp. 189–209. doi: 10.1177/0271678X18809547.

Strader, C. D. *et al.* (1994) 'Structure and Function of G Protein-Coupled Receptors', *Annual Review of Biochemistry*, 63(1), pp. 101–132. doi: 10.1146/annurev.bi.63.070194.000533.

Stucky, C. . L. (2016) 'Mechanisms of pain', *Cognitive Neuroscience Robotics B: Analytic Approaches to Human Understanding*, 98(21), pp. 121–145. doi: 10.1007/978-4-431-54598-9_6.

Swain, S. *et al.* (2019) 'Comorbidities in Osteoarthritis: A systematic review and meta-analysis of observational studies.', *Arthritis care & research*. doi: 10.1002/acr.24008.

Tanasescu, R. *et al.* (2016) 'Functional reorganisation in chronic pain and neural correlates of pain sensitisation: A coordinate based meta-analysis of 266 cutaneous pain fMRI studies', *Neuroscience & Biobehavioral Reviews*, 68, pp. 120–133. doi: 10.1016/j.neubiorev.2016.04.001.

Teeple, E. *et al.* (2013) 'Animal models of osteoarthritis: Challenges of model selection and analysis', *AAPS Journal*, pp. 438–446. doi: 10.1208/s12248-013-9454-x.

Thompson, S. J. *et al.* (2018) 'Chronic neuropathic pain reduces opioid receptor availability with associated anhedonia in rat.', *Pain*, 159(9), pp. 1856–1866. doi: 10.1097/j.pain.0000000000001282.

Tiemann, L. *et al.* (2015) 'Differential neurophysiological correlates of bottom-up and top-down modulations of pain', *Pain*. Lippincott Williams and Wilkins, 156(2), pp. 289–296. doi: 10.1097/01.j.pain.0000460309.94442.44.

Todd, A. J. *et al.* (2002) 'Projection Neurons in Lamina I of Rat Spinal Cord with the Neurokinin 1 Receptor Are Selectively Innervated by Substance P-Containing Afferents and Respond to Noxious Stimulation', *Journal of Neuroscience*, 22(10), pp. 4103–4113. doi: 10.1523/jneurosci.22-10-04103.2002.

Todd, A. J. (2010) 'Neuronal circuitry for pain processing in the dorsal horn.', *Nature reviews. Neuroscience*. Europe PMC Funders, 11(12), pp. 823–36. doi: 10.1038/nrn2947.

Tölle, T. R. *et al.* (1999) 'Region-specific encoding of sensory and affective components of pain in the human brain: A positron emission tomography correlation analysis', *Annals of Neurology*. John Wiley & Sons, Ltd, 45(1), pp. 40–47. doi: 10.1002/1531-8249(199901)45:1<40::AID-ART8>3.0.CO;2-L.

Tracey, I. and Mantyh, P. W. (2007) 'The Cerebral Signature for Pain Perception and Its Modulation', *Neuron*, 55(3), pp. 377–391. doi: 10.1016/j.neuron.2007.07.012.

Treede, R. D. *et al.* (2015) 'A classification of chronic pain for ICD-11', *Pain*. Lippincott Williams and Wilkins, pp. 1003–1007. doi: 10.1097/j.pain.0000000000000160.

Tsurugizawa, T., Takahashi, Y. and Kato, F. (2016) 'Distinct effects of isoflurane on basal BOLD signals in tissue/vascular microstructures in rats', *Scientific Reports*. Nature Publishing Group, 6(1), p. 38977. doi: 10.1038/srep38977.

Uhlhaas, P. J. (2011) 'High-Frequency Oscillations in Schizophrenia', *Clinical EEG and Neuroscience*, 42(2), pp. 77–82. doi: 10.1177/155005941104200208.

Urban, M. O., Zahn, P. K. and Gebhart, G. F. (1999) 'Descending facilitatory influences from the rostral medial medulla mediate secondary, but not primary hyperalgesia in the rat', *Neuroscience*. Pergamon, 90(2), pp. 349–352. doi: 10.1016/S0306-4522(99)00002-0.

Uth, K. (2014) 'Stem cell application for osteoarthritis in the knee joint: A minireview', *World Journal of Stem Cells*. Baishideng Publishing Group Inc., 6(5), p. 629. doi: 10.4252/wjsc.v6.i5.629.

Valdes, A. M. *et al.* (2015) 'Use of prescription analgesic medication and pain catastrophizing after total joint replacement surgery', *Seminars in Arthritis and Rheumatism*, 45(2), pp. 150–155. doi: 10.1016/j.semarthrit.2015.05.004.

Veening, J. *et al.* (1991) 'Hypothalamic Projections to the PAG in the Rat: Topographical, Immuno-Electronmicroscopical and Functional Aspects', in *The Midbrain Periaqueductal Gray Matter*. Springer US, pp. 387–415. doi: 10.1007/978-1-4615-3302-3_21.

Veiga, D. R. *et al.* (2018) 'Effectiveness of Opioids for Chronic Noncancer Pain: A Two-Year Multicenter, Prospective Cohort Study With Propensity Score Matching', *The Journal of Pain*. Churchill Livingstone. doi: 10.1016/J.JPAIN.2018.12.007.

Veinante, P., Yalcin, I. and Barrot, M. (2013) 'The amygdala between sensation and affect: a role in pain.', *Journal of molecular psychiatry*. BioMed Central, 1(1), p. 9. doi: 10.1186/2049-9256-1-9.

Vincent, J. L. *et al.* (2007) 'Intrinsic functional architecture in the anaesthetized monkey brain', 447. doi: 10.1038/nature05758.

Vowles, K. E. *et al.* (2015) 'Rates of opioid misuse, abuse, and addiction in chronic pain: A systematic review and data synthesis', *Pain*. Lippincott Williams and Wilkins, pp. 569–576. doi: 10.1097/01.j.pain.0000460357.01998.f1.

Vukojević, K., Lovrić-Kojundžić, S. and Sapunar, D. (2007) 'HYPERALGESIA-TYPE RESPONSE REVEALS NO DIFFERENCE IN PAIN-RELATED BEHAVIOR BETWEEN WISTAR AND SPRAGUE-DAWLEY RATS', *Bosnian Journal of Basic Medical Sciences*. Association of Basic Medical Sciences of Federation of Bosnia and Herzegovina, 7(2), p. 123.

Waldhoer, M., Bartlett, S. E. and Whistler, J. L. (2004a) 'OPIOID

RECEPTORS'. doi: 10.1146/annurev.biochem.73.011303.073940.

Waldhoer, M., Bartlett, S. E. and Whistler, J. L. (2004b) 'OPIOID RECEPTORS'. doi: 10.1146/annurev.biochem.73.011303.073940.

Wardach, J. *et al.* (2016) 'Lateral Hypothalamic Stimulation Reduces Hyperalgesia Through Spinally Descending Orexin-A Neurons in Neuropathic Pain.', *Western journal of nursing research*. NIH Public Access, 38(3), pp. 292–307. doi: 10.1177/0193945915610083.

Wasan, A. D., Davar, G. and Jamison, R. (2005a) 'The association between negative affect and opioid analgesia in patients with discogenic low back pain', *Pain*, 117(3), pp. 450–461. doi: 10.1016/j.pain.2005.08.006.

Wasan, A. D., Davar, G. and Jamison, R. (2005b) 'The association between negative affect and opioid analgesia in patients with discogenic low back pain', *Pain*, 117(3), pp. 450–461. doi: 10.1016/j.pain.2005.08.006.

Weber, R. *et al.* (2006) 'A fully noninvasive and robust experimental protocol for longitudinal fMRI studies in the rat', *NeuroImage*, 29(4), pp. 1303–1310. doi: 10.1016/j.neuroimage.2005.08.028.

Wells, J. A. *et al.* (2017a) 'Functional MRI of the Reserpine-Induced Putative Rat Model of Fibromyalgia Reveals Discriminatory Patterns of Functional Augmentation to Acute Nociceptive Stimuli', *Scientific Reports*. Nature Publishing Group, 7(November 2016), p. 38325. doi: 10.1038/srep38325.

Wells, J. A. *et al.* (2017b) 'Functional MRI of the Reserpine-Induced Putative Rat Model of Fibromyalgia Reveals Discriminatory Patterns of Functional Augmentation to Acute Nociceptive Stimuli', *Scientific Reports*. Nature Publishing Group, 7(1), p. 38325. doi: 10.1038/srep38325.

Westlund, K. N. and Willis, W. D. (2012) 'Chapter 32 – Pain System', *The Human Nervous System*, pp. 1144–1186. doi: 10.1016/B978-0-12-374236-0.10032-X.

Williams, K. A. *et al.* (2010) 'Comparison of α-chloralose, medetomidine and isoflurane anesthesia for functional connectivity mapping in the rat', *Magnetic Resonance Imaging*, 28(7), pp. 995–1003. doi: 10.1016/j.mri.2010.03.007.

Winkler, A. M. *et al.* (2014) 'Permutation inference for the general linear model', *NeuroImage*, 92, pp. 381–397. doi: 10.1016/j.neuroimage.2014.01.060.

Winters, B. L. *et al.* (2017) 'Endogenous opioids regulate moment-to-moment neuronal communication and excitability', *Nature Communications*. Nature Publishing Group, 8, p. 14611. doi: 10.1038/ncomms14611.

Woods, S. B. *et al.* (2019) 'Close relationships as a contributor to chronic pain pathogenesis: Predicting pain etiology and persistence', *Social Science & Medicine*, 237, p. 112452. doi: 10.1016/j.socscimed.2019.112452.

Woolf, C. J. (1983) 'Evidence for a central component of post-injury pain hypersensitivity', *Nature*. Nature Publishing Group, 306(5944), pp. 686–688. doi: 10.1038/306686a0.

Woolf, C. J. and Ma, Q. (2007) 'Nociceptors-Noxious Stimulus Detectors', *Neuron*, 55(3), pp. 353–364. doi: 10.1016/j.neuron.2007.07.016.

Wu, L. *et al.* (2018) 'An approach to directly link ICA and seed-based functional connectivity: Application to schizophrenia', *NeuroImage*, 179, pp. 448–470. doi: 10.1016/j.neuroimage.2018.06.024.

Xia, X. L. *et al.* (2016) 'Laser-evoked cortical responses in freely-moving rats reflect the activation of C-fibre afferent pathways', *NeuroImage*. Academic Press, 128, pp. 209–217. doi: 10.1016/J.NEUROIMAGE.2015.12.042.

Yaksh, T. L. (1988) 'Substance P release from knee joint afferent terminals: modulation by opioids.', *Brain research*, 458(2), pp. 319–24.

Available at: http://www.ncbi.nlm.nih.gov/pubmed/2463049 (Accessed: 13 June 2019).

Yaksh, T. L., Yeung, J. C. and Rudy, T. A. (1976) 'Systematic examination in the rat of brain sites sensitive to the direct application of morphine: Observation of differential effects within the periaqueductal gray', *Brain Research*. Elsevier, 114(1), pp. 83–103. doi: 10.1016/0006-8993(76)91009-X.

Yang, C. F. *et al.* (2014) 'Dose-dependent effects of isoflurane on cardiovascular function in rats', *Tzu Chi Medical Journal*. Elsevier Taiwan LLC, 26(3), pp. 119–122. doi: 10.1016/j.tcmj.2014.07.005.

Yu, R. *et al.* (2014) 'Disrupted functional connectivity of the periaqueductal gray in chronic low back pain', *NeuroImage: Clinical*. Elsevier Inc., 6, pp. 100–108. doi: 10.1016/j.nicl.2014.08.019.

Yushkevich, P. A. *et al.* (2006) 'User-guided 3D active contour segmentation of anatomical structures: Significantly improved efficiency and reliability', *NeuroImage*, 31(3), pp. 1116–1128. doi: 10.1016/j.neuroimage.2006.01.015.

Zaitsev, M., Maclaren, J. and Herbst, M. (2015) 'Motion artifacts in MRI: A complex problem with many partial solutions', *Journal of Magnetic Resonance Imaging*. John Wiley and Sons Inc., pp. 887–901. doi: 10.1002/jmri.24850.

Zhang, R. X. *et al.* (2003) 'Strain differences in pain sensitivity and expression of preprodynorphin mRNA in rats following peripheral inflammation', *Neuroscience Letters*. Elsevier Ireland Ltd, 353(3), pp. 213–216. doi: 10.1016/j.neulet.2003.09.043.

Zhao, F. *et al.* (2012) 'NeuroImage fMRI of pain processing in the brain : A within-animal comparative study of BOLD vs . CBV and noxious electrical vs . noxious mechanical stimulation in rat', *NeuroImage*. Elsevier Inc., 59(2), pp. 1168–1179. doi: 10.1016/j.neuroimage.2011.08.002.

Zhao, F. *et al.* (2014) 'NeuroImage Quali fi cation of fMRI as a biomarker for pain in anesthetized rats by comparison with behavioral response in conscious rats', *NeuroImage*. Elsevier Inc., 84, pp. 724–732. doi: 10.1016/j.neuroimage.2013.09.036.

Zywiel, M. G. *et al.* (2011) 'Chronic opioid use prior to total knee arthroplasty', *Journal of Bone and Joint Surgery - Series A*. Journal of Bone and Joint Surgery Inc., 93(21), pp. 1988–1993. doi: 10.2106/JBJS.J.01473.